SÃO PAULO STATE UNIVERSITY
SCHOOL OF ENGINEERING
ILHA SOLTEIRA

JONATHAN PABLO AYALA MARCELO

MULTISTAGE PLANNING FOR ACTIVE DISTRIBUTION SYSTEMS UNDER UNCERTAINTY: A COMPREHENSIVE APPROACH

Ilha Solteira
2023

JONATHAN PABLO AYALA MARCELO

MULTISTAGE PLANNING FOR ACTIVE DISTRIBUTION SYSTEMS UNDER UNCERTAINTY: A COMPREHENSIVE APPROACH

Thesis submitted to the School of Engineering of Ilha Solteira – UNESP in partial fulfillment of the requirements for the degree of Doctor of Philosophy in Electrical Engineering.

Concentration Area: Electrical Engineering

Prof. Dr. José Roberto Sanches Mantovani
Advisor

Prof. Dr. Diogo Rupolo
Prof. Dr. Javier Contreras
Associate advisors

Ilha Solteira
2023

FICHA CATALOGRÁFICA
Desenvolvido pelo Serviço Técnico de Biblioteca e Documentação

A973m

Ayala Marcelo, Jonathan Pablo.
multistage planning for active distribution systems under uncertainty: a comprehensive approach / Jonathan Pablo Ayala Marcelo. -- Ilha Solteira: [s.n.], 2023
100 f. : il.

Tese (doutorado) - Universidade Estadual Paulista. Faculdade de Engenharia de Ilha Solteira. Área de conhecimento: Automação, 2023

Orientador: José Roberto Sanches Mantovani
Co-orientador: Diogo Rupolo
Co-orientador: Javier Contreras
Inclui bibliografia

1. Sistemas ativos de distribuição. 2. Incertezas. 3. Prosumidores. 4. Veículo elétricos. 5. Avaliação da confiabilidade do planejamento. 6. Mateuristica.

Amanda Sertori dos Santos
Bibliotecária - CRB/8-9061
Seção Técnica de Referência, Atendimento ao Usuário e Documentação
Diretoria Técnica de Biblioteca e Documentação

Potencial impact of this research

This research reduces the gap between the academic development and the practical applicability of solution approaches for the planning of electrical power distribution systems (a realistic and practical model together with a novel solution technique are proposed). Also, it is committed to sustainable development, proposing necessary actions to achieve optimal results while reducing carbon emissions.

Impacto potencial desta pesquisa

Neste trabalho de pesquisa propõe-se uma redução entre o desenvolvimento acadêmico e a aplicabilidade prática das abordagens de solução para o planejamento de sistemas de distribuição de energia elétrica (é proposto um modelo realista e prático juntamente com uma nova técnica de solução). Além disso, está comprometida com o desenvolvimento sustentável, propondo as ações necessárias para alcançar ótimos resultados e, ao mesmo tempo, reduzir as emissões de carbono.

Impacto potencial de esta investigación

Esta investigación reduce la brecha entre el desarrollo académico y la aplicabilidad práctica de los enfoques de solución para la planificación de sistemas de distribución de energía eléctrica (se propone un modelo realista y práctico junto con una técnica de solución novedosa). Además, apuesta por el desarrollo sostenible, proponiendo acciones necesarias para lograr resultados óptimos mientras se reducen las emisiones de carbono.

CERTIFICADO DE APROVAÇÃO

TÍTULO DA TESE: MULTISTAGE PLANNING FOR ACTIVE DISTRIBUTION SYSTEMS UNDER UNCERTAINTY: A COMPREHENSIVE APPROACH

AUTOR: JONATHAN PABLO AYALA MARCELO
ORIENTADOR: JOSE ROBERTO SANCHES MANTOVANI
COORIENTADOR: DIOGO RUPOLO
COORIENTADOR: JAVIER CONTRERAS SANZ

Aprovado como parte das exigências para obtenção do Título de Doutor em Engenharia Elétrica, área: Automação pela Comissão Examinadora:

Prof. Dr. JOSE ROBERTO SANCHES MANTOVANI (Participaçao Presencial)
Departamento de Engenharia Eletrica / Faculdade de Engenharia de Ilha Solteira - UNESP

Prof. Dr. RUBEN AUGUSTO ROMERO LAZARO (Participaçao Presencial)
Departamento de Engenharia Eletrica / Faculdade de Engenharia de Ilha Solteira - UNESP

Prof. Dr. JONATAS BOAS LEITE (Participaçao Presencial)
Departamento de Engenharia Eletrica / Faculdade de Engenharia de Ilha Solteira - UNESP

Dr. OZY DANIEL MELGAR DOMINGUEZ (Participaçao Virtual)
Departamento de Planejamento da Expansão da Geração / Operador do Sistema Elétrico Nacional (CND-ODS), Tegucigalpa, Honduras

Prof. Dr. BENVINDO RODRIGUES PEREIRA JÚNIOR (Participaçao Virtual)
Departamento de Engenharia Elétrica e de Computação / Escola de Engenharia de São Carlos - USP

Ilha Solteira, 22 de setembro de 2023

This work is dedicated for all the people who have passed through my life leaving a mark, a memorable memory or simply a smile. Especially for my family.

ACKNOWLEDGMENTS

I thank God for everything. This work is just a small sample of what Him wanted for me.

To my family, who have always supported and encouraged me over all the time dedicated to the development of this work.

To my advisor, Prof. Dr. José Roberto Sanches Mantovani, for the mentorship, support and trust throughout the doctoral program. To my co-advisor, Prof. Dr. Diogo Rupolo, for his friendship and support. To my co-advisor, Prof. Dr. Javier Contreras, for their mentorship and support. To Prof. Dr. Gregorio Muñoz Delgado for his advice that has lead to improving the quality of this work. Also, to Prof. Ruben Romero for his compromise with research.

To colleagues and friends of the Laboratorio de Planejamento de Sistemas de Energia Elétrica (LAPSEE), for friendship and companionship during this work. Also, to colleagues and friends of the Power and Energy Analysis and Research Laboratory (PEARL), for friendship and companionship during my international PhD internship (Sandwich Ph.D) in the Universidad de Castilla-La Mancha, Spain.

The present work was carried out with the support of the National Council for Scientific and Technological Development (CNPq) by Grant 140363/2020-3. Also, by the Brazilian Federal Agency for Support and Evaluation of Graduate Education (CAPES) by Finance Code 001, and through the process number 88887.310463/ 2018-00, Mobility number 88887.685344/2022-00 in the scope of the program CAPES-PrInt. My gratitude to these institutions.

“Don’t chase success, strive for excellence, and success will follow you.”

(Rajkumar Hirani, 3 Idiots)

RESUMO

Neste trabalho propõe-se um novo modelo estocástico de dois estágios baseado em cenários para o planejamento multiestágio de sistemas ativos de distribuição de energia elétrica considerando um tratamento adequado das incertezas. O problema de planejamento é formulado como um modelo de programação quadrática inteira mista e resolvido mediante uma nova técnica matheurística que pode obter soluções de alta qualidade garantindo sua factibilidade em relação ao problema original (não linear e não convexo). Como o planejamento ótimo depende tanto da qualidade dos dados quanto da modelagem e da técnica de solução, os dados (parâmetros operacionais) e as incertezas são modeladas detalhadamente, considerando incertezas de curto e longo prazo. Propõe-se também um novo método para estimar as cargas dos veículos elétricos com base em distribuições de probabilidades. Para capturar a diversidade dos cenários de operação a partir das incertezas de demanda e recursos energéticos, preservando a transição temporal da operação do sistema (útil para a modelagem dos sistemas de armazenamento de energia elétrica), são utilizados cenários representativos de operação de duração diária e resolução horária. Para isso, é proposto um novo método para determinar cenários representativos robustos que permitem ênfase em cenários críticos, como aqueles de demandas máxima e mínima. Um grande portfólio de ações de planejamento é considerado visando obter o melhor plano de investimento com base nos recursos tecnológicos atuais, bem como investigar seus impactos na operação do sistema. Essas ações incluem repotencialização das subestações, instalação de comutadores de tap sob carga (OLTCs), sistemas de geração distribuída, sistemas de armazenamento de energia elétrica, bancos de capacitores fixos e chaveados, compensadores estáticos de reativos (SVCs), reguladores de tensão e recondutoramento. Adicionalmente, o modelo garante reduções periódicas de CO_2, para atender o compromisso de limitar o aquecimento global. Para ponderar adequadamente estas emissões, são contabilizadas as emissões de CO_2 provenientes da operação do sistema de distribuição e dos veículos a combustão, considerando a redução de emissões resultante da adoção dos veículos elétricos. Após o planejamento, a confiabilidade dos planos de investimento é analisada quantitativamente, mostrando as vantagens de considerar adequadamente as incertezas no processamento dos dados. Para demonstrar a eficácia do modelo proposto, são realizados testes em um sistema de distribuição de 69 nós e em um sistema real de 135 nós, considerando três estudos de casos com diferentes tratamentos de incerteza e diferentes seleções de cenários representativos.

Palavras-chave: Sistemas ativos de distribuição; incertezas; prosumidores; veículos elétricos; avaliação da confiabilidade do planejamento; matheurística.

ABSTRACT

This work proposes a new scenario-based two-stage stochastic model for the multistage planning of active distribution systems considering a proper handling of the uncertainties. The planning problem is formulated as a Mixed Integer Quadratic Programming (MIQP) model and solved through a matheuristic technique that can attain high-quality solutions guaranteeing their feasibility regarding the original non-linear and non-convex problem. Since an optimal planning depends on both data quality and modeling, due importance is given to data analysis (about operating parameters) and the uncertainties are modeled in detail, considering short and long term uncertainties. Also, a new method to estimate the Electrical Vehicle (EV) loads based on probability distributions is proposed. In order to capture the diversity of operation scenarios from demand and energy resource uncertainties while preserving the temporal transition of the system operation (useful for Electrical Energy Storage (EES) modeling), Representative Operating Scenarios (ROSs) of daily duration and hourly resolution are used. For that, a new method to determine robust ROSs is proposed, which allows to emphasize in critical scenarios, as those of maximum and minimum demand. A large portfolio of planning actions is considered with the aim of improving the system planning and investigating its impacts on system operation. These actions include substation replacement, installation of On Load Tap Changers (OLTCs), Distributed Generation (DG) systems, EES systems, fixed and switchable Capacitor Banks (CBs), Static VAr Compensators (SVCs), Voltage Regulators (VRs) and reconductoring. Moreover, the model guarantees periodical CO_2 reductions in order to be on track to limit global warming. To properly weight up these emissions, CO_2 emissions from distribution system operation and CO_2 emission reduction from EV adoption are accounted for. After planning, the reliability of the obtained investment plans are addressed and measured and the advantages of considering properly the uncertainties in data processing are shown. To show the effectiveness of the proposed model, tests are carried out in a 69-node distribution test system and a real 135-node distribution system, considering three case studies with different uncertainty handling and different selection of representative scenarios.

Keywords: Active distribution systems; uncertainties; prosumers; electrical vehicles; planning reliability assestment; matheuristics.

LIST OF FIGURES

Figure 1 – Application of long-term and short-term uncertainties 31
Figure 2 – (a) Probability function of charging decision. (b) PDF of SOC at the end of charging 33
Figure 3 – (a) PDF of SOC at the charging start. (b)–(d) PDF of charging start time for b) charging level 1, c) charging level 2 and d) charging level 3 34
Figure 4 – Methodology to generate random EV load profiles 36
Figure 5 – Relationship between operating scenarios and comprised operating scenarios 39
Figure 6 – Simplified scheme for obtaining ROSs 41
Figure 7 – Methodology to determine robust ROS 43
Figure 8 – Capability curve of DG systems 49
Figure 9 – Sketch of the solution technique heuristics 55
Figure 10 – Block diagram of the solution technique methodology 59
Figure 11 – Topology and candidate location for equipment installation of the 69-node test system 61
Figure 12 – Topology and candidate location for equipment installation of the real 135-node system 62
Figure 13 – Demand integration by planning period 66
Figure 14 – Robust ROSs for each planning period 67
Figure 15 – Losses composition by planning period for Case III 73

LIST OF TABLES

Table 1 – Comparison of this work with the state of art - part 1 28
Table 2 – Comparison of this work with the state of art - part 2 29
Table 3 – Lifespan of the system assets (years) 65
Table 4 – EV charging preferences by charging level (%) 65
Table 5 – Solution overview: Distribution and energy costs 69
Table 6 – Investment and planning actions 71
Table 7 – Performance Overview for the Case III 74
Table 8 – Planning Reliability Assestment 76
Table 9 – Solution overview for the real 135-node system: Distribution and energy costs 78
Table 10 – Expected number of EVs by node for selected years 86
Table 11 – Data of the 69-node test system 88
Table 12 – Data of the real 135-node system 91
Table 13 – Hourly average energy prices for each planning period (\$/MWh) 96
Table 14 – Hourly average CO_2 intensity for each planning period ($kgCO_2$/MWh) 97
Table 15 – Substation costs 98
Table 16 – Conductor replacement costs 98
Table 17 – Support replacement costs 99
Table 18 – VR costs 99
Table 19 – Investment costs of DER systems 99
Table 20 – O&M costs of DER systems (\$/kW) 100

LIST OF ACRONYMS AND ABBREVIATIONS

CB	Capacitor Bank
C&CG	Column-and-Constraint Generation
DISCO	Distribution Company
DG	Distributed Generation
DER	Distributed Energy Resource
EES	Electrical Energy Storage
EV	Electrical Vehicle
EVCS	Electric Vehicle Charging Station
HMM	Heuristic Moment Matching
KKT	Karush-Kuhn-Tucker
LP	Linear Programming
MILP	Mixed Integer Linear Programming
MINLP	Mixed Integer Non-Linear Programming
MISOCP	Mixed Integer Second Order Cone Programming
MICP	Mixed Integer Conic Programming
MIQP	Mixed Integer Quadratic Programming
NSGA-II	Non-Dominated Sorting Genetic Algorithm
O&M	Operation and Maintenance
OLTC	On Load Tap Changer
OPF	Optimal Power Flow
PDF	Probability Density Function
PWL	Piece-Wise Linearization
QP	Quadratic Programming
ROS	Representative Operating Scenario
SOC	State of Charge
SVC	Static VAr Compensator

TSO	Transmission System Operator
VR	Voltage Regulator

LIST OF SYMBOLS

Index sets and indices

Ω_B,Ω_{B+},(i,j)	Index set/index of branches/branches including transformer windings.
Ω_N, i, j, j'	Index set/indices of nodes.
$\Omega_{\bar{N}}, \Omega_{ss}$	Index set of load/substation nodes.
Ω_B^{vr}	Index set of candidate branches to install VRs.
Ω_{ees},Ω_{pv},Ω_{wd}	Index set of candidate nodes to install EES/photovoltaic (PV) DG/wind DG systems.
Ω_{rc}	Index set of candidate nodes to install reactive compensation devices.
Ω_C, a, a';	Index set/indices of conductor/support types
Ω_{sp}, e, e'	for reconductoring.
$\Omega_{\overline{ss}}, u$	Index set/index of substation types.
Ω_{vr}, v	Index set/index of VR types.
Ω_V, ν	Index set/index of EV charging levels.
Ω_T, t, t'	Index set/indices of planning periods.
Ω_Y, y	Index set/ index of years of each planning period.
Ω_D, d	Index set/index of days within a year.
Ω_H, h	Index set/index of hours within a day.
Ω_R^t, r	Index set/index of representative operating scenarios.

Planning and investment parameters

$c_{a',a}^{cr}$	Investment cost for the replacement of type a' conductor by type a (\$/km).
$c_{e',e}^{sp}$	Investment cost for the replacement of type e' structure by type e (\$/km).
$c_{t,h}^{en}$	Cost of energy supplied by the substation (\$/kWh).
c_f^{fcb}, c_v^{fcb}	Fixed/Variable investment cost of fixed CBs (\$).
c_f^{scb}, c_v^{scb}	Fixed/Variable investment cost of switchable CBs (\$).
$c_t^{ees}, com_{t,y}^{ees}$	Investment/O&M cost of EES systems (\$/kW).
$c_t^{pv}, com_{t,y}^{pv}$	Investment/O&M cost of PV systems (\$/kW).
$c_t^{wd}, com_{t,y}^{wd}$	Investment/O&M cost of wind systems (\$/kW).
c_t^{svc}	Investment cost of a SVC (\$).
$c_t^{ss,k}$	Investment cost of substations (\$).
$c_t^{vr,v}$	Investment cost of VR units (\$).
$n_T, n_Y, n_{t,y}$	Number of planning periods/of years of each planning period/of years until planning period t and year y inclusive.

ι	Annual discount rate.
T, T_t	Planning horizon/time span from the beginning of planning period t (years).
β_t^{inv}	Present value factor for investments.
$\beta_{t,y}^{en}$	Present value factor for energy purchase.
$\beta_{t,y}^{om}$	Present value factor for O&M costs.
ω_t^{as}	Use factor for asset as.

Distribution network parameters

$a_0^{i,j}/e_0^{i,j}$	Initial conductor/ structure type of line (i,j).
$\mathrm{p}_{ss}^{ind}/\mathrm{p}_{ss}^{cap}$	Minimum inductive/capacitive power factor allowed at substations.
$\bar{I}_a$	Nominal current of type a conductor.
$(i,j)_c/(i,j)_s$	Existing conductor/supports of branch (i,j).
$l_{i,j}$	Length of line (i,j) (km).
R_a, X_a, Z_a	Resistance/Reactance/Impedance of type a conductor (Ω/km).
$R_{ss}^i, X_{ss}^i, Z_{ss}^i$	Equivalent resistance/reactance referred to secondary of the power transformers (Ω).
L_{ss}^i	No-load losses of the power transformers (kW).
ss_i	Existing substation at node i.
$S_0^{ss,i}$	Nominal power of the existing substations (kVA).
T_{as}, T_{as}^0	Lifespan/Elapsed life until the beginning of the planning horizon of system asset as.
$\overline{V}, \underline{V}$	Upper/Lower voltage limit.

Parameters related to operating parameters

c_{ev}	EV energy consumption rate (kWh/km).
$\dot{\mathrm{f}}_{t,d,h}^D, \dot{\mathrm{f}}_{t,d,h}^R$	Active/Reactive power demand factor.
$\mathrm{f}_{t,d,h}^D, \mathrm{f}_{t,d,h}^R$	Active/Reactive power demand factor for representative days.
$\bar{\ell}, \ell_d$	Average/Day-d commute route length (km).
$\bar{n}^{ev}, n_0^{ev}$	Number of EVs over all the planning horizon/at the beginning of the planning horizon.
$n_{t,y}^{ev}, n_{t,y}^{ev,i}$	Number of EVs powered by the system/by the node i.
$n_{t,y}^{v,i}$	Number of vehicles within node i area, in period t and year y.
$N_0^{v,i}$	Number of EVs present at the beginning of the planning horizon.
$\hat{\mathrm{p}}_{pr}$	Power factor of DG systems owned by prosumers.
p_{ev}	Power factor of EV chargers.
p_v	EV charging power.
$P_{0,d,h}^{cd,i}, Q_{0,d,h}^{cd,i}$	Estimated active/reactive conventional demand at the beginning of the planning horizon (kW/kVAr).

$\bar{P}^{D}_{t}, \bar{Q}^{D}_{t}$	Maximum active/reactive system power demand (kW).
$\bar{P}^{D,i}_{t,d}, \bar{Q}^{D,i}_{t,d}$	Maximum active/reactive power demand of node i on representative day d (kW).
$\dot{P}^{D,i}_{t,y,d,h}, \dot{Q}^{D,i}_{t,y,d,h}$	Total active/reactive power demand (kW/kVAr).
$P^{D,i}_{t,y,d,h}, Q^{D,i}_{t,y,d,h}$	Total active/reactive power demand of representative days (kW/kVAr).
$P^{ev}_{\mu,h}$	Diversified EV load (kW).
$P^{ev,i}_{t,y,d,h}, Q^{ev,i}_{t,y,d,h}$	Active/Reactive expected load of the EV fleet powered by node i (kW/kVAr).
$P^{pr,i}_{t,y,d,h}, Q^{pr,i}_{t,y,d,h}$	Active/Reactive power output of prosumers' DG systems (kW/kVAr).
soc_{min}	Minimum State of Charge (SOC) value needed to complete an EV daily trip.
$\alpha^{ev}_{t,v}, \phi^{ev,i}_{t,v}$	Percentage of EV owners who have access and prefer charging their EVs with charging level v/with charging level v at node i.
$\lambda^{ev,i}_{t,y} / \lambda^{pr,i}_{t,y}$	EV/Prosumers' DG penetration.
$\varsigma^{p,i}, \varsigma^{q,i}$	Annual growth rate of active/reactive conventional demand at the beginning of the planning horizon.
$\tau^{ev}_{i} / \tau^{pr}_{i}$	Expected date of maximum EV penetration/prosumer penetration (year).

Parameters associated to planning actions

$\dot{\mathrm{f}}^{pv}_{t,d,h}, \dot{\mathrm{f}}^{wd}_{t,d,h}$	PV/wind generation factor.
$\mathrm{f}^{pv}_{t,d,h}, \mathrm{f}^{wd}_{t,d,h}$	PV/wind generation factor for representative days.
$\bar{I}_{vr,v}$	Nominal capacity of a type v VR.
m^{cb}_{max}	Maximum number of modules that can be integrated in a capacitor bank.
$n^{wd,i}_{max}$	Maximum number of wind system units that can be installed at node i (kW).
n_{tap}	Number of positions of an OLTC.
$\mathrm{p}^{ind}_{pv} / \mathrm{p}^{cap}_{pv}$	Minimum inductive/capacitive power factor allowed in PV systems.
$\mathrm{p}^{ind}_{wd} / \mathrm{p}^{cap}_{wd}$	Minimum inductive/capacitive power factor allowed in wind systems.
$P^{pv,i}_{max}$	Maximum PV system nominal power that can be installed at node i.
$P^{+ees,i}_{t,d,h} / P^{-ees,i}_{t,d,h}$	Power delivered by EES system to the grid/ vice versa, at node i, year t, representative day d, hour h (kW).
$\hat{P}^{pr}_{t}$	Total installed power by prosumers at node i.
$\bar{P}^{ees}_{\mu}$	Nominal capacity of an EES system unit.
P^{wd}_{μ}	Nominal power of a wind system unit (kW).
Q^{cb}_{μ}	Nominal capacity of an unitary module of capacitor banks (kVAr).
soc^{ees}_{min}	Minimum charge allowed in EES systems (%).
$S^{ss,k}$	Nominal power of a type k substation (kVA).
$\pm v_R$	Regulation range of VRs (p.u.).
$\overline{V}^{i'}_{t,d,h}$	Primary voltage of substation transformers (p.u.).
$\eta^{ees}_{ch} / \eta^{ees}_{dch}$	Charging/ Discharging efficiency of EES systems.
κ	Storage duration of EES systems (h).

Parameters associated to CO_2 emissions

n_t^{cv}	Expected number of combustion vehicles to be replaced by EVs until the end of period t.
n_t^{ev}, n_0^{ev}	Expected number of EVs present at the end of planning period t/Number of EVs at the beginning of the planning horizon.
r_{co_2}	Carbon rate (\$/kg CO_2).
$\alpha\%$	Reduction of CO_2 emissions required for each planning period.
$\gamma\%$	CO_2 intensity reduction of the energy supplied by substations.
$\Gamma_{t,h}^{co_2}$	Average hourly CO_2 intensity of the energy supplied by substations in period t (kg CO_2/kWh).
$\varepsilon_{cv}^{co_2}$	Average CO_2 emission of an engine combustion vehicle (kg CO_2/km).
$\xi_{S,0}^{co_2}$	Average annual CO_2 emissions from distribution system for a period precedent to the planning (kg CO_2).
$\xi_{cv,0}^{co_2,t}$	Annual CO_2 emissions from the combustion vehicles expected to be replaced by EVs until the end of planning period t (kg CO_2).

Parameters associated to the solution technique

g_I	Maximum optimality gap allowed.
k	Iteration index.
(P^*, Q^*, V^*, I^*)	Reference operating point.
$(P^{ss,*}, Q^{ss,*})$	Reference operating point of substations.
$(P, Q, V)_k^{inc}$	Incumbent solution at iteration k.
M_1, M_2, M_3	Feasibility error coefficients.
$\varepsilon_R, \varepsilon_S$	Maximum feasibility error allowed for the relax stage/solution.
ξ_{feas}	Feasibility error (kVA).

Continuous variables

$c_t^{fcb,i}/c_t^{scb,i}$	Investment cost required for fixed/ switchable CBs.
$c_t^{wd,i}$	Investment cost required for wind systems.
$\bar{E}_t^{ees,i}, \bar{P}_t^{ess,i}$	Total energy storage capacity (kWh)/Total rated power (kW) of EES systems.
$E_t^{ees,i}, P_t^{ess,i}$	Energy storage capacity (kWh)/Rated power (kW) of EES systems installed in period t.
$E_{t,0}^{ees,i}$	Initial charge of EES systems.
$I_{t,d,h}^{i,j}$	Square of branch current.
$P_{t,d,h}^{i,j}, Q_{t,d,h}^{i,j}$	Active/Reactive power flow.
$P_{t,d,h}^{+ees,i}, P_{t,d,h}^{-ees,i}$	Power delivered/received by EES systems.
$\bar{P}_t^{pv,i}, \bar{P}_t^{wd,i}$	Total PV/wind system capacity.

$P_t^{pv,i}, P_t^{wd,i}$	PV/wind system capacity installed in period t.
$P_{t,d,h}^{pv,i}, P_{t,d,h}^{wd,i}$	Active power supplied by PV/wind systems.
$P_{t,d,h}^{ss,i'}, Q_{t,d,h}^{ss,i'}$	Active/Reactive power supplied at the primary terminals of the substation transformers.
$Q_{t,d,h}^{cb,i}$	Reactive power supply by CBs.
$Q_{t,d,h}^{svc,i}$	Reactive power supply by SVCs.
$Q_{t,d,h}^{pv,i}, Q_{t,d,h}^{wd,i}$	Reactive power supplied by PV/wind systems.
$V_{t,d,h}^{i}$	Nodal voltage squared.
$\Delta V_{t,d,h}^{i}$	Regulation of nodal voltage squared.
$\Delta_{t,d,h}^{i,j}$	Linearization control variable.
$\xi_{S,t}^{co_2}, \xi_{cv,t}^{co_2}$	Expected annual CO_2 emissions from system operation/combustion engine vehicles (kg CO_2).

Integer variables

$\bar{m}_t^{fcb,i}, \bar{m}_t^{scb,i}$	Number of modules of the fixed/switchable CB allocated at node i.
$m_{t,d,h}^{scb,i}$	Number of active modules of the switchable CB allocated at node i.
$n_t^{ees,i}$	Number of EES system units installed at node i.
$n_t^{wd,i}$	Number of wind turbines installed at node i.
$tap_{t,d,h}^{i}$	Tap position of the OLTC installed at node i.

Binary variables

$x_t^{a,i,j}, z_t^{e,i,j}$	State variable that indicates if the conductor/structure of line (i,j) have been replaced by one of type *a*/*e*.
$x_t^{fcb,i}, x_t^{scb,i}$	Decision variable for fixed/switchable CB installation.
$x_t^{oltc,i}, x_t^{ss,u,i}$	Decision variable for OLTC/type u substation installation.
$x_t^{svc,i}$	Decision variable for SVC installation.
$x_t^{wd,i}$	Decision variable for wind system installation.
$\varkappa_t^{v,i,j}$	Decision variable for VR installation.
$\varkappa_t^{i,j}$	State variable that indicates that a VR has been installed.

Random variables

$\tilde{\mathrm{f}}_{d,h}^{pv}, \tilde{\mathrm{f}}_{d,h}^{wd}$	PV/Wind generation factor.
$\tilde{h}_v^{in}, \tilde{h}_v^{fi}$	Charging start time/end time.
$\tilde{n}_{t,y}^{ev,i}$	Number of EVs.
$\tilde{P}_{t,y,d,h}^{cd,i}, \tilde{Q}_{t,y,d,h}^{cd,i}$	Active/Reactive conventional demand (kW/kVAr).
$\tilde{P}_{t,y,d,h}^{ev,i}, \tilde{Q}_{t,y,d,h}^{ev,i}$	Active/Reactive EV load (kW/kVAr).
$\tilde{P}_{t,y,d,h}^{pr,i}, \tilde{Q}_{t,y,d,h}^{pr,i}$	Active/Reactive power generated by prosumers (kW/kVAr).
$s\tilde{o}c_d^{in}, s\tilde{o}c_d^{fi}$	EV battery SOC at the charging start/at the end of charging .

$\tilde{x}_d$	EV charging decision.
$\tilde{z}^{s,i,h}_{cd,p}, \tilde{z}^{s,i,h}_{cd,q}$	Short-term uncertainty related to hourly active/reactive demand.
$\tilde{z}^{\ell,t}_{cd}$	Long-term uncertainty related to demand growth.
$\tilde{z}_{ev}$	Uncertainty related to the date of maximum EV penetration.
$\Delta\tilde{h}_d$	Charging duration (h).
$\tilde{\tau}^{ev,i}, \tilde{\tau}^{pr,i}$	EV/Prosumer peak penetration date (years).

Operators and symbols

$\mathbb{E}(x)$	Expected value of the random variable x.
$\lfloor n \rceil$	Rounding of n to the nearest integer.
$\langle s \rangle$	Logical value (0,1) of statement s.
∂	Customized metric used in K-means.
$:=$	Equal by definition.
$\|x\|^*$	Euclidean norm column by column of matrix x.
$[x]_{\Omega_1,..\Omega_n}$	Array indexed by the ordered sets $\Omega_1,..\Omega_n$.

CONTENTS

1	**INTRODUCTION**	**20**
1.1	LITERATURE REVIEW	23
1.2	OBJECTIVES	26
1.3	CONTRIBUTIONS	27
1.4	DOCUMENT STRUCTURE	28
2	**SYSTEM OPERATING PARAMETERS UNDER UNCERTAINTIES**	**30**
2.1	CONVENTIONAL DEMAND	30
2.2	ELECTRICAL VEHICLE LOADS	31
2.2.1	EV quantity by charging level	31
2.2.2	Charging habits of EV owners	32
2.2.3	Methodology	34
2.3	DISTRIBUTED GENERATION MODELING	35
2.3.1	Energy production	36
2.3.2	Prosumer participation	37
2.4	GENERATION OF SYSTEM OPERATING SCENARIOS	37
3	**PROBLEM FORMULATION**	**40**
3.1	DETERMINATION OF ROSs	40
3.1.1	Robust ROSs	40
3.2	OBJECTIVE FUNCTION	43
3.3	CONSTRAINTS	45
3.3.1	Kirchhoff's first law	45
3.3.2	Kirchhoff's second law	46
3.3.3	Power, voltage and current relationship	46
3.3.4	Substation operation	46
3.3.5	Installation and operating limits of DG systems	47
3.3.6	Voltage and current limits	48
3.3.7	Reconductoring constraints	49
3.3.8	Reactive compensation modeling	50
3.3.9	VR modeling	51
3.3.10	EES system constraints	51
3.3.11	Reduction of CO_2 emissions	52
4	**SOLUTION TECHNIQUE**	**54**

4.1 MATHEMATICAL JUSTIFICATION 54
4.2 METHODOLOGY 56
4.2.1 Relaxed stage 56
4.2.2 Integral stage 57
4.2.3 Feasibility fix stage 57
4.2.4 Error coefficient update 58

5 CASE STUDY AND RESULTS 60
5.1 TEST SYSTEMS 60
5.2 PLANNING DATA 61
5.3 SIMULATION OF THE OPERATING CONDITIONS 64
5.4 RESULTS 65
5.4.1 Solution overview 68
5.4.2 Investment plans 69
5.4.3 Network operation analysis 72
5.4.4 Performance of the proposed model and solution technique 73
5.4.5 Planning reliability assessment 75
5.4.6 Solution overview for the real 135-node distribution system 77

6 CONCLUSIONS AND FUTURE WORKS 79
6.1 CONCLUSIONS 79
6.2 FUTURE WORKS 80

BIBLIOGRAPHY 81

APPENDIX A - Expected quantity of EVs 86

APPENDIX B - Scientific Production 87

ANNEX A - Test System of 69 Nodes 88

ANNEX B - Real System of 135 Nodes 91

ANNEX C - Energy prices and CO_2 intensity 96

ANNEX D - Investment and O&M costs related to planning actions 98

1 INTRODUCTION

The operation of distribution systems is facing significant changes due to the increasing participation of Distributed Energy Resources (DERs), as DG and EES systems (owned by prosumers, independent agents or Distribution Companies (DISCOs)), and the increasing adoption of EVs. These changes include the presence of bidirectional power flows, increased demand variability (usually translated into duck curves) and increased operating uncertainty. In this context, the traditional distribution systems are turning into active distribution systems for both taking advantage of the DER capabilities and dealing with their adverse effects. Here, note that active distribution systems are those that include in their infrastructure systems capable of controlling their distributed energy resources (ADAMO *et al.*, 2011), and also other system assets, as OLTCs, CBs, SVCs and VRs. On the one hand, this feature allows the system to be operated more flexibly and efficiently and it points to investment plans that lead to cheaper distribution and energy costs compared with that for traditional systems. On the other hand, determining the optimal investment plan becomes a more challenging task, since more variables are involved in the planing problem while uncertain operating conditions need to be handled.

Planning actions, typically, have involved the allocation of capacitor banks for reactive compensation (SUNDHARARAJAN; PAHWA, 1994), the installation of voltage regulators at critical points of the network for voltage regulation (SAFIGIANNI; SALIS, 2000), and reconductoring to upgrade the power capacity of selected lines while reducing both power losses and voltage drops (FRANCO *et al.*, 2013). Subsequently, with the emergence and adoption of DG, the planning problem shifted its focus to the optimal allocation and sizing of DG systems within the grid (GEORGILAKIS; HATZIARGYRIOU, 2013), as well as to an integrated planning, considering also the typical planning actions previously mentioned (SHAHEEN; EL-SEHIEMY, 2021). The participation of prosumers has been studied in the field of smart grids with the aim of managing DG systems units and other DERs owned by prosumers (normally through an agregator) to reduce their electricity bills while improving system operational flexibility (HU *et al.*, 2021). However, prosumer participation has not been yet considered in the context of distribution system planning. Since prosumers are increasing rapidly to levels capable to affect the normal system operation, their participation is considered in this work.

Regarding system planning objectives, traditionally they consisted of minimizing investment and operating costs as well as improving efficiency and reliability (VAHIDINASAB; MEMBER; TABARZADI, 2020). In recent years, due to the urgent need to reduce the global warming and promoted by Kyoto Protocol (1997) and Paris Agreement (2015), reducing CO_2 emission has become a novel and significant objective of the planning problem (ZENG *et al.*, 2014). This has led to several actions, such as, increased participation of renewable DG (mainly PV and wind) (MELGAR-DOMINGUEZ; POURAKBARI-KASMAEI; MANTOVANI, 2019); the development and application of emission abatement polices, such as cap and trade, and carbon taxes (POURAKBARI-KASMAEI *et al.*, 2020); the modeling and integration of EVs into the distribution network (SHA; FOTUHI-FIRUZABAD, 2013); and a greater interest in determining and increasing renewable DG hosting capacity (CAPITANESCU *et al.*, 2015). About the last point, note that the integration of EES systems into the grid stands out as a plausible solution, which also improves the flexibility and reliability of system operation (JAYASEKARA *et al.*, 2016).

The distribution planning, in short, involves currently the following planning actions: construction or upgrade of substations, installation of OLTCs to regulate the substations voltages, allocation of fixed and switchable CBs as well as SVCs for reactive compensation, installation of voltage regulators at critical points of the network, reconductoring to upgrade the power capacity of selected lines while reducing both power losses and voltage drops, allocation and sizing of DG systems and installation of EES systems to increase the DG hosting capacity while improving system flexibility (XIE *et al.*, 2018; MELGAR-DOMINGUEZ; POURAKBARI-KASMAEI; MANTOVANI, 2019; MEJIA *et al.*, 2022). In order to obtain the optimal investment plan, ideally, all the available planning actions should be considered in the problem modeling, however, since this involves a high computational burden for the traditional solution approaches, it has not yet been addressed in the existing literature. Thus, the present work aims to cover this gap.

Currently, to address the planning problem, three different techniques can be used: Mathematical programming, metaheuristics and matheuristics (BOSCHETTI; MANIEZZO, 2022). In general, the planning problem can be accurately formulated as a non-convex Mixed Integer Non-Linear Programming (MINLP) model, but this model correspond to a NP-hard problem, even undecidable for some cases, and extremely difficult and computationally expensive to solve in practice (BELOTTI *et al.*, 2013). Thus, to get around these issues, the mathematical programming approaches use convex relaxations or approximations to model the problem. Hence, conic relaxation and Piece-Wise Linearization (PWL) are widely used, leading to Mixed Integer Second Order Cone Programming (MISOCP) and Mixed Integer Linear Programming (MILP) models, respectively (HAGHIGHAT; ZENG, 2018; TABARES *et al.*, 2016). The main feature of these techniques is their ability to obtain the global optimum of their models. However, they can not guarantee that their solutions are feasible for the original planning problem. Additionally, these techniques are usually too computationally expensive (and sometimes not suitable) for large-scale problems. On the other hand, metaheuristics are a good option to provide feasible solutions in relative short times, what makes them appropriate for large problems (ARASTEH *et al.*, 2016); but they neither recognize global optimality nor provide a measure to indicate the proximity to the optimal solution of the problem. Finally, matheuristic is a relative new term that refers to heuristic algorithms based on mathematical programming. Generally, this technique solves a series of sub-problems formulated according to a given metaheuristic via mathematical programming (BOSCHETTI; MANIEZZO, 2022; HOME-ORTIZ *et al.*, 2020). Matheuristics are supposed to be computationally less expensive than mathematical programming and has the advantage over metaheuristics that it can guarantee the optimality of the addressed sub-problems, thus, the obtained solution is likely to be a high-quality local optimal. Hence, in order to attain feasible and high-quality solutions in a reasonable computational time, the present work proposes a novel solution technique based on a matheuristic approach.

Distribution system planning aims at allowing safe and sustainable operation of the system under different operating conditions at minimum cost. Compared with traditional network operation, the variability of the operating conditions of modern distribution systems has increased significantly mainly due to the increasing penetration of prosumers and EVs. Thus, the variability and uncertainty from PV generation (prosumers) and EV loads are more and more noticeable in the load profiles. Additionally, medium and large renewable DG systems owned by independent agents or DISCO makes the operation system dependent to some degree of the energy resources variations (solar irradiation and wind). In this context, the modeling of the variation and uncertainty from demand (conventional and EVs) and renewable energy resources are of special interest for the planning of modern distribution networks, and even more if the planning is long-term because it adds forecast uncertainty to the modeling. In order to address the planning problem considering the variable and uncertain operation of the system, optimization-under-uncertainty methods are used in the literature (ROALD *et al.*, 2023). Due to the large quantity of random variables involved in the system operation and the large-scale nature of the planning problem, this work use the two-stage stochastic optimization method on a finite set of representative scenarios.

The random variables associated to system operation are of continues type, therefore, the number of their realizations is infinite. Thus, in order to get a solvable model in the context of scenario-based two-stage stochastic optimization, a finite set of representative realizations is required (ROALD *et al.*, 2023). From this point it follows that the quality of the solution is strongly related to the selection of that representative realizations (scenarios). In this way, there is no use finding the global optimal of a problem based on no-representative scenarios. Therefore, the data analysis and selection is as important as the formulation and solution technique of the planning problem. The two-stage stochastic optimization method is widely used in distribution system planning, but most of the works from literature only consider the historical data and their expected forecasts leaving aside the associated uncertainty (EHSAN; YANG, 2020a; XIE *et al.*, 2018; LIMA *et al.*, 2022; MEJIA *et al.*, 2022), which can lead to get representative scenarios that do not really represent all (of most of) the possible realizations of uncertainties. The impact of this fact can be visualized with a simple example: consider that two different instances of a variable are represented by normally random variables, e.g., $n_{t_1} \sim \mathcal{N}(4,4)$ and $n_{t_2} \sim \mathcal{N}(7,9)$. If K-means clustering with $K = 2$ is performed over those variable instances, the obtained representative values are 3.56 and 8.48. In contrast, if the random nature of the variables is ignored the result will correspond to their expected values (4 and 7), losing data variability, which is an important feature for planning purposes. Thus, this work models in detail the uncertainty from operating parameters and obtains the representative scenarios on a large set of realizations of that uncertainty.

In this work, a novel multistage planning model for active distribution systems under uncertainty is proposed. The work addresses properly the operating uncertainty and proposes a customized K-means clustering especially designed for planning purposes (in the context of scenario-based two-stage stochastic programming). Also, a post-planning stage to address and measure the planning reliability is proposed. Additionally, this work considers important practical planning and operating aspects not addressed before in the existing literature (to the best of the author's knowledge), such as the elapsed life of the existing system assets (as substations, conductors and supports), the increasing penetration of both prosumers and EVs and the losses in substation transformers.

1.1 LITERATURE REVIEW

Developing an optimal planning for distribution systems is of utmost interest to all involved agents, such as consumers, DISCOs and society. This is because a proper planning results in reduced investments and operational costs, leading to lower electricity rates, as well as in improved energy efficiency and reduced greenhouse gas emissions. Therefore, the distribution system planning problem is an important topic in both industry and academia, and it has been widely discussed in the specialized literature considering different approaches in terms of mathematical models, objectives and solution techniques. Thus, relevant works about distribution system planning are discussed below, with focus on those related to multistage planning for active distribution systems under uncertainty.

Pereira, Cossi and Mantovani (2013) propose a multi-objective short-term model for the planning of electric power distribution systems. The model corresponds to a MINLP model and it is solved through the metaheuristic Non-Dominated Sorting Genetic Algorithm (NSGA-II). The problem objective is minimize the investment and operating costs as well as the voltage magnitude deviations in the network buses. For that, the installation of CBs, VRs and reconductoring are considered as planning actions. This work shows that nonlinearities from the objective and constraints of the model can be successfully handle through metaheuristics to obtain feasible solutions. However, it can not be informed how close is the solution from the global optimal.

Tabares *et al.* (2016) propose a multistage long-term expansion planning of electrical distribution systems considering multiple planning actions. The planning problem is modeled as a MILP model based on PWL technique. The planning actions include increasing the capacity of existing substations, constructing new substations, allocating capacitor banks, voltage regulators, DG systems , constructing or reinforcing circuits, and modifying the system topology. The work presents six case studies that include, independently and then jointly, the participation of CBs, VRs and DGs. However, the variation and uncertainty from the operating parameters within each planning period are not considered.

Xie *et al.* (2018) propose a multi-objective and scenario-based stochastic programming model. The model uses uncertain random network theory in order to take into account the uncertainty associated with the reliability and stability of distribution lines. For the operating parameters, demand and renewable-based energy resources, the uncertainty is modeled through representative scenarios obtained as the combinations of individual representative values of each parameter. Thus, the temporal correlation among the operating parameters is not preserved. The model includes the installation of OLTCs for voltage regulation in substations and SVCs for reactive power compensation. The model is formulated using a conic relaxation as a MISOCP model. Then, the accuracy of the results regarding the original MINLP model is evaluated. It is shown that, due to the negligible errors obtained in the conic relaxation for the employed test system, the solution found with the MISOCP model corresponds to the solution of the original MINLP model, corresponding therefore to the global optimal. Thus, the MISOCP can led to global optimality occasionally, but in fact, this is unusual in the context of modern distribution system planning.

Arias *et al.* (2018) propose a chance-constraint MILP model for the expansion planning that guarantees that substations do not operate above their nominal capacity within a specified confidence level. For that, the uncertainties from conventional and EV demand are considered and modeled as normally distributed variables. The MILP model is obtained through the PWL of the squares of the active and reactive powers present in the operating constraints. Also, the model considers the increasing penetration of EVs and the installation of Electric Vehicle Charging Stations (EVCSs) over the planning horizon. However, the participation of prosumers is not considered. Finally, the compliance of the preset confidence level is verified through Monte Carlo simulations.

Melgar-Dominguez, Pourakbari-Kasmaei and Mantovani (2019) present a two-stage robust optimization model for the short-term planning. The system parameters are modeled using a representative day for each season, which allows to model properly the EES transition, but since it does not take into account the correlation among the operating parameters, the obtained representativeness is not necessarily the best. The uncertainties of demand and renewable power output factors are modeled through uncertainty intervals built based on normal probability distributions within a confidence level of 95%. The two-stage robust model is formulated as a bilevel optimization model that then is recast to a single-level MILP model through Karush-Kuhn-Tucker (KKT) optimality conditions. Since the joint use of PWL and KKT conditions is not appropriate for optimality, a linearization based on Taylor series is proposed. Finally, the problem is solved applying the Column-and-Constraint Generation (C&CG) algorithm.

Home-Ortiz *et al.* (2020) propose a matheuristic approach based on a Mixed Integer Conic Programming (MICP) model to address the expansion planning. The proposal shows that a matheuristic approach can perform better than solving the original MICP problem via mathematical programming. However, it is worth indicating that since the model is based on a conic relaxation, the feasibility of the original MINLP planning problem is not guaranteed. To handle the uncertainties, the model is formulated as a scenario-based two-stage stochastic programming model and the uncertainties from demand, solar irradiation and wind speed are addressed trough representative scenarios obtained via k-means clustering on historical data. The matheuristic approach used to solve the problem consist of the joint application of MICP and the philosophy of the meta-heuristic Variable Neighborhood Descent (VND).

Ehsan and Yang (2020a), Ehsan and Yang (2020b) propose a scenario-based stochastic model formulated as a MILP model for the multistage joint reinforcement planning of distribution systems and EVCSs. The work uses a Markov-based approach to model the EV charging demand and the Heuristic Moment Matching (HMM) method to generate representative scenarios based on historical data of wind and PV generation, conventional demand and expected EV demand. The HMM method aims at preserving the first four stochastic moments of historical scenarios, i.e., expectation, standard deviation, skewness and kurtosis. Thus, reliable representative scenarios regarding the historical data are expected to be obtained. However, since uncertainties are not considered, some information could be missing. Additionally, the work evaluates the expansion planning solution in terms of failure rate of substation capacities through Monte Carlo simulations.

Lima *et al.* (2022) present a scenario-based stochastic MILP model for the long-term expansion planning. This work proposes a method to estimate and generate EV load profiles for one year range. Representative scenarios are obtain through the application of k-means clustering on historical data of demand, solar irradiation and wind speed, in addition to the EV load profiles previously generated. The model considers the installation of EES systems as planning action. Since their current prices do not favor their participation on the investment plans, a sensitivity analysis for different EES system prices is performed in order to investigate the instances in which installing EES systems will be required (being the best option). The reactive power is supplied only by substations and DG systems. Thus, reactive compensation equipment are not considered. Additionally, in this work is stated that the investment plans obtained by the proposed MILP model are the same of those obtained by solving the original MINLP problem (possibly by a non-linear solver).

Mejia *et al.* (2022) propose a scenario-based stochastic MILP model to address the multistage planning of active distribution systems. The model includes EVCS installation, several planning actions and voltage-dependent load behavior. The EV charging demand is estimated by zones based on real travel patterns and assumptions about when and where EVs should be charged. The work considers five uncertain parameters: demand, wind speed, solar irradiation, energy prices, and EVCS loads. Representative scenarios are obtained from historical data. This data is classified in sub-groups by season and day/night, then the algorithm k-means++ is applied to each sub-group. The model assumes that there is an environmental policy that penalizes excess of CO_2 emissions from the distribution system. Thus, CO_2 emission limits are imposed in order to prevent penalties for excess emissions. However, the CO_2 emission reduction from EV adoption (through the replacement of combustion vehicles) is not considered.

Finally, it is worth indicating that important aspects about the planning and operation of distribution systems have not yet been addressed in the existing literature, such as the elapsed life of the existing system assets (as substations, conductors and supports), the mechanical correlation between conductors and supports and the losses of substation transformers. Also, the increasing penetration of prosumers has not been considered in the long-term planning. Another important point is that the works that use scenario-based two-stage stochastic programming only take into account expected values of the operating parameters, overlooking their associated short-term and long-term uncertainty. Additionally, about the solution approaches used to solve the planning problem, it is observed that most of the existing works do not take care of guaranteeing the feasibility of solution regarding the original MINLP problem, which can lead to pseudo-solutions with significant errors as shown in (MARCELO *et al.*, 2023).

1.2 OBJECTIVES

The main goal of this work is obtaining a realistic planning model for active distribution systems in order to determine the investment plan to be executed in the short-term (knowing the possible future operating scenarios) and anticipate the future investment actions and the network operation to prevent possible issues or improve certain operating or policy aspects. Aiming to fulfill this goal the following objectives are established.

- Propose a multistage planning model for active distribution systems considering the operating uncertainty.

- Propose a solution technique to solve the planning problem aiming to obtain the global optimal solution or high-quality local solutions guaranteeing the feasibility regarding the original problem (non-linear and non-convex). This solution technique must solve the planning problem in adequate computational times for practical purposes and must perform well for large problems involving a high number of discrete variables.
- Model the operating uncertainty in a proper and detail way in such a manner that it allows generating realistic operating scenarios as the realizations of that uncertainties.
- Include important and realistic aspects about the planning and operation of distribution systems in the optimization model in order to represent the system as realistically as possible and convenient.
- Assess the reliability of the obtain investment plans in order to verify or, if necessary, modify the investment decisions.

1.3 CONTRIBUTIONS

The main contributions of this work are summarized as follows. Additionally, the novelties of this work regarding the state of the art are presented in Tables 1 and 2.

- A new scenario-based two-stage stochastic model for the multistage planning of active distribution systems under uncertainty is proposed. The model considers the data uncertainty and not only their expected forecast values as done in previous related works. This leads to investment plans that better withstand uncertainty.
- A novel solution technique for the planning problem is proposed, which can obtain high-quality local optimal solutions in relative short times guaranteeing its feasibility regarding the original non-convex MINLP planning problem. The application of this technique allows to solve the planning problem considering a large portfolio of planning actions and several scenarios over a broad planning horizon.
- A detailed modeling of the operating parameters under uncertainty is proposed. The modeling includes short-term uncertainties related to the realization of a random variable in a given time and long-term uncertainties related to the growth forecast of conventional demand, prosumers and EVs over the planning horizon.
- The planning modeling considers the elapsed life of existing assets in decision making, which in practice is a determining factor to decide the optimal timing of assets replacement or installation. To the best of the author's knowledge this topic is addressed for the first time in the existing literature.

Table 1 – Comparison of this work with the state of art - part 1

Reference	System modeling					Solution technique						
							Solution quality[1]					
	Assets elapsed life	Prosumers	EVs	EES temporal transition	CO_2 reduction	Approach	Global optimum	Local optimum	Approximate solution	Lower bound	Upper bound	Feasible
Pereira, Cossi and Mantovani (2013)	✗	✗	✗	✗	✗	Metaheuristic (NSGA-II)	✗	✗	✗	✗	✓	✓
Tabares et al. (2016)	✗	✗	✗	✗	✗	MP (MILP)	✗	✗	✓	✗	✗	✗
Xie et al. (2018)	✗	✗	✗	✗	✗	MP (MISOCP[2])	✗	✗	✓	✓	✗	✗
Arias et al. (2018)	✗	✗	✓	✗	✗	MP (MILP)	✗	✗	✓	✗	✗	✗
Melgar-Dominguez, Pourakbari-Kasmaei and Mantovani (2019)	✗	✗	✗	✓	✗	MP (C&CG MILP)	✗	✗	✓	✗	✗	✗
Home-Ortiz et al. (2020)	✗	✗	✗	✗	✓	MP (MICP)	✗	✗	✓	✗	✗	✗
Ehsan and Yang (2020a) Ehsan e Yang (2020b)	✗	✗	✓	✗	✗	MP (MILP)	✗	✗	✓	✗	✗	✗
Lima et al. (2022)	✗	✗	✓	✗	✓	MP (MILP)	✗	✗	✓	✗	✗	✗
Mejia et al. (2022)	✗	✗	✓	✗	✓	MP (MILP)	✗	✗	✓	✗	✗	✗
This work	✓	✓	✓	✓	✓	Matheuristic (MIQP)	✗	✓	✗	✗	✓	✓

[1] regarding the original non-convex MINLP planning model, [2] occasionally can attain global optimality, but it can not recognize or prove it by itself
MP: Mathematical Programming, ✓: considered, ✗: not considered

Source: Elaborated by the author.

- A new methodology to estimate and generate EV load profiles is proposed, considering different charging levels and preferences about charging schedules.
- The impact of using different representative scenarios on planning reliability is analyzed. Also, it is proposed a new method to determine representative scenarios that aim to improve the planning reliability.

1.4 DOCUMENT STRUCTURE

This work, in addition to its introductory chapter, is organized as follows:

In Chapter 2, the system operating parameters are modeled under uncertainty. This includes the modeling of conventional demand, EV loads and DG systems (including prosumers). Then, the integration of these parameters is done while presenting the generation of system operating scenarios.

In Chapter 3, the formulation for the planning problem is proposed. At first, the use of ROSs is addressed and a new method to determine them (in order to improve the planning reliability) is proposed. Then, the objective function and the constraints of optimization model (corresponding to the planning problem) are presented and justified.

Table 2 – Comparison of this work with the state of art - part 2

Reference	Planning features										
	Uncertainty approach	Planning actions									Planning reliability assessment
		Substation update	OLTC	Re-conductoring	CBs		SVC	VR	DG	EES	
					Fixed	Switchable					
Pereira, Cossi and Mantovani (2013)	Deterministic	×	×	✓	✓	✓	×	✓	×	×	×
Tabares et al. (2016)	Deterministic	✓	×	✓	×	✓	×	✓	✓	×	×
Xie et al. (2018)	Scenario-based stochastic	✓	✓	✓	×	×	✓	×	✓	×	×
Arias et al. (2018)	Chance constraint	✓	×	✓	✓	×	×	×	✓	×	✓
Melgar-Dominguez, Pourakbari-Kasmaei and Mantovani (2019)	Two-stage Robust	×	×	✓	✓	✓	×	✓	✓	✓	✓
Home-Ortiz et al. (2020)	Scenario-based stochastic	✓	×	✓	×	×	×	×	✓	✓	✓
Ehsan and Yang (2020a) Ehsan e Yang (2020b)	Scenario-based stochastic	✓	×	✓	✓	×	×	×	✓	×	✓
Lima et al. (2022)	Scenario-based stochastic	✓	×	✓	×	×	×	×	✓	✓	×
Mejia et al. (2022)	Scenario-based stochastic	×	×	✓	✓	×	×	✓	✓	✓	×
This work	Scenario-based stochastic	✓	✓	✓	✓	✓	✓	✓	✓	✓	✓

✓: considered, ×: not considered

Source: Elaborated by the author.

In Chapter 4, the proposed solution technique is described. The mathematical justification is presented first and then the proposed methodology is described in detail.

In Chapter 5, the case studies are presented and numerical results are analyzed and discussed. Also, key information about planning data is presented and the planning reliability is addressed and measured.

Finally, in Chapter 6, the conclusions are drawn and related future works are suggested.

2 SYSTEM OPERATING PARAMETERS UNDER UNCERTAINTIES

Distribution systems must be prepared to operate efficiently in different conditions along time in response to the variation of operating parameters, such as conventional demand, EV charging and DG system production. This is not an easy task to accomplish due to the significant variability and uncertainty associated to these parameters. Thus, a proper modeling and integration of them in the planning problem is required in order to obtain a reliable system planning. To model conventional demand both long-term and short-term uncertainty are considered (VELLOSO; POZO; STREET, 2020). Short-term uncertainty is related to the uncertainty that exists just before the event happens (the event can correspond to a certain time or a very short period). Long-term uncertainty refers to the uncertainty associated to the forecast process of a future event (usually with a long-term scope). Thus, to model the growth of EVs and prosumers along the planning horizon long-term uncertainties are considered, while for PV and wind generation only short-term uncertainty is required (divided in hourly and daily uncertainty). Additionally, EV load modeling includes several random parameters associated to charging decision, charging start time and the SOC at the charging start.

2.1 CONVENTIONAL DEMAND

This type of demand corresponds to the electrical energy demanded by residential, commercial and industrial consumers, with exception of EV charging. Note that conventional demand generally grows linearly year after year. Also, their intra-day profiles have not face significant shape changes during the last decade and they are not expected to do so significantly in the future (OPERADOR NACIONAL DO SISTEMA ELÉTRICO – ONS, 2023). Thus, historical data offer valuable information to estimate the expected values of conventional demand along the planning horizon, which will serve as a basis for its modeling under uncertainty.

The expected growth rates $\varsigma^{p,i}, \varsigma^{q,i}$ are obtained through linear regression of historical demand data. Notice that these growth rates are determined in relation to the current calculated demand, i.e., the demand corresponding to year 0 in the regression line, which not necessarily correspond to the actual current demand. Long-term and short-term uncertainties are represented by normally distributed variables $\tilde{z}_{cd}^{\ell,t}$ and $\tilde{z}_{cd,p}^{s,i,h}, \tilde{z}_{cd,q}^{s,i,h}$, respectively. Then, $\tilde{z}_{cd}^{\ell,t}$ is applied to the expected growth rate every planning period and $\tilde{z}_{cd,p}^{s,i,h}, \tilde{z}_{cd,q}^{s,i,h}$ are applied every hour, after the realization of the long-term uncertainty. Note that long-term uncertainty affects both the active and reactive power of all nodes while short-term uncertainty is independent for each. Also, since forecast uncertainty increases over time, $\tilde{z}_{cd}^{\ell,t}$ is modeled in such a way that its standard deviation

Figure 1 – Application of long-term and short-term uncertainties

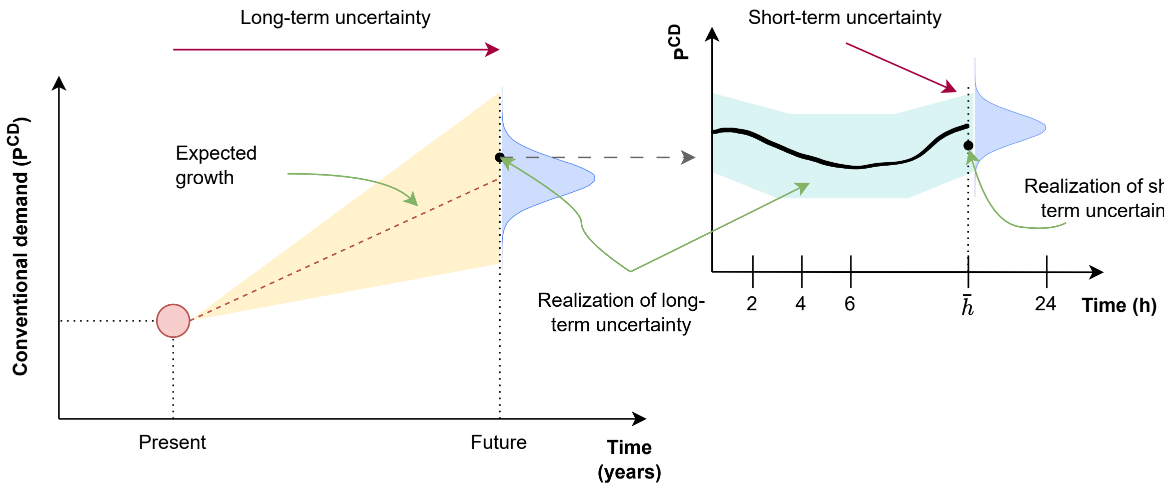

Source: Elaborated by the author.

increases every planning period. Finally, active and reactive nodal demand are modeled through (2.1)–(2.2), respectively.

$$\tilde{P}^{cd,i}_{t,y,d,h}(\tilde{z}^{s,i,h}_{cd,p}, \tilde{z}^{\ell,t}_{cd}) = \tilde{z}^{s,i,h}_{cd,p}\left[1 + (n_{t,y} + \tilde{z}^{\ell,t}_{cd})\varsigma^{p,i}\right] P^{cd,i}_{0,d,h}, \quad (2.1)$$
$$\forall (t \in \Omega_T, y \in \Omega_Y, i \in \Omega_{\bar{N}}, d \in \Omega_D, h \in \Omega_H)$$

$$\tilde{Q}^{cd,i}_{t,y,d,h}(\tilde{z}^{s,i,h}_{cd,q}, \tilde{z}^{\ell,t}_{cd}) = \tilde{z}^{s,i,h}_{cd,q}\left[1 + (n_{t,y} + \tilde{z}^{\ell,t}_{cd})\varsigma^{q,i}\right] Q^{cd,i}_{0,d,h}, \quad (2.2)$$
$$\forall (t \in \Omega_T, y \in \Omega_Y, i \in \Omega_{\bar{N}}, d \in \Omega_D, h \in \Omega_H)$$

$$n_{t,y} = (t-1)n_Y + y, \forall (t \in \Omega_T, y \in \Omega_Y) \quad (2.3)$$

The application of long-term and short-term uncertainties to conventional demand can be visualized in Fig. 1.

2.2 ELECTRICAL VEHICLE LOADS

EV loads are modeled considering EV penetration growth, available charging levels and charging habits of EV owners.

2.2.1 EV quantity by charging level

The number of EVs is estimated considering that EV penetration follows a S-shape growth curve (2.4). Here, notice that S-curves are suitable for modeling technology diffusion, particularly EV adoption (FLUCHS, 2020). This S-shape curve is built as a sigmoid function δ_{ev}^{i} that passes through the points corresponding to EV appearance, current and maximum penetration. Note that EV appearance date and the current EV penetration are assumed to be known while the maximum penetration date is uncertain. Therefore, the maximum penetration date is represented by the normally distributed random variable $\tilde{\tau}_{ev}^{i}$, defined as $\tilde{\tau}_{ev}^{i} = \tau_{ev}^{i} + \tilde{z}_{ev}$. Also, the growth of vehicles is considered through the annual growth rate $\varsigma^{v,i}$.

$$\tilde{n}_{t,y}^{ev,i}(\tilde{\tau}_{ev}^{i}) = \lfloor \delta_{ev}^{i}(t,y,\tilde{\tau}_{ev}^{i})(1+n_{t,y}\varsigma^{v,i})N_0^{v,i} \rceil, \tag{2.4}$$

Charging powers are classified into three levels based on SAE J1772 standard (AL-HANAHI *et al.*, 2021). However, the nominal charging powers may vary according to regulatory jurisdiction. Thus, the capacities adopted in this work aim at using representative or typical values considering the lower voltage in the range of 120–230V. They are established as follows.

- Charging level 1: Corresponding to charging at residential level. It has a charging power of 2.2kW.
- Charging level 2: Installed mainly in private or commercial facilities. It has a charging power of 12.2kW.
- Charging level 3: Supplied by EV charging stations. It corresponds to fast charging and has a power of 50kW.

Then, the quantity of EVs at each node using each charging level is estimated considering the accessibility and preferences of EV owners about charging level and charging location (2.5). Note that only knowledge of charging level preference is required to estimate the quantity of EVs with charging level 1 (residential), while for charging levels 2 and 3 is necessary to know also the charging location preference (possibly in the way home - work).

$$\tilde{n}_{t,y}^{ev,v,i}(\tilde{\tau}_{ev}^{i}) = \begin{cases} \lfloor \alpha_{t,v}^{ev} \tilde{n}_{t,y}^{ev,i}(\tilde{\tau}_{ev}^{i}) \rceil, & v = 1 \\ \lfloor \phi_{t,v}^{ev,i} \sum\limits_{i \in \Omega_{\bar{N}}} \tilde{n}_{t,y}^{ev,i}(\tilde{\tau}_{ev}^{i}) \rceil, & v \in \{2,3\} \end{cases} \tag{2.5}$$
$$\forall (t \in \Omega_T, y \in \Omega_Y, i \in \Omega_{\bar{N}}, v \in \Omega_V)$$

2.2.2 Charging habits of EV owners

The charging habits of EV owners are defined mainly by the following parameters: charging decision, charging start time and charging duration. Both charging decision and charging duration depend on the SOC at the charging start. Charging decision is determined considering the probability function presented in Fig. 2(a), where charging is considered mandatory when

Figure 2 – (a) Probability function of charging decision. (b) PDF of SOC at the end of charging

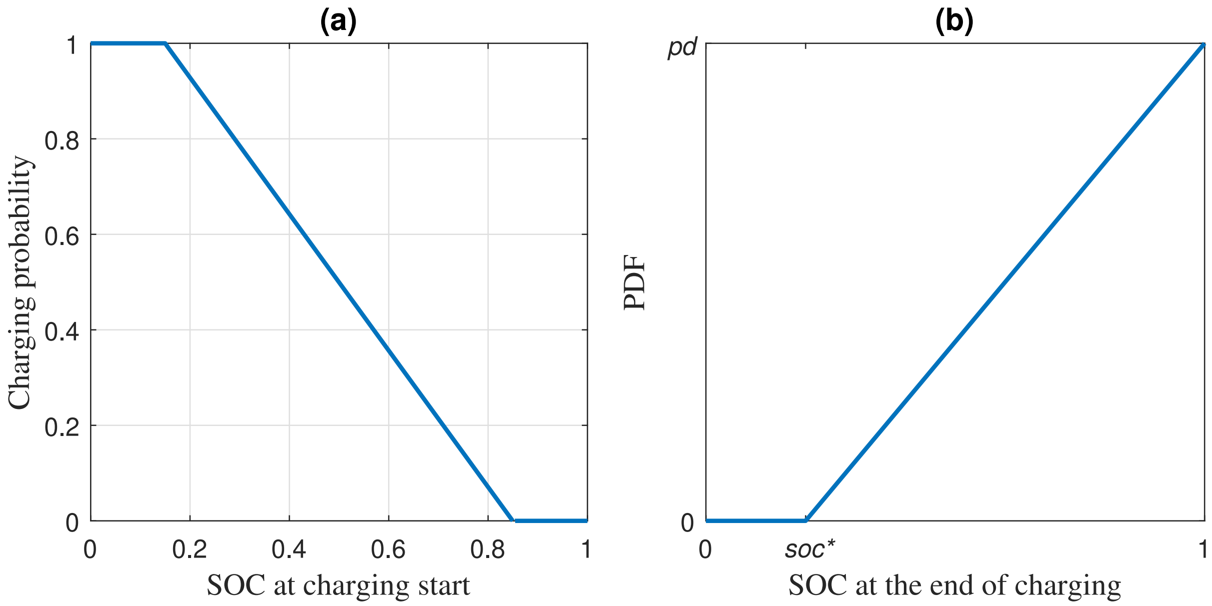

Source: Elaborated by the author.

SOC is lower than 15% and unnecessary when SOC is greater than 85%. On the other hand, charging duration is modeled as a function of charging decision and the SOCs at the start and end of charging (2.6). The SOC at the end of charging is determined through the Probability Density Function (PDF) presented in Fig. 2(b), where $soc^* = \max\{soc_{min}, s\tilde{o}c_d^{in}\}$ and $pd = 2/(1-soc^*)$. This function considers that it is most likely to charge the EV battery until it reaches 100% charge, while it is less likely to be charged and unplugged shortly after. The SOC at the charging start of some day is equal to the analogous SOC of the previous day, plus energy supplied during charging, minus energy spent on daily trip (only a charging per day is assumed) (2.7). Here it is important indicating that since SOC at charging start depends of its previous day value, its PDF is not expected to be uniform; therefore, Monte Carlo simulations are carried out and their results are displayed in Fig. 3(a).

$$\Delta\tilde{h}_d(\tilde{x}_d, s\tilde{o}c_d^{in}, s\tilde{o}c_d^{fi}) = \tilde{x}_d \frac{C_b(s\tilde{o}c_d^{fi} - s\tilde{o}c_d^{in})}{\eta_{ev} p_v} \tag{2.6}$$

$$s\tilde{o}c_d^{in} = s\tilde{o}c_{d-1}^{in} + \frac{\eta_{ev} p_v \Delta\tilde{h}_{d-1}}{C_b} - \frac{c_{ev}\ell_{d-1}}{C_b} \tag{2.7}$$

EV owner preferences regarding charging start times are modeled through the PDFs presented in Fig. 3(b)–(d). It is worth mentioning that for charging level 1, the most probable times for charging start happen at night, while the least probable ones happen at dawn; for charging level 2, the charging usually take place in parking lots, which generally attend between

Figure 3 – (a) PDF of SOC at the charging start. (b)–(d) PDF of charging start time for b) charging level 1, c) charging level 2 and d) charging level 3

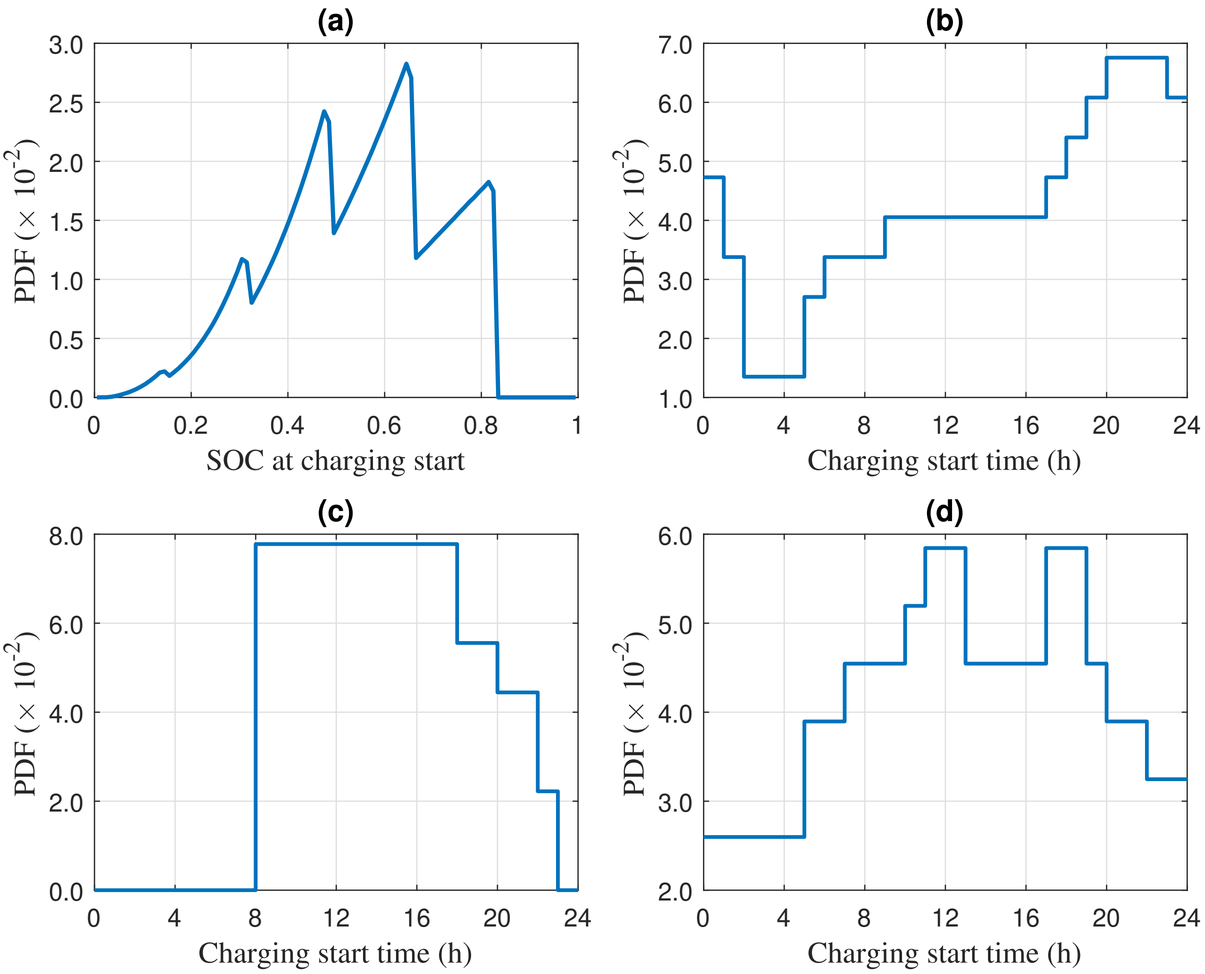

Source: Elaborated by the author.

8h and 23h; and, for charging level 3 is considered that these preferences are similar to those of gas stations.

2.2.3 Methodology

Finally, the proposed methodology to build EV load profiles is described as follows.

(i) Provide the following information: number of existing EVs per node, expected vehicle growth, EV appearance date, current EV penetration and expected EV peak penetration date.

(ii) Define the normal distribution parameters of $\tilde{z}_{ev}$ and the values of $\alpha^{ev}_{t,v}$ and $\phi^{ev,i}_{t,v}$.

(iii) Generate the quantity of EVs for a given node and time through (i) and (ii) (2.6). Afterward, based on (iii), estimate the quantity of EVs that will be charged by each charging level (2.7).

(iv) Generate a random EV load profile for each EV considered in (iii) (2.8)–(2.10). Note that, in order to generate independent daily profiles, when charging occurs in two consecutive days, the charging period is split at hour 0 and the parts are placed on a same day at their corresponding hours (2.9).

$$\tilde{P}^{ev,\nu}_{\mu,h}(\tilde{h}^{in}_{\nu},\tilde{x}_d,s\tilde{o}c^{in}_{d},s\tilde{o}c^{fi}_{d}) = \begin{cases} p_\nu, & h \in H^* \\ 0, & h \in H - H^*, \end{cases} \tag{2.8}$$

$$H^* = \{h \in H | \exists h^* \in \langle \tilde{h}^{in}_{\nu}, \tilde{h}^{fi}_{\nu}] : h \equiv h^* \mod 24\} \tag{2.9}$$

$$\tilde{h}^{fi}_{\nu} = \tilde{h}^{in}_{\nu} + \lfloor \Delta\tilde{h}_d \rceil \tag{2.10}$$

(v) Calculate the random EV load profile for the preset node and time as the sum of the individual profiles generated in (iv) (2.11)–(2.12). Its corresponding reactive load profile is calculated considering the power factors of the chargers (QUIRÓS-TORTÓS; OCHOA; LEES, 2015) (2.13). For the sake of simplicity, the random variables associated with the modeling of an unitary EV $(\tilde{h}_{in},\tilde{x}_d,s\tilde{o}c^{in}_{d},s\tilde{o}c^{fi}_{d})$ are replaced by the variable $\tilde{\varphi}_{ev}$.

$$\tilde{P}^{ev,i}_{t,y,d,h}(\tilde{\tau}^{i}_{ev},\tilde{\varphi}_{ev}) = \sum_{\nu\in\Omega_V}\sum_{n=1}^{\eta_\nu}\tilde{P}^{ev,\nu}_{\mu,h}(\tilde{\varphi}_{ev}),$$
$$\forall(t\in\Omega_T, y\in\Omega_Y, i\in\Omega_{\bar{N}}, d\in\Omega_D, h\in\Omega_H) \tag{2.11}$$

$$\eta_\nu = \tilde{n}^{ev,\nu,i}_{t,y}(\tilde{\tau}^{i}_{ev}), \forall(t\in\Omega_T, y\in\Omega_Y, i\in\Omega_{\bar{N}}, \nu\in\Omega_V) \tag{2.12}$$

$$\tilde{Q}^{ev,i}_{t,y,d,h}(\tilde{\tau}^{i}_{ev},\tilde{\varphi}_{ev}) = \tilde{P}^{ev,i}_{t,y,d,h}(\tilde{\tau}^{i}_{ev},\tilde{\varphi}_{ev})\tan(\cos^{-1}\mathrm{p}_{ev}), \tag{2.13}$$
$$\forall(t\in\Omega_T, y\in\Omega_Y, i\in\Omega_{\bar{N}}, d\in\Omega_D, h\in\Omega_H)$$

This methodology is summarized in the diagram of Fig. 4.

2.3 DISTRIBUTED GENERATION MODELING

DG systems are modeled in terms of energy production and prosumer participation. Since the renewable energy resources can not be predicted with certainty, to model their energy production under an uncertainty environment is vitally important to properly simulate the system operation and evaluate the risks involved in renewable DG system investments (PRILLIMAN *et al.*, 2023). Also, due to the increasing participation of prosumers, their impacts on the network are

Figure 4 – Methodology to generate random EV load profiles

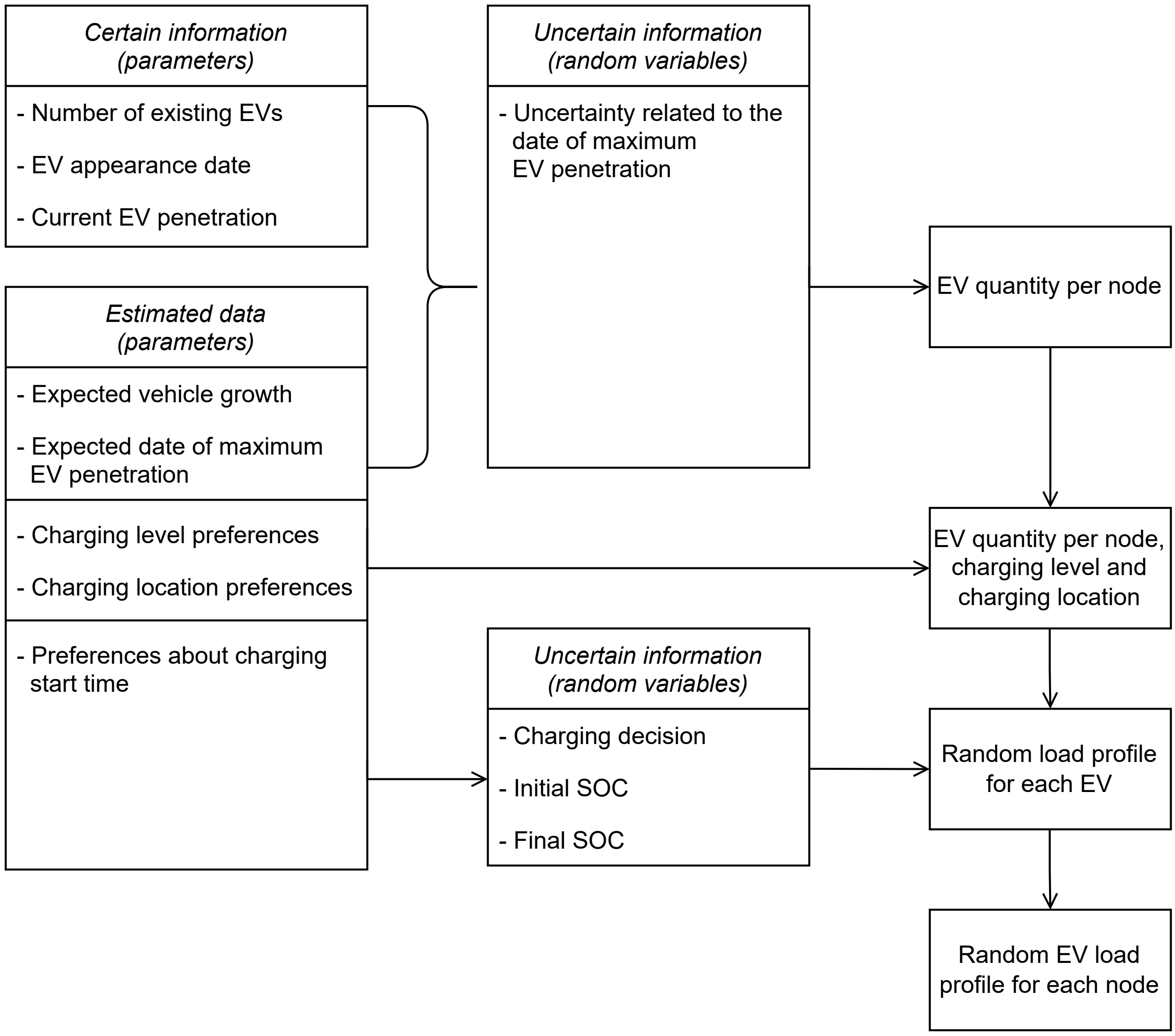

Source: Elaborated by the author.

expected to be significant within the planning horizon. Therefore, their participation is addressed and included in the planning problem.

2.3.1 Energy production

Electrical energy production is calculated based on the nominal power of the DG system and energy resources availability in its zone of installation (2.14). The utilization of energy resources by DG systems is measured through the generation factors $\tilde{f}^{pv,i}_{d,h}$ and $\tilde{f}^{wd,j}_{d,h}$, which are modeled as random variables considering the uncertainty related to daily energy production ($\tilde{z}^{pv}_{d}, \tilde{z}^{wd}_{d}$) and the short-term uncertainty regarding hourly production ($\tilde{z}^{pv}_{h}, \tilde{z}^{wd}_{h}$) (2.15). These uncertainties are modeled as normally distributed variables whose parameters are defined based on historical data of solar irradiation, temperature and wind speed. Note that the uncertainties are indistinctly applied to all the nodes of the system while the expected generation factors are considered with nodal resolution in order to take advantage of the available software about PV and wind generation, which usually present their data with resolutions of around 250m (SOLARGIS; ESMAP; GROUP, 2023; Technical University of Denmark (DTU) *et al.*, 2023). Additionally, to know the mathematical relationship among the energy resources and the generation factors, the work of Montoya-Bueno, Muñoz and Contreras (2015) can be consulted.

$$\left[\tilde{P}^{pv,i}_{t,y,d,h},\tilde{P}^{wd,j}_{t,y,d,h}\right]=\left[\tilde{\mathrm{f}}^{pv,i}_{d,h}\bar{P}^{pv,i}_{t},\tilde{\mathrm{f}}^{wd,j}_{d,h}\bar{P}^{wd,j}_{t}\right],\forall(t\in\Omega_T,y\in\Omega_Y,d\in\Omega_D,h\in\Omega_H,i\in\Omega_{pv})\quad(2.14)$$

$$\left[\tilde{\mathrm{f}}^{pv,i}_{d,h},\tilde{\mathrm{f}}^{wd,j}_{d,h}\right]=\left[\tilde{z}^{pv}_{d}\tilde{z}^{pv}_{h}\bar{\mathrm{f}}^{pv.i}_{d,h},\tilde{z}^{wd}_{d}\tilde{z}^{wd}_{h}\bar{\mathrm{f}}^{wd.j}_{d,h}\right],\forall(t\in\Omega_T,y\in\Omega_Y,d\in\Omega_D,h\in\Omega_H,j\in\Omega_{wd})\quad(2.15)$$

2.3.2 Prosumer participation

Prosumer participation in distribution networks is modeled considering that the vast majority of them use PV systems as generation technology (EMPRESA DE PESQUISA ENERGÉTICA – EPE, 2023). Total power installed by prosumers can be estimated based on prosumer penetration, which will be defined as the ratio between the average annual values of prosumers' production and system demand (2.16). As in the hypothesis assumed for EV adoption, prosumer growth is assumed to follow a S-curve, δ^i_{pr}, built since the start of prosumer activity in the network until the date $\tilde{\tau}^i_{pr}$ to achieve a given maximum hosting capacity. Note that $\tilde{\tau}^i_{pr}=\tau^i_{pr}+\tilde{z}_{pr}$. Afterward, the active and reactive power generated by prosumers is calculated in (2.17) and (2.21), respectively, considering that prosumers need to inject reactive power with a given power factor to support the grid (2.18).

$$\tilde{P}^{pr,i}_{t,y}(\tilde{\tau}^i_{pr})=\delta^i_{pr}(t,y,\tilde{\tau}^i_{pr})P^{cd,ev}_{t,y}/cf_{pv},\forall(t\in\Omega_T,y\in\Omega_Y)\quad(2.16)$$

$$\tilde{P}^{pr,i}_{t,y,d,h}(\tilde{\tau}^i_{pr},\tilde{\mathrm{f}}^{pv}_{d,h})=\tilde{\mathrm{f}}^{pv}_{d,h}\hat{P}^{pr,i}_{t,y}(\tilde{\tau}^i_{pr}),\forall(t\in\Omega_T,y\in\Omega_Y,d\in\Omega_D,h\in\Omega_H)\quad(2.17)$$

$$\tilde{Q}^{pr,i}_{t,y,d,h}(\tilde{\tau}^i_{pr},\tilde{\mathrm{f}}^{pv}_{d,h})=\tilde{P}^{pr,i}_{t,y,d,h}(\tilde{\tau}^i_{pr},\tilde{\mathrm{f}}^{pv}_{d,h})\tan\left(\cos^{-1}\hat{\mathrm{p}}_{pr}\right),\forall(t\in\Omega_T,y\in\Omega_Y,d\in\Omega_D,h\in\Omega_H)\quad(2.18)$$

2.4 GENERATION OF SYSTEM OPERATING SCENARIOS

The system operation at a given time is characterized, for planning purposes, by the set of active and reactive demands (both seen by the DISCO) and by the DG generation factors of all the system nodes. Thus, a system operating scenario should include the following components: active demand, reactive demand, PV generation factor and wind generation factor. Also, in order to take into account the temporal transition of EES systems, it is considered that system operating scenarios comprises a day of operation with hourly resolution.

Aggregated demand seen by the DISCO is determined through the balance of conventional demand, EV load and prosumers' power generation for each node (2.19)–(2.20) and for the whole system (2.21)–(2.22). Note that all random variables related to demand are comprised in $\tilde{z}^{D,i}_{t,d,h}$ and that PV generation uncertainty is embedded in the aggregated demand uncertainty (2.23). It is worth indicating that this last fact is overlooked in the existing literature, which cause a loss of correlation in the system modeling.

$$\tilde{P}^{D,i}_{t,y,d,h}(\tilde{z}^{D,i}_{t,d,h}) = \tilde{P}^{cd,i}_{t,y,d,h}(\tilde{z}^{s,i,h}_{cd,p}, \tilde{z}^{\ell,t}_{cd}) + \tilde{P}^{ev,i}_{t,y,d,h}(\tilde{\tau}^{i}_{ev}, \tilde{\varphi}_{ev}) - \tilde{P}^{pr,i}_{t,y,d,h}(\tilde{\tau}^{i}_{pr}, \tilde{\mathrm{f}}^{pv,i}_{d,h}),$$
$$\forall(t \in \Omega_T, y \in \Omega_Y, d \in \Omega_D, h \in \Omega_H, i \in \Omega_{\bar{N}}) \tag{2.19}$$

$$\tilde{Q}^{D,i}_{t,y,d,h}(\tilde{z}^{D,i}_{t,d,h}) = \tilde{Q}^{cd,i}_{t,y,d,h}(\tilde{z}^{s,i,h}_{cd,q}, \tilde{z}^{\ell,t}_{cd}) + \tilde{Q}^{ev,i}_{t,y,d,h}(\tilde{\tau}^{i}_{ev}, \tilde{\varphi}_{ev}) - \tilde{Q}^{pr,i}_{t,y,d,h}(\tilde{\tau}^{i}_{pr}, \tilde{\mathrm{f}}^{pv,i}_{d,h}),$$
$$\forall(t \in \Omega_T, y \in \Omega_Y, d \in \Omega_D, h \in \Omega_H, i \in \Omega_{\bar{N}}) \tag{2.20}$$

$$\tilde{P}^{D}_{t,y,d,h}([\tilde{z}^{D,i}_{t,d,h}]_{\{i\in\Omega_{\bar{N}}\}}) = \sum_{i\in\Omega_{\bar{N}}} \tilde{P}^{D,i}_{t,y,d,h}(\tilde{z}^{D,i}_{t,d,h}), \forall(t \in \Omega_T, y \in \Omega_Y, d \in \Omega_D, h \in \Omega_H) \tag{2.21}$$

$$\tilde{Q}^{D}_{t,y,d,h}([\tilde{z}^{D,i}_{t,d,h}]_{\{i\in\Omega_{\bar{N}}\}}) = \sum_{i\in\Omega_{\bar{N}}} \tilde{Q}^{D,i}_{t,y,d,h}(\tilde{z}^{D,i}_{t,d,h}), \forall(t \in \Omega_T, y \in \Omega_Y, d \in \Omega_D, h \in \Omega_H) \tag{2.22}$$

$$\tilde{z}^{D,i}_{t,d,h} = (\tilde{z}^{\ell,t}_{cd}, \tilde{z}^{s,i,h}_{cd,p}, \tilde{z}^{s,i,h}_{cd,q}, \tilde{\tau}^{i}_{ev}, \tilde{\varphi}_{ev}, \tilde{\tau}^{i}_{pr}, \tilde{\mathrm{f}}^{pv,i}_{d,h}), \forall(t \in \Omega_T, d \in \Omega_D, h \in \Omega_H) \tag{2.23}$$

Finally, a system operating scenario is defined by the tuple $\tilde{S}_{t,y,d} = [\tilde{s}^{i}_{t,y,d}]_{\{i\in\Omega_{\bar{N}}\}}$, which includes demand and generation factors for all load nodes along a given day (2.24)–(2.25). Additionally, a compressed version of $\tilde{S}_{t,y,d}$, denominated as comprised operating scenario, is defined by the matrix $\tilde{s}_{t,y,d}$, which accounts for total system demand and average generation factors while setting aside the nodal information (2.26)–(2.27).

$$\tilde{s}^{i}_{t,y,d}([\tilde{z}^{i}_{t,d,h}]_{\{h\in\Omega_H\}}) := [s]_{\Omega_H} : s_{h\in\Omega_H} =$$
$$\Big[\tilde{P}^{D,i}_{t,y,d,h}(\tilde{z}^{D,i}_{t,d,h}), \tilde{Q}^{D,i}_{t,d,h}(\tilde{z}^{D,i}_{t,d,h}), \tilde{\mathrm{f}}^{pv}_{d,h}(\tilde{z}^{pv}_{d}, \tilde{z}^{pv}_{h}), \tilde{\mathrm{f}}^{wd}_{d,h}(\tilde{z}^{wd}_{d}, \tilde{z}^{wd}_{h})\Big], \forall(t \in \Omega_T, d \in \Omega_D, i \in \Omega_{\bar{N}}) \tag{2.24}$$

$$\tilde{z}^{i}_{t,d,h} = (\tilde{z}^{\ell,t}_{cd}, \tilde{z}^{s,i,h}_{cd,p}, \tilde{z}^{s,i,h}_{cd,q}, \tilde{\tau}^{i}_{ev}, \tilde{\varphi}_{ev}, \tilde{\tau}^{i}_{pr}, \tilde{z}^{pv}_{d}, \tilde{z}^{pv}_{h}, \tilde{z}^{wd}_{d}, \tilde{z}^{wd}_{h}), \forall(t \in \Omega_T, d \in \Omega_D, h \in \Omega_H, i \in \Omega_{\bar{N}}) \tag{2.25}$$

$$\tilde{s}_{t,y,d}([\tilde{z}^{i}_{t,d,h}]_{\{h\in\Omega_H\},\{i\in\Omega_{\bar{N}}\}}) := [s]_{\Omega_H} : s_{h\in\Omega_H} =$$
$$\Big[\tilde{P}^{D}_{t,y,d,h}([\tilde{z}^{D,i}_{t,d,h}]_{\{i\in\Omega_{\bar{N}}\}}), \tilde{Q}^{D}_{t,y,d,h}([\tilde{z}^{D,i}_{t,d,h}]_{\{i\in\Omega_{\bar{N}}\}}), \tilde{\mathrm{f}}^{pv}_{d,h}(\tilde{z}^{pv}_{d}, \tilde{z}^{pv}_{h}), \tilde{\mathrm{f}}^{wd}_{d,h}(\tilde{z}^{wd}_{d}, \tilde{z}^{wd}_{h})\Big],$$
$$\forall(t \in \Omega_T, d \in \Omega_D) \tag{2.26}$$

$$\Big[\tilde{\mathrm{f}}^{pv}_{d,h}, \tilde{\mathrm{f}}^{wd}_{d,h}\Big] = \left[\sum_{i\in\Omega_{\bar{N}}} \tilde{\mathrm{f}}^{pv,i}_{d,h}/|\Omega_{\bar{N}}|, \sum_{j\in\Omega_{wd}} \tilde{\mathrm{f}}^{wd,j}_{d,h}/|\Omega_{wd}|\right], \forall(t \in \Omega_T, d \in \Omega_D, i \in \Omega_{\bar{N}}, j \in \Omega_{wd}) \tag{2.27}$$

The relationship between operating scenarios and their corresponding comprised operating scenarios is schematized in Fig. 5.

Figure 5 – Relationship between operating scenarios and comprised operating scenarios

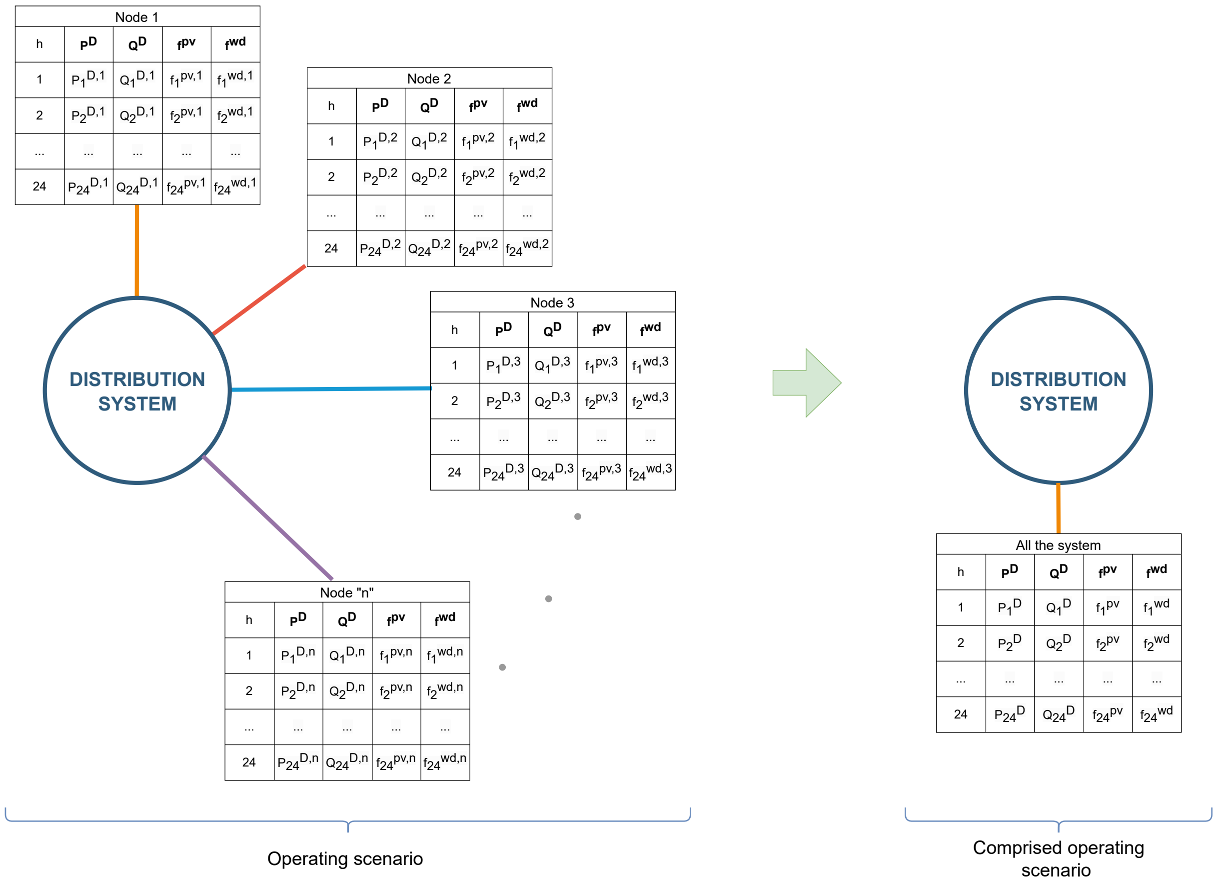

Source: Elaborated by the author.

3 PROBLEM FORMULATION

The proposed model aims to determine an optimal investment plan that leads to reliable and proper operation of the system at minimum cost, while reducing its CO_2 emissions over the planning horizon. In order to achieve that, representative operating scenarios are carefully determined and several planning actions are considered. Planning actions include the installation of DG systems (PV and wind), EES systems, fixed and switchable CBs, SVCs, OLTCs and VRs, as well as reconductoring and substation reinforcement. It is worth indicating that switchable CBs, SVCs, OLTCs and VRs are supposed to be centrally controlled together with the DERs (DG and EES systems). Investments are assumed to be made by the DISCO, but in the case of DERs could also be made by an independent agent in agreement with the DISCO considering the information obtained through this model. The problem is formulated as a two-stage stochastic programming model based on discrete scenarios, where the investment costs correspond to the first stage and the Operation and Maintenance (O&M) costs to the second one. In order to handle the non-linear nature of network equations and to guarantee feasibility of the solution, a novel MIQP model is proposed..

3.1 DETERMINATION OF ROSs

Representative operating scenarios (ROSs) correspond to a reduced set of virtual operating scenarios, which have the quality of preserving as much as possible the most relevant features of system operation that impact on the planning (Fig. 6). Traditionally, the most used method to obtain ROSs is the K-means clustering, which presents the advantages of being easy to implement and scalable (GARCÍA-CEREZO; BARINGO; GARCÍA-BERTRAND, 2020; MAHDI; HOSNY; ELHENAWY, 2021) . However, since K-means is a generic clustering technique, it does not take into account particular information about the purpose of its application. Thus, a customized K-means is required to obtain proper ROSs for distribution system planning.

3.1.1 Robust ROSs

Robust ROSs are obtained from a large set of system operating scenarios (generated according to Chapter 2) through a novel method based on K-means clustering, named as robust K-means. The proposed method has the advantage of considering customized metrics that allow assigning different weights to system operating parameters. Also, it allows to assign different weights to the distances (with respect to each cluster centroid) used to determine the clusters and, which is useful to emphasize in critical scenarios through the reduction of their neighborhood.

Figure 6 – Simplified scheme for obtaining ROSs

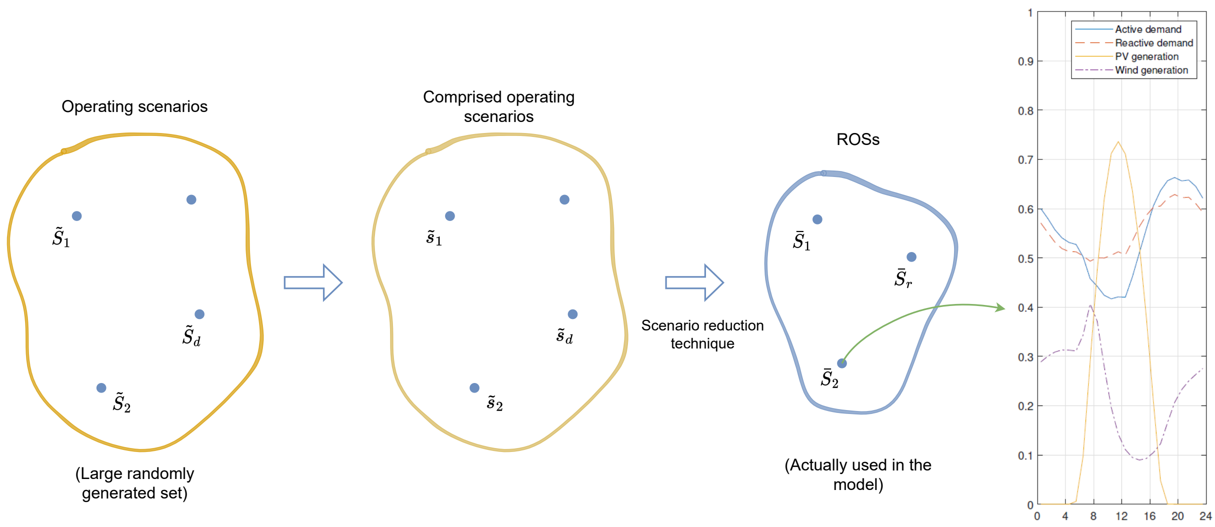

Source: Elaborated by the author.

The weight assignation for the operating parameters is important since allows to focus in parameters according their impact in system operation. Thus, e.g., it has no much sense to consider demand and PV generation with the same importance if PV penetration is expected to be only of 5%. On the other hand, emphasize in critical scenarios allows to increase the planning reliability, which is important given the appreciable uncertainties to which the system is subjected. The method is described below.

- Generate a large set $\hat{S}_t$ of random operating scenarios ($\bar{S}_{t,y,d}$) for each planning period t as realizations of the random array $[\tilde{z}^i_{t,d,h}]$, considering the same quantity of scenarios for each given tuple (t,y,d).

- Due to the data from $\hat{S}_t$ is considerably large (since includes nodal information), any clustering method applied to them is expected to be too computationally expensive. Thus, clustering will be performed over the set $\hat{S}^{\prime}_t$ composed of the corresponding comprised operating scenarios ($\bar{s}_{t,y,d}$), which account only for the total system demand and average generation factors.

- Normalize the data so that each operating parameter value belongs to the interval $[0,1]$ for each planning period.

- Define the number of ROSs for each planning period (K_t) and the set of ROS indices as $\Omega^t_R = \{1,..K_t\}$. Note that, ideally, this number should correspond to the minimum number of ROSs that represent the data variability incident in the system planning. For practical purposes, the Elbow's method or a sufficient number of days that aims to represent the min/max values of the operating parameters (as adopted in this work) can be used.

- Define the initial centroids for the robust K-means clustering including critical scenarios, as those of minimum and maximum demand or generation.

- Define the metric to be used in the K-means clustering, as indicated in (3.1). Note that $\{\{\mathscr{C}_1^t, ..\mathscr{C}_{K_t}^t\} : t \in \Omega_T\}$ denotes the cluster centroids. Also, notice that the vector $[w_D, w_R, w_{pv}, w_{wd}]$ comprises the weights of operating parameters, while w_r^t refers to the weights of the distances to each centroid.

$$\partial(\mathscr{C}_r^t, s) = w_r^t [w_D, w_R, w_{pv}, w_{wd}] \cdot \|\mathscr{C}_r^t - s\|^*, \\ \forall t \in \Omega_T, s \in \hat{S}_t^{\prime}, r \in \Omega_R^t \tag{3.1}$$

- Apply the K-means method over $\hat{S}_t^{\prime}$ considering K_t clusters and the metric ∂ previously defined, for each planning period t. Denote the obtained clusters (make up of $\bar{s}_{t,y,d}$) as $\mathtt{C}_r^{t\,\prime}, \forall t \in \Omega_T, r \in \{1, ..K_t\}$, respectively. Then, define the corresponding clusters that include nodal information (make up of $\bar{S}_{t,y,d}$) and their respective cardinality as $\mathtt{C}_r^t$ and $|\mathtt{C}_r^t|$, $\forall t \in \Omega_T, r \in \{1, ..K_t\}$, respectively. Finally, the ROSs ($\bar{S}_{t,r}$) are obtained through (3.2), after reverting the normalization. The set of ROSs is denoted as Ω_S.

$$\bar{S}_{t,r} = \frac{1}{|\mathtt{C}_r^t|} \sum_{s \in \mathtt{C}_r^t} s, \forall t \in \Omega_T, r \in \Omega_R^t \tag{3.2}$$

- As each ROS represents all the operating scenarios inside its corresponding cluster, its probability of occurrence (in the modeling) can be obtained as $\pi_{t,r} = |\mathtt{C}_r^t|/|\hat{S}_t|$. Additionally, the probability of occurrence of a ROS within a given year can be calculated as $\pi_{t,y,r} = |\mathtt{C}_r^{t,y}|/|\hat{S}_{t,y}|$, where $\hat{S}_{t,y}$ denotes the set of operating scenarios in period t and year y, and $\mathtt{C}_r^{t,y}$ denotes the set of operating scenarios in $\mathtt{C}_r^t$ corresponding to year y.

Finally, the equation (3.3) is established in order to identify each operating parameter used in the mathematical model.

$$\bar{S}_{t,r} = \left[P_{t,r,h}^{D,i}, Q_{t,r,h}^{D,i}, \mathrm{f}_{t,r,h}^{pv}, \mathrm{f}_{t,r,h}^{wd}\right]_{\{h \in \Omega_H\},\{i \in \Omega_{\bar{N}}\}}, \\ \forall (t \in \Omega_T, r \in \Omega_R^t) \tag{3.3}$$

The proposed methodology is summarized in Fig. 7.

Figure 7 – Methodology to determine robust ROS

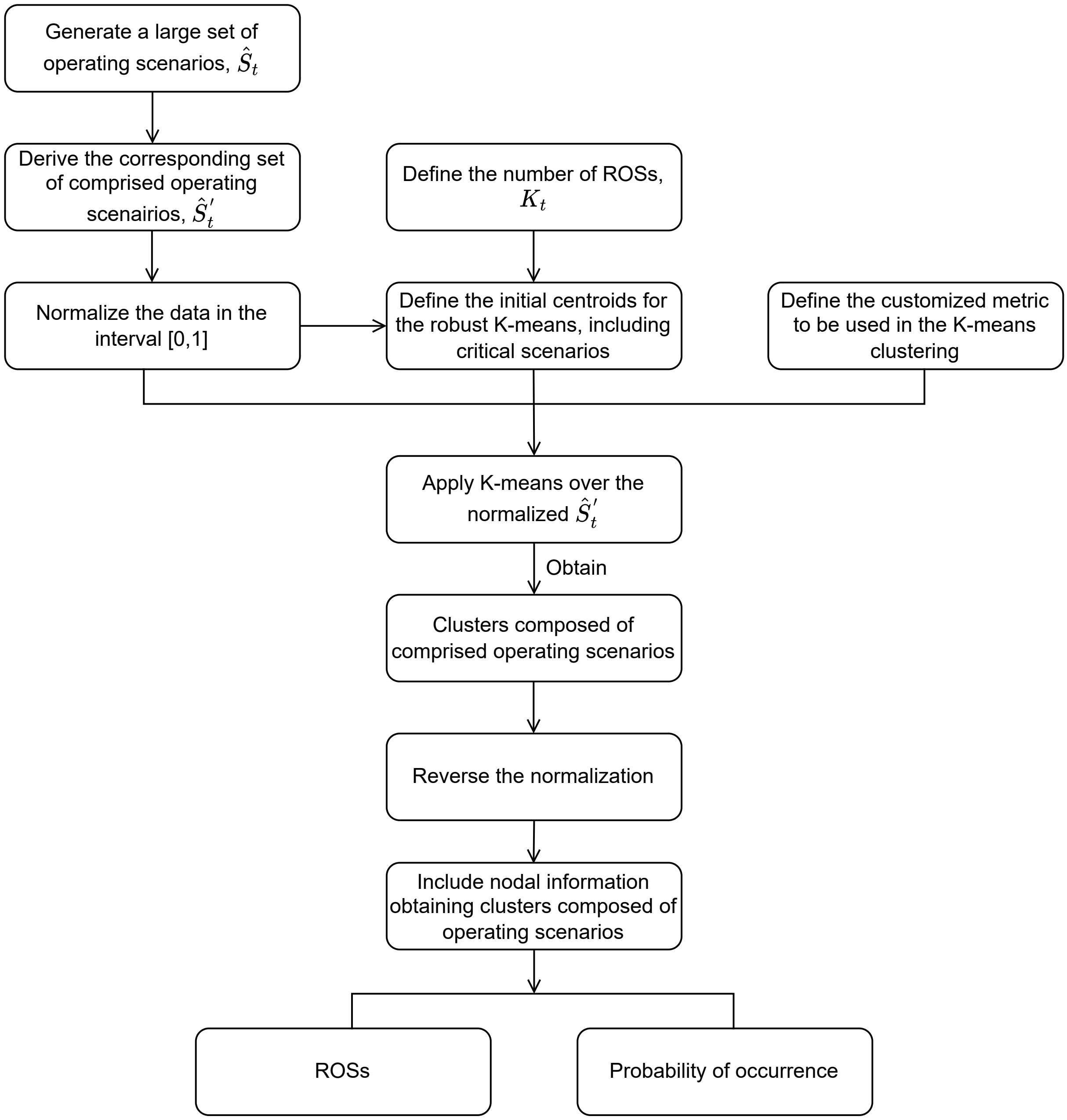

Source: Elaborated by the author.

3.2 OBJECTIVE FUNCTION

The objective of the model aims at minimizing the aggregate present value of investment costs and expected costs of operation and maintenance (O&M) over the planning horizon, while minimizing the feasibility error (f_ξ) (3.4)–(3.6).

$$\min C_T = C_I + \mathbb{E}_{\Omega_S}[\tilde{C}_{om}] + f_\xi \tag{3.4}$$

$$\begin{aligned}
C_I = \sum_{t\in\Omega_T} \beta_t^{inv} \Bigg[& \omega_t^{pv} \sum_{i\in\Omega_{pv}} c_t^{pv} \bar{P}_t^{pv,i} + \omega_t^{wd} \sum_{i\in\Omega_{wd}} c_t^{wd,i} \\
& + \sum_{i\in\Omega_{ss}} \Big(\omega_t^{ss} \sum_{u\in\Omega_{\overline{ss}}} x_t^{ss,u,i} c_t^{ss,u} + \omega_t^{oltc} x_t^{oltc,i} c_t^{oltc} \Big) + \sum_{i\in\Omega_{rc}} \Big(\omega_t^{cb} (c_t^{fcb,i} + c_t^{scb,i}) + \omega_t^{svc} x_t^{svc,i} c_t^{svc} \Big) \\
& + \omega_t^{con} \sum_{i,j\in\Omega_B} \sum_{a\in\Omega_C} c^{cr}_{a_0^{i,j},a} l_{i,j} (x_t^{a,i,j} - x_{t-1}^{a,i,j}) + \omega_t^{sp} \sum_{i,j\in\Omega_B} \sum_{e\in\Omega_E} c^{sp}_{e_0^{i,j},e} l_{i,j} (z_t^{e,i,j} - z_{t-1}^{e,i,j}) \\
& + \omega_t^{vr} \sum_{i,j\in\Omega_B^{vr}} \sum_{v\in\Omega_{vr}} c_t^{vr} \varkappa_t^{v,i,j} + \omega_t^{ees} \sum_{i\in\Omega_{ees}} c_t^{ees} P_t^{ees,i} \Bigg]
\end{aligned} \tag{3.5}$$

$$\begin{aligned}
\mathbb{E}_{\Omega_S}[\tilde{C}_{om}] = \sum_{t\in\Omega_T} \sum_{y\in\Omega_Y} \Bigg[& \beta_{t,y}^{om} \sum_{i\in\Omega_{pv}} com_{t,y}^{pv} \bar{P}_t^{pv,i} + \beta_{t,y}^{om} \sum_{i\in\Omega_{wd}} com_{t,y}^{wd} \bar{P}_t^{wd,i} \\
& + \beta_{t,y}^{om} \sum_{i\in\Omega_{ees}} com_{t,y}^{ees} \bar{P}_t^{ees,i} + \beta_{t,y}^{en} \sum_{i\in\Omega_{ss}} \sum_{r\in\Omega_R^t} \sum_{h\in\Omega_H} \pi_{t,y,r} P_{t,r,h}^{ss,i'} (c_{t,h}^{en} + r_{co_2} \Gamma_t^{co_2}) \Bigg]
\end{aligned} \tag{3.6}$$

The investment cost, C_I, includes acquisition, installation or replacement costs corresponding to substations, OLTCs, PV, wind and EES systems; equipment for reactive compensation as fixed and switchable CBs and SVCs; VRs and reconductoring (through conductor and support replacement). O&M cost, $\tilde{C}_{om}$, includes cost of energy purchased at the substations, CO_2 carbon taxes and O&M costs of PV, wind and EES systems. In order to take into account the power transformer losses in the modeling (which are significant), the topology includes node indices i' and an branch indices $(i,i'), \forall i \in \Omega_{ss}$, to represent the primary terminals of the transformers and their windings, respectively. Thus, the energy purchased in the substations are referred to these nodes i'. The feasibility error function, f_ξ, corresponds to the sum of squares of the differences between actual and reference values of some given parameters. It is described in more detail in Chapter 4. Also, in order to consider the time required for engineering, procurement and construction (EPC) of the investment assets, investments are considered to be 3 months earlier than the beginning of each planning period (3.7). The payments for the energy purchased at the substations is assumed to be monthly (3.8). Other O&M costs are assumed to take place at the beginning of each year (3.9).

$$\beta_t^{inv} = \frac{1}{(1+\iota)^{n_Y(t-1)-1/4}} \tag{3.7}$$

$$\beta_{t,y}^{en} = \frac{(1+\iota/12)^{12} - 1}{\iota(1+\iota/12)^{12}(1+\iota)^{n_Y(t-1)+y-1}} \tag{3.8}$$

$$\beta_{t,y}^{om} = \frac{1}{(1+\iota)^{n_Y(t-1)+y-1}} \tag{3.9}$$

In addition, in order to properly model the cost-benefit of assets to be installed, i.e., substations, OLTCs, conductors, supports, CBs, SVCs, VRs and PV, wind and EES systems, the application of usage factors ω_t^{as} is proposed, as expressed in (3.10).

$$\omega_t^{as} = \begin{cases} 1 - \dfrac{(1+\imath)^{T_{as}-T_t}}{(1+\imath)^{T_{as}}-1}, & T_{as} > T_t \\ 1, & T_{as} \leq T_t \end{cases} \tag{3.10}$$

$$T_t = T - n_Y(t-1), \forall t \in \Omega_T \tag{3.11}$$

3.3 CONSTRAINTS

The network operating conditions, including physical and operating limits, asset costs and CO_2 emission reduction targets are modeled through (3.12)–(3.68). It is worth indicating that some constraints are modeled around a reference point ($P^*, Q^*, V^*, I^*, P^{ss,*}, Q^{ss,*}$) in order to bring the advantages of the proposed solution technique to the modeling, and vice versa.

3.3.1 Kirchhoff's first law

Kirchhoff's first law is modeled through the balance of active and reactive powers. The modeling is done for the power transformers in (3.12)–(3.13) and for the network nodes through (3.14)–(3.15). Notice that the effect of reconductoring is recursively modeled in terms of I^*, which avoids the use of variables indexed by conductor types ($P_a, Q_a, I_a : a \in \Omega_C$), thereby reducing the size and sparseness of the matrices involved in the numerical solution process.

$$P_{t,r,h}^{ss,i'} - P_{t,r,h}^{i',i} - R_{ss}^{i} I_{t,r,h}^{i',i} - L_{ss}^{i} = 0, \forall (t \in \Omega_T, r \in \Omega_R^t, h \in \Omega_H, i \in \Omega_{ss}) \tag{3.12}$$

$$Q_{t,r,h}^{ss,i'} - Q_{t,r,h}^{i',i} - X_{ss}^{i} I_{t,r,h}^{i',i} = 0, \forall (t \in \Omega_T, r \in \Omega_R^t, h \in \Omega_H, i \in \Omega_{ss}) \tag{3.13}$$

$$\begin{aligned} &\sum_{(j,i) \in \Omega_{B+}} P_{t,r,h}^{j,i} + P_{t,r,h}^{pv,i} + P_{t,r,h}^{wd,i} + P_{t,r,h}^{+ess,i} - P_{t,r,h}^{-ess,i} - P_{t,d,h}^{D,i} \\ &- \sum_{(i,j) \in \Omega_B} \Big[P_{t,r,h}^{i,j} + R_{a_0^{i,j}} l_{i,j} I_{t,r,h}^{i,j} + \sum_{a \in \Omega_C} x_a^{i,j} (R_a - R_{a_0^{i,j}}) l_{i,j} I_{t,r,h}^{i,j,*} \Big] = 0, \\ &\forall (t \in \Omega_T, r \in \Omega_R^t, h \in \Omega_H, i \in \Omega_N) \end{aligned} \tag{3.14}$$

$$\begin{aligned} &\sum_{(j,i) \in \Omega_{B+}} Q_{t,r,h}^{j,i} + Q_{t,r,h}^{pv,i} + Q_{t,r,h}^{wd,i} + Q_{t,r,h}^{cb,i} + Q_{t,r,h}^{svc,i} - Q_{t,r,h}^{D,i} \\ &- \sum_{(i,j) \in \Omega_B} \Big[Q_{t,r,h}^{i,j} + X_{a_0^{i,j}} l_{i,j} I_{t,r,h}^{i,j} + \sum_{a \in \Omega_C} x_a^{i,j} (X_a - X_{a_0^{i,j}}) l_{i,j} I_{t,r,h}^{i,j,*} \Big] = 0, \\ &\forall (t \in \Omega_T, r \in \Omega_R^t, h \in \Omega_H, i \in \Omega_N) \end{aligned} \tag{3.15}$$

3.3.2 Kirchhoff's second law

Based on Kirchhoff's second law, drop of voltage squared is modeled through (3.16). Analogously with the modeling of Kirchhoff's first law, the effect of reconductoring is recursively modeled in terms of P^*, Q^*, I^*.

$$V^i_{t,r,h} + \Delta V^i_{t,r,h} - V^j_{t,r,h} = 2l_{i,j}(R_{a^0_{i,j}} P^{i,j}_{t,r,h} + X_{a^0_{i,j}} Q^{i,j}_{t,r,h}) + Z^2_{a^0_{i,j}} l^2_{i,j} I^{i,j}_{t,r,h}$$
$$+ \sum_{a \in \Omega_C} x^{i,j}_a \Big[2l_{i,j}(R_a - R_{a^{i,j}_0}) P^{i,j,*}_{t,r,h} + 2l_{i,j}(X_a - X_{a^{i,j}_0}) Q^{i,j,*}_{t,r,h} + (Z^2_a - Z^2_{a^0_{i,j}}) l^2_{i,j} I^{i,j,*}_{t,r,h} \Big],$$
$$\forall (t \in \Omega_T, d \in \Omega^t_R, h \in \Omega_H, (i,j) \in \Omega_B) \tag{3.16}$$

3.3.3 Power, voltage and current relationship

The apparent power relationship among $P, Q, V, I : VI = P^2 + Q^2$ (non-linear and non-convex) is modeled through a linearized model (3.17)–(3.18). This model consists of an approximation in the left side (assuming $V \approx V^*$) and a relaxation, based on Taylor series around (P^*, Q^*), in the right side.

$$V^{j,*}_{t,r,h} I^{i,j}_{t,r,h} = 2P^{i,j}_{t,r,h} P^{i,j,*}_{t,r,h} + 2Q^{i,j}_{t,r,h} Q^{i,j,*}_{t,r,h} - (P^{i,j,*}_{t,r,h})^2 - (Q^{i,j,*}_{t,r,h})^2 + \Delta^{i,j}_{t,r,h},$$
$$\forall (t \in \Omega_T, r \in \Omega^t_R, h \in \Omega_H, (i,j) \in \Omega_{B^+}) \tag{3.17}$$

$$\Delta^{i,j}_{t,r,h} \geq 0, \forall (t \in \Omega_T, r \in \Omega^t_R, h \in \Omega_H, (i,j) \in \Omega_{B^+}) \tag{3.18}$$

3.3.4 Substation operation

Power exchange in substations is limited by their nominal powers and by the power exchange flexibility at the transmission/distribution interface established by the Transmission System Operator (TSO) (STANKOVIĆ *et al.*, 2021). The limitation about nominal power is modeled through the linearization proposed in (3.19). Note that, to prevent overloading the substations, their upgrades are considered through their replacements, which is mandatory at the end of their lifespan (3.19). Regarding the transmission/distribution flexibility, it is assumed that active power supply to the transmission system is not allowed and that reactive power flow in substations is delimited by given power factors (3.20)–(3.21). The operation of OLTCs is modeled through (3.22)–(3.23). Note that (3.23) corresponds to a pretty accurate linearization of the voltage square variation due to the OLTC operation, which also includes the voltage drop due to transformer impedance. The decision to install OLTCs is modeled in (3.24). Since substation lifespan is greater than the planning horizon, at most one upgrade is expected (3.25).

$$P_{t,r,h}^{ss,i'} P_{t,r,h}^{ss,i',*} + Q_{t,d,h}^{ss,i'} Q_{t,d,h}^{ss,i',*} \leq S_0^{ss,i2} \left\langle t \leq \frac{T_{ss_i} - T_{ss_i}^0}{n_T} \right\rangle$$
$$+ \sum_{t'=1}^{t} \sum_{u \in \Omega_{\overline{ss}}} x_t^{ss,u,i} \left(S^{ss,u2} - S_0^{ss,i2} \left\langle t \leq \frac{T_{ss_i} - T_{ss_i}^0}{n_T} \right\rangle \right),$$
$$\forall (t \in \Omega_T, r \in \Omega_{R'}, h \in \Omega_H, i \in \Omega_{ss}) \tag{3.19}$$

$$0 \leq P_{t,d,h}^{ss,i'}, \forall (t \in \Omega_T, r \in \Omega_{R'}, h \in \Omega_H, i \in \Omega_{ss}) \tag{3.20}$$

$$-P_{t,r,h}^{ss,i'} \tan(\cos^{-1} \mathrm{p}_{ss}^{cap}) \leq Q_{t,d,h}^{ss,i'} \leq P_{t,r,h}^{ss,i'} \tan(\cos^{-1} \mathrm{p}_{ss}^{ind})$$
$$\forall (t \in \Omega_T, r \in \Omega_{R'}, h \in \Omega_H, i \in \Omega_{ss}) \tag{3.21}$$

$$-\frac{n_{tap} - 1}{2} \leq tap_{t,r,h}^i \leq \frac{n_{tap} - 1}{2}, \forall (t \in \Omega_T, r \in \Omega_{R'}, h \in \Omega_H, i \in \Omega_{ss}) \tag{3.22}$$

$$V_{t,r,h}^i = \overline{V}_{t,r,h}^{i'} \left(1.001 + \frac{tap_{t,r,h}^i}{5(n_{tap} - 1)} \right) - 2R_{ss}^i P_{t,r,h}^{i',i} - 2X_{ss}^i Q_{t,r,h}^{i',i} - {Z_{ss}^i}^2 I_{t,r,h}^{i',i},$$
$$\forall (t \in \Omega_T, r \in \Omega_{R'}, h \in \Omega_H, i \in \Omega_{ss}) \tag{3.23}$$

$$x_t^{oltc,i} \geq \left| \frac{2tap_{t,r,h}^i}{n_{tap} - 1} \right|, \forall (t \in \Omega_T, r \in \Omega_{R'}, h \in \Omega_H, i \in \Omega_{ss}) \tag{3.24}$$

$$\sum_{t' \in \Omega_T, u \in \Omega_{\overline{ss}}} x_{t'}^{ss,u,i} \leq 1, \forall (i \in \Omega_{ss}) \tag{3.25}$$

3.3.5 Installation and operating limits of DG systems

The capacity of wind systems is calculated based on the number of wind system units that comprise it (3.26). The total DG installed capacity in each planning period can be calculated through (3.27). On the other hand, since PV systems are usually made up of modules with nominal capacity of about 0.3kW, their nominal capacity is considered as a continuous variable. Due to physical space limits in distribution networks, the capacity of DG systems that can be installed is limited by (3.28)–(3.29). In order to take advantage of the reactive power control capacity offered by PV inverters and wind converters, the power ouput of DG systems is controlled according their reactive power capabilities considering a reactive power limit of 60% of the nominal capacity (DING; MEMBER; BAGGU, 2018; ELLIS *et al.*, 2012). These capability curves are modeled through piece-wise linearization in (3.30)–(3.37) according to the Fig. 8. In addition, since it can not be guaranteed that injecting all the energy from DG systems to the grid leads always to an optimal system operation, energy curtailment is taken into account through (3.38)–(3.39). Finally, wind system cost is modeled in (3.40) considering cost reduction due to turbines grouping (BHASKAR; STEHLY, 2021).

$$P_t^{wd,j} = n_t^{wd,j} P_{\mu}^{wd}, \forall (t \in \Omega_T, i \in \Omega_{pv}, j \in \Omega_{wd}) \tag{3.26}$$

$$\left[\bar{P}_t^{pv,i}, \bar{P}_t^{wd,j} \right] = \left[\sum_{t'=1}^{t} P_{t'}^{pv,i}, \sum_{t'=1}^{t} P_{t'}^{wd,j} \right], \forall (t \in \Omega_T, i \in \Omega_{pv}, j \in \Omega_{wd}) \tag{3.27}$$

$$\sum_{t \in \Omega_T} \bar{P}_t^{pv,i} \leq P_{max}^{pv,i}, \forall i \in \Omega_{pv} \tag{3.28}$$

$$\sum_{t'=1}^{t} n_{t'}^{wd,j} \leq n_{max}^{wd}, \forall j \in \Omega_{wd} \tag{3.29}$$

$$-0.6\bar{P}_t^{pv,i} \leq Q_{t,r,h}^{pv,i} \leq 0.6\bar{P}_t^{pv,i}, \forall (t \in \Omega_T, r \in \Omega_R^t, h \in \Omega_H, i \in \Omega_{pv}) \tag{3.30}$$

$$\tfrac{9+5\sqrt{10}}{13} P_{t,r,h}^{pv,i} - \tfrac{15+4\sqrt{10}}{13} \bar{P}_t^{pv,i} \leq Q_{t,r,h}^{pv,i}, \forall (t \in \Omega_T, r \in \Omega_R^t, h \in \Omega_H, i \in \Omega_{pv}) \tag{3.31}$$

$$Q_{t,r,h}^{pv,i} \leq \tfrac{15+4\sqrt{10}}{13} \bar{P}_t^{pv,i} - \tfrac{9+5\sqrt{10}}{13} P_{t,r,h}^{pv,i}, \forall (t \in \Omega_T, r \in \Omega_R^t, h \in \Omega_H, i \in \Omega_{pv}) \tag{3.32}$$

$$P_{t,r,h}^{pv,i} - \bar{P}_t^{pv,i} \leq (10 - \sqrt{3}) Q_{t,r,h}^{pv,i} \leq \bar{P}_t^{pv,i} - P_{t,r,h}^{pv,i}, \forall (t \in \Omega_T, r \in \Omega_R^t, h \in \Omega_H, i \in \Omega_{pv}) \tag{3.33}$$

$$-0.6\bar{P}_t^{wd,i} \leq Q_{t,r,h}^{wd,i} \leq 0.6\bar{P}_t^{wd,i}, \forall (t \in \Omega_T, r \in \Omega_R^t, h \in \Omega_H, j \in \Omega_{wd}) \tag{3.34}$$

$$\tfrac{9+5\sqrt{10}}{13} P_{t,r,h}^{wd,i} - \tfrac{15+4\sqrt{10}}{13} \bar{P}_t^{wd,i} \leq Q_{t,r,h}^{wd,i}, \forall (t \in \Omega_T, r \in \Omega_R^t, h \in \Omega_H, j \in \Omega_{wd}) \tag{3.35}$$

$$Q_{t,r,h}^{wd,i} \leq \tfrac{15+4\sqrt{10}}{13} \bar{P}_t^{wd,i} - \tfrac{9+5\sqrt{10}}{13} P_{t,r,h}^{wd,i}, \forall (t \in \Omega_T, r \in \Omega_R^t, h \in \Omega_H, j \in \Omega_{wd}) \tag{3.36}$$

$$P_{t,r,h}^{wd,i} - \bar{P}_t^{wd,i} \leq (10 - \sqrt{3}) Q_{t,r,h}^{wd,i} \leq \bar{P}_t^{wd,i} - P_{t,r,h}^{wd,i}, \forall (t \in \Omega_T, r \in \Omega_R^t, h \in \Omega_H, j \in \Omega_{wd}) \tag{3.37}$$

$$P_{t,r,h}^{pv,i} \leq \mathrm{f}_{t,r,h}^{pv} \bar{P}_t^{pv,i}, \forall (t \in \Omega_T, r \in \Omega_R^t, h \in \Omega_H, i \in \Omega_{pv}) \tag{3.38}$$

$$P_{t,r,h}^{wd,i} \leq \mathrm{f}_{t,r,h}^{wd} \bar{P}_t^{wd,i}, \forall (t \in \Omega_T, r \in \Omega_R^t, h \in \Omega_H, j \in \Omega_{wd}) \tag{3.39}$$

$$c_t^{wd,j} = (0.3125 x_t^{wd,j} + 0.6875 n_t^{wd,j}) c_t^{wd} P_{\mu}^{wd}, \forall (t \in \Omega_T, j \in \Omega_{wd}) \tag{3.40}$$

3.3.6 Voltage and current limits

In order to ensure that voltage levels meet power quality requirements and prevent conductors from operating overloaded, limits of voltage and current are established (3.41)–(3.42).

$$\underline{V}^2 \leq V_{t,r,h}^{i} \leq \overline{V}^2, \forall (t \in \Omega_T, d \in \Omega_{\widehat{D}}, h \in \Omega_H, i \in \Omega_N) \tag{3.41}$$

$$0 \leq I_{t,r,h}^{i,j} \leq \bar{I}_{a_{i,j}^0}^2 + \sum_{a \in \Omega_C} x_t^{a,i,j} (\bar{I}_a^2 - \bar{I}_{a_{i,j}^0}^2), \forall (t \in \Omega_T, r \in \Omega_R^t, h \in \Omega_H, (i,j) \in \Omega_B) \tag{3.42}$$

Figure 8 – Capability curve of DG systems

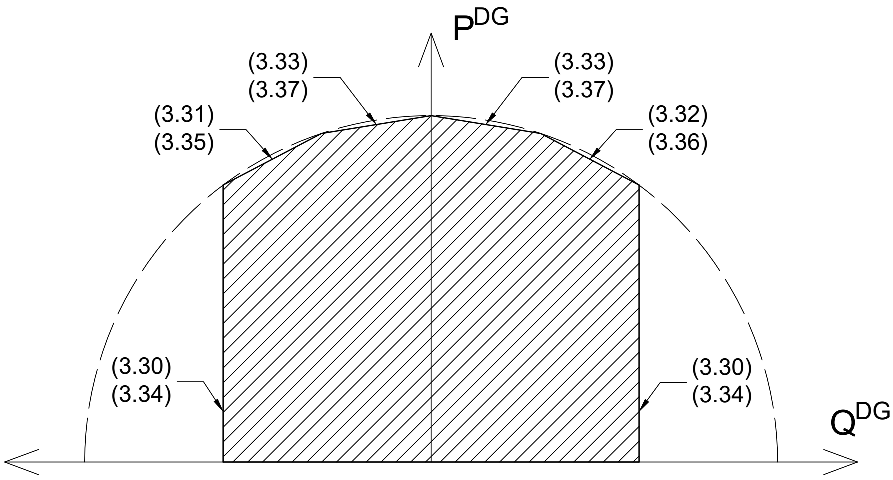

Source: Elaborated by the author.

3.3.7 Reconductoring constraints

Reconductoring consists of the replacement of conductors (by others of the same or different gauge) and/or supports (such as poles or structures). It is modeled considering that existing conductors and supports can be replaced only once within the planning horizon (3.43)–(3.46), and that the replacement is mandatory when their lifespan is attained (3.47). Also, within the lifespan of existing conductors or supports, their replacement is not expected to be by others of lesser capacity (3.48). Besides, installation requirements about mechanical correlation between conductors and supports are taken into account. Thus, it is considered that type 4 conductors or higher can be installed only in type 2 supports (3.49). The state of the variables at the initial state of network is set to 0 (3.50).

$$\sum_{a \in \Omega_C} x_t^{a,i,j} \leq 1, \forall (t \in \Omega_T, (i,j) \in \Omega_B) \tag{3.43}$$

$$x_{t-1}^{a,i,j} \leq x_t^{a,i,j}, \forall (t \in \Omega_T, (i,j) \in \Omega_B, a \in \Omega_C) \tag{3.44}$$

$$\sum_{e \in \Omega_E} z_t^{e,i,j} \leq 1, \forall (t \in \Omega_T, (i,j) \in \Omega_B) \tag{3.45}$$

$$z_{t-1}^{e,i,j} \leq z_t^{e,i,j}, \forall (t \in \Omega_T, (i,j) \in \Omega_B, e \in \Omega_{sp}) \tag{3.46}$$

$$\sum_{a \in \Omega_C} x_t^{a,i,j} = \sum_{e \in \Omega_{sp}} x_{t'}^{e,i,j} = 1,$$

$$\forall \big((i,j) \in \Omega_B, t, t' \in \Omega_T : t = \frac{T_{(i,j)_c} - T^0_{(i,j)_c}}{n_T} + 1 \wedge t' = \frac{T_{(i,j)_{sp}} - T^0_{(i,j)_{sp}}}{n_T} + 1 \big) \tag{3.47}$$

$$x_t^{a,i,j} = z_{t'}^{e,i,j} = 0,$$
$$\forall\big((i,j) \in \Omega_B, t, t' \in \Omega_T : t \leq \frac{T_{(i,j)_c} - T^0_{(i,j)_c}}{n_T} \wedge t' \leq \frac{T_{(i,j)_{sp}} - T^0_{(i,j)_{sp}}}{n_T},$$
$$a \in \Omega_C : a \leq a^0_{i,j}, e \in \Omega_E : e \leq e^0_{i,j}\big) \tag{3.48}$$

$$\sum_{a \in \Omega_C : a \geq 4} x_t^{a,i,j} \leq z_t^{2,i,j}, \forall(t \in \Omega_T, (i,j) \in \Omega_B) \tag{3.49}$$

$$x_0^{a,i,j} = z_0^{e,i,j} = 0, \forall((i,j) \in \Omega_B, a \in \Omega_C, e \in \Omega_{sp}) \tag{3.50}$$

3.3.8 Reactive compensation modeling

In order to supply reactive power, help control voltage level and improve operation efficiency, the following equipment are considered: fixed CBs, switchable CBs and SVCs. The capacity of each CB is limited by a maximum number of modules that can be integrated in a bank (3.51). The operation of switchable CBs is limited by their nominal capacity (3.52). The reactive power supplied by both fixed and switchable CBs is calculated in (3.53), while that provided by SVC is modeled in (3.54). Note that the SVC capacity is set to be the same of the CB modules in order to allow a continuous reactive compensation at least cost. Also, the installation of at most one SVC per node is expected over the horizon planning (3.55). The decision of installing fixed or switchable CBs is modeled through (3.56) and (3.57), respectively. Investment costs of fixed and switchable CBs are modeled via (3.58) and (3.59), respectively.

$$\bar{m}_t^{fcb,i}, \bar{m}_t^{scb,i} \leq m_{max}^{cb}, \forall(t \in \Omega_T, i \in \Omega_{rc}) \tag{3.51}$$

$$m_{t,r,h}^{scb,i} \leq \sum_{t'=1}^{t} n_{t'}^{scb,i}, \forall(t \in \Omega_T, r \in \Omega_R^t, h \in \Omega_H, i \in \Omega_{rc}) \tag{3.52}$$

$$Q_{t,r,h}^{cb,i} = \left(\sum_{t'=1}^{t} \bar{m}_{t'}^{fcb,i} + m_{t,d,h}^{scb,i}\right) Q_\mu^{cb}, \forall(t \in \Omega_T, r \in \Omega_R^t, h \in \Omega_H, i \in \Omega_{rc}) \tag{3.53}$$

$$Q_{t,r,h}^{svc,i} \leq \sum_{t'=1}^{t} x_{t'}^{svc,i} Q_\mu^{cb}, \forall(t \in \Omega_T, r \in \Omega_R^t, h \in \Omega_H, i \in \Omega_{rc}) \tag{3.54}$$

$$\sum_{t' \in T} x_{t'}^{svc,i} \leq 1, \forall i \in \Omega_{rc} \tag{3.55}$$

$$x_t^{fcb,i} \geq \bar{m}_t^{fcb,i} / m_{max}^{cb}, \forall(t \in \Omega_T, i \in \Omega_{rc}) \tag{3.56}$$

$$x_t^{scb,i} \geq \bar{m}_t^{scb,i} / m_{max}^{cb}, \forall(t \in \Omega_T, i \in \Omega_{rc}) \tag{3.57}$$

$$c_t^{fcb,i} = c_f^{fcb} x_t^{fcb,i} + c_v^{fcb} \bar{m}_t^{fcb,i}, \forall (t \in \Omega_T, i \in \Omega_{rc}) \tag{3.58}$$

$$c_t^{scb,i} = c_f^{scb} x_t^{scb,i} + c_v^{scb} \bar{m}_t^{scb,i}, \forall (t \in \Omega_T, i \in \Omega_{rc}) \tag{3.59}$$

3.3.9 VR modeling

Considering that commercial voltage regulators usually provide a considerable number of steps, and taking into account that the planning has a long-term scope, the voltage regulation by VRs is considered as a continuous variable (TABARES *et al.*, 2016). Also, it is considered that VRs are installed next to the sending nodes of branches. Thus, the range regulation for ΔV is established in (3.60). The decision of installing VRs is modeled through (3.61)–(3.62). Note that only one VR (at most) is expected to be installed per branch over the horizon planning (3.63). Additionally, the power capacity limit is modeled in (3.64).

$$V_{t,r,h}^{i}(-2v_R + v_R^2) \leq \Delta V_{t,r,h}^{i} \leq V_{t,r,h}^{i}(2v_R + v_R^2), \forall (t \in \Omega_T, r \in \Omega_R^t, h \in \Omega_H, (i,j) \in \Omega_{vr}) \tag{3.60}$$

$$\varkappa_t^{i,j} \geq \max\left(\frac{-\Delta V_{t,r,h}^{i}}{\overline{V}^2(-2v_R + v_R^2)}, \frac{\Delta V_{t,r,h}^{i}}{\overline{V}^2(2v_R + v_R^2)} \right), \forall (t \in \Omega_T, r \in \Omega_R^t, h \in \Omega_H, (i,j) \in \Omega_{vr}) \tag{3.61}$$

$$\varkappa_t^{i,j} = \sum_{t'=1}^{t} \sum_{v \in \Omega_{vr}} \varkappa_t^{v,i,j}, \forall (t \in \Omega_T, (i,j) \in \Omega_{vr}) \tag{3.62}$$

$$\sum_{t' \in \Omega_T} \sum_{v \in \Omega_{vr}} \varkappa_{t'}^{v,i,j} \leq 1, \forall (i,j) \in \Omega_{vr} \tag{3.63}$$

$$M_{vr}(1 - \varkappa_t^{i,j}) + \sum_{t'=1}^{t} \sum_{v \in \Omega_{vr}} \varkappa_t^{v,i,j} \bar{I}_{vr,v}^2 \geq I_{t,r,h}^{i,j}, \forall (t \in \Omega_T, r \in \Omega_R^t, h \in \Omega_H, (i,j) \in \Omega_{vr}) \tag{3.64}$$

3.3.10 EES system constraints

EES systems are constituted by modules of a given storage duration (3.65)–(3.66). Physical space limits (most likely in substations) are considered in (3.67). Then, the nodal EES system capacity and rated power in each planning period is calculated taking into account that the lifespan of EES systems is less than the planning horizon (3.68). Intra-day energy balance, with hourly transition, is modeled through (3.69). Here, charging and discharging losses are considered, while self-discharging losses are omitted because of their negligible values. To ensure that inter-day energy balance is accomplished, energy stored at the beginning and at the end of each day are set to be the same (3.70). Also, it is taken into account that the charge of EES systems can not fall more than a predefined level, and that it is bounded above by its storage nominal capacity (3.71). The power exchange is limited by the rated power of the EES systems, and, since charging and discharging are not expected to happen simultaneously, this condition can be formulated by (3.72). Besides, it is considered that EES systems can be installed with a given initial charge, which is limited in each planning period by (3.73).

$$P_t^{ees,i} = n_t^{ees,i} P_\mu^{ees}, \forall (t \in \Omega_T, i \in \Omega_{ees}) \tag{3.65}$$

$$E_t^{ees,i} = \kappa P_t^{ees,i}, \forall (t \in \Omega_T, i \in \Omega_{ees}) \tag{3.66}$$

$$\sum_{t'=1}^{t} n_{t'}^{ees,i} \leq n_{max}^{ees,i}, \forall (t \in \Omega_T, i \in \Omega_{ees}) \tag{3.67}$$

$$\left[\bar{P}_t^{ees,i}, \bar{E}_t^{ees,i} \right] = \left[\sum_{t'=\max(1,t-2)}^{t} P_{t'}^{ees,i}, \sum_{t'=\max(1,t-2)}^{t} E_{t'}^{ees,i} \right], \forall (t \in \Omega_T, i \in \Omega_{ees}) \tag{3.68}$$

$$E_{t,r,h}^{ees,i} = E_{t,r,h-1}^{ees,i} + \eta_{ch}^{ees} P_{t,r,h}^{-ees,i} - \frac{P_{t,r,h}^{+ees,i}}{\eta_{dch}^{ees}}, \forall (t \in \Omega_T, r \in \Omega_R^t, h \in \Omega_H, i \in \Omega_{ees}) \tag{3.69}$$

$$E_{t,0}^{ees,i} = E_{t,r,0}^{ees,i} = E_{t,r,24}^{ees,i}, \forall (t \in \Omega_T, r \in \Omega_R^t, i \in \Omega_{ees}) \tag{3.70}$$

$$soc_{min}^{ees} \bar{E}_t^{ees,i} \leq E_{t,r,h}^{ees} \leq \bar{E}_t^{ees,i}, \forall (t \in \Omega_T, r \in \Omega_R^t, h \in \Omega_H, i \in \Omega_{ees}) \tag{3.71}$$

$$P_{t,r,h}^{+ees,i} + P_{t,r,h}^{-ees,i} \leq \bar{P}_t^{ees,i}, \forall (t \in \Omega_T, r \in \Omega_R^t, h \in \Omega_H, i \in \Omega_{ees}) \tag{3.72}$$

$$\begin{aligned} &E_{t-1,0}^{ees,i} \leq E_{t,0}^{ees,i} \leq E_{t-1,0}^{ees,i} + \bar{E}_t^{ees,i}, \\ &\forall (t \in \Omega_T : t > 1, r \in \Omega_R^t, h \in \Omega_H, i \in \Omega_{ees}) \end{aligned} \tag{3.73}$$

3.3.11 Reduction of CO_2 emissions

Global electricity generation mix has a considerable participation of fossil fuels (IEA, 2020). In that sense, energy bought by the DISCO can be associated with significant CO_2 emissions. On the other hand, EV adoption increases electrical demand but reduces CO_2 emissions from the replaced combustion vehicles. In order to evaluate the temporal variation of CO_2 emissions, including EV impact, the expected annual average CO_2 emissions from distribution system operation for each planning period and the estimated annual CO_2 emissions at the beginning of the planning horizon from the combustion vehicles to be replaced (until the end of a given planning period) are calculated via (3.74) and (3.75), respectively. Note that to estimate the number of the combustion vehicles to be replaced it is assumed that 70% of new EV owners replaced their old engine combustion vehicles, while the remaining 30% acquired a vehicle for the first time (3.76). Finally, to ensure a periodical reduction of CO_2 emissions, a reduction of $\alpha\%$ is established per planning period regarding the pre-planning emission levels (3.77).

$$\xi_{S,t}^{co_2} = \sum_{i\in\Omega_{ss}} \sum_{r\in\Omega_R^t} \sum_{h\in\Omega_H} 365\pi_{t,r}\Gamma_{t,h}^{co_2} P_{t,r,h}^{ss,i}, \forall t \in \Omega_T \tag{3.74}$$

$$\xi_{cv,0}^{co_2,t} = 365 n_t^{cv} \varepsilon_{cv}^{co_2} \bar{\ell}, \forall t \in \Omega_T \tag{3.75}$$

$$n_t^{cv} = 0.7(n_t^{ev} - n_0^{ev}), \forall t \in \Omega_T \tag{3.76}$$

$$\xi_{S,t}^{co_2} \leq (1-\alpha\%)^t \left(\xi_{S,0}^{co_2} + \xi_{cv,0}^{co_2,t}\right), \forall t \in \Omega_T \tag{3.77}$$

4 SOLUTION TECHNIQUE

Techniques that use mathematical tools for the design of heuristics are known as matheuristics (BOSCHETTI; MANIEZZO, 2022). In this context, the proposed solution technique corresponds to a novel matheuristic technique that consist in an iterative local search algorithm based on mathematical programming. The proposed method solves the planning model (proposed in Chapter 3) successively around a given operating reference point that is updated and improved at each iteration while reducing neighborhood search until getting a high quality feasible solution. The neighborhood reduction is made implicitly through the application of penalty functions that penalize the feasibility error regarding the original non-convex MINLP planning model.

It is important mentioning that this solution technique is mainly proposed to handle the non-convexity and non-linearity of the planning problem. Thus, the heuristic part of the method is concern with the solution feasibility (regarding the original non-convex MINLP planning model), while the mathematical programming guarantees the optimality of incumbent solutions. Unlike the traditional heuristic approaches that look for local optimal solutions in different sub-spaces of the feasibility region, the proposed solution technique seek global optimums in neighborhood spaces (not necessarily inside the feasibility region) that are likely to include the global optimum of the original planning problem. The philosophy of the proposal is summarized in Fig. 9. The proposed model has been formulated around the reference point $(P^{ss,*}, Q^{ss,*}, P^{*}, Q^{*}, V^{*}, I^{*})$ (3.14)–(3.17), (3.19). This reference point is trivially determined in the first iteration and then is updated at each iteration. Note that the physical relationship among their components needs to be considered (4.1)–(4.3).

$$I^{i,j,*}_{t,r,h} = \frac{{P^{i,j,*}_{t,r,h}}^2 + {Q^{i,j,*}_{t,r,h}}^2}{V^{j,*}_{t,r,h}}, \forall (t \in \Omega_T, r \in \Omega^t_R, h \in \Omega_H, (i,j) \in \Omega_{\bar{B}}) \tag{4.1}$$

$$P^{ss,i',*}_{t,r,h} = P^{i',i,*}_{t,r,h} + R^{i,*}_{ss} I^{i',i,*}_{t,r,h} + L^{i}_{ss}, \forall (t \in \Omega_T, r \in \Omega^t_R, h \in \Omega_H, i \in \Omega_{ss}) \tag{4.2}$$

$$Q^{ss,i',*}_{t,r,h} = Q^{i',i,*}_{t,r,h} + X^{i}_{ss} I^{i',i,*}_{t,r,h}, \forall (t \in \Omega_T, r \in \Omega^t_R, h \in \Omega_H, i \in \Omega_{ss}) \tag{4.3}$$

4.1 MATHEMATICAL JUSTIFICATION

The feasibility of the solution regarding the original non-convex MINLP planning model is guaranteed through the fulfillment of the conditions (necessary and sufficient) given by (4.4)–(4.5). Here, note that the solution of the proposed model satisfies the exact model when $I = I^*$

Figure 9 – Sketch of the solution technique heuristics

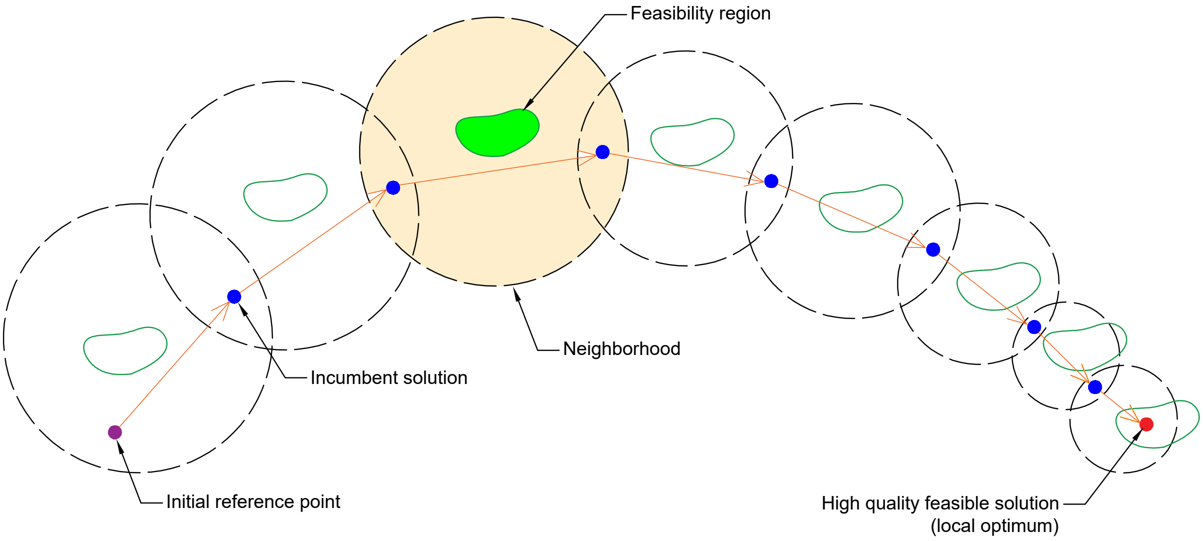

Source: Elaborated by the author.

(3.14)–(3.16), $(P,Q) = (P^*,Q^*)$ (3.16)–(3.17), $\Delta = 0$ (3.17) and $(P^{ss},Q^{ss}) = (P^{ss,*},Q^{ss,*})$ (3.16). To accomplish that, a successive local search process that aims for (P,Q,V) and (P^*,Q^*,V^*) to converge while reducing Δ is used. Note that $(P,Q,V) = (P^*,Q^*,V^*) \rightarrow I = I^*, P^{ss} = P^{ss,*}, Q^{ss} = Q^{ss,*}$.

$$\begin{aligned}&(P^{i,j}_{t,r,h}, Q^{i,j}_{t,r,h}, V^{j}_{t,r,h}, I^{i,j}_{t,r,h}) = (P^{i,j,*}_{t,r,h}, Q^{i,j,*}_{t,r,h}, V^{j,*}_{t,r,h}, I^{i,j,*}_{t,r,h}),\\ &\forall (t \in \Omega_T, r \in \Omega^t_R, h \in \Omega_H, (i,j) \in \Omega_{\bar{B}})\end{aligned} \tag{4.4}$$

$$\Delta^{i,j}_{t,r,h} = 0, \forall (t \in \Omega_T, r \in \Omega^t_R, h \in \Omega_H, (i,j) \in \Omega_{\bar{B}}) \tag{4.5}$$

In order to ensure convergence, a feasibility error function (penalty function), f_ξ, is defined and included in the objective function (4.6)–(4.7). Note that f_ξ includes error coefficients M_1, M_2 and M_3 that are updated at each iteration. Also, when $f_\xi \rightarrow 0$ and M_1, M_2, M_3 are large enough, then $\xi_\Delta, \xi_p, \xi_q \rightarrow 0$ and $\Delta = 0, (P,Q) = (P^*,Q^*)$. Besides, given the narrow limits imposed to V (3.41) and because of the iterative process, V is driven to converge and fulfill $V = V^*$ (which is verified in practice). Thus, at the final of the solution process both (4.4) and (4.5) will be satisfied.

$$f_\xi = M_1 \xi_\Delta + M_2 \xi_p + M_3 \xi_q, \tag{4.6}$$

$$[\xi_\Delta, \xi_p, \xi_q] = \sum_{\substack{t \in \Omega_T, r \in \Omega^t_R,\\ h \in \Omega_H, (i,j) \in \Omega_B}} [\Delta^{i,j}_{t,r,h}, (P^{i,j}_{t,r,h} - P^{i,j,*}_{t,r,h})^2, (Q^{i,j}_{t,r,h} - Q^{i,j,*}_{t,r,h})^2] \tag{4.7}$$

On the other hand, since the feasibility error function corresponds to a quadratic expression and all the constrains of the proposed model are linear, the resulting optimization model corresponds to a convex MIQP model. Here, it is worth indicating that since MIQP solvers are based on MILP techniques, MIQP is not expected to be much more expensive than MILP, while it is less expensive than MISOCP (BLIEK; BONAMI; LODI, 2014).

4.2 METHODOLOGY

The solution technique consists in an iterative process that improves the incumbent solution feasibility until obtaining a feasible solution regarding the original non-convex MINLP problem. For that, the planning problem modeled through (3.4)–(3.77) is iteratively solved while updating both the operating reference points and the error coefficients. The update of error coefficients is based on the variation of the feasibility error, measured according the metric proposed in (4.8)–(4.9). Note that this metric determines the greatest average error of feasibility, which in practice presents enough precision for planning purposes. Instead, for problems that need to focus on feasibility the ∞ - norm can be employed. Additionally, in order to establish a metric that can measure the solution feasibility for different solution techniques, (4.10)–(4.11) are proposed, which measure the deviation regarding the P,Q,V,I relationship: $P^2+Q^2=VI$.

$$\bar{\xi}_{feas} = \sqrt{\frac{\xi_{max}}{\sum_{t\in\Omega_T} |\Omega_R^t \times \Omega_H \times \Omega_B|}} \tag{4.8}$$

$$\xi_{max} = \max\left(\xi_\Delta, \xi_p, \xi_q\right) \tag{4.9}$$

$$\xi_{t,r,h}^{lin,i,j} = \left| \sqrt{V_{t,r,h}^{j} I_{t,r,h}^{i,j}} - \sqrt{{P_{t,r,h}^{i,j}}^2 + {Q_{t,r,h}^{i,j}}^2} \right|, \forall (t\in\Omega_T, r\in\Omega_R^t, h\in\Omega_H, (i,j)\in\Omega_B) \tag{4.10}$$

$$\xi_{max}^{lin} = \max_{t\in\Omega_T, r\in\Omega_R^t, h\in\Omega_H, (i,j)\in\Omega_B} \xi_{t,d,h}^{lin,i,j} \tag{4.11}$$

The solution technique is divided in three stages: relaxed, integral and feasibility fix. Each of them is described below. Also, the error coefficient update immersed in the solution process is explained.

4.2.1 Relaxed stage

The objective of this stage is to obtain a good quality reference point (P^*, Q^*, V^*, I^*) in a relative short time, before moving to the integral stage, which is expected to be computationally more expensive. The stage starts with a predefined trivial reference point and it finishes when a given feasibility exactness is reached ($\xi_{feas} \leq \varepsilon_R$). It is composed of the following steps:

(i) Relax integrality assuming integer variables as continuous.

(ii) Set $k := 1$, $(P^*, Q^*, V^*) = (0,0,1)$ and $M_1 = M_2 = M_3 = 0$. Then, solve the resulting Linear Programming (LP) problem.

(iii) Set $k := k+1$ and $(P^*, Q^*, V^*) = (P,Q,V)^{inc}_{k-1}$. Set $P^{ss,*}, Q^{ss,*}, I^*$ according (4.1)–(4.3). Update M_1, M_2 and M_3. Then, solve the resulting convex Quadratic Programming (QP) problem.

(iv) Repeat (iii) until $\xi_{feas} \leq \varepsilon_R$. Then, pass to the integral stage

It is worth indicating that the solution of this stage corresponds to a local and approximate relaxed solution of the problem. Thus, it is likely to be an approximate lower bound for the integral problem.

4.2.2 Integral stage

This stage seeks to find a very good quality solution for the integer variables involved in the investment cost. The stage consists of the following steps:

(i) Resume integrality and set the optimality gap so that $gap \leq g_I$.

(ii) Set $k := k+1$ and $(P^*, Q^*, V^*) = (P,Q,V)^{inc}_{k-1}$. Set $P^{ss,*}, Q^{ss,*}, I^*$ according (4.1)–(4.3). Keep the values of M_1, M_2 and M_3. Then, solve the resulting convex MIQP problem.

4.2.3 Feasibility fix stage

Based on the nature of the proposed heuristic, the solution found in the integral stage is expected to be of high quality in terms of investment decisions. However, the feasibility error of the solution found in the integral stage is not expected to be lower than the one of the relaxed stage. Thus, it is necessary to fix the feasibility of the current solution keeping fixed the values of the discrete variables associated with investment decisions. For that, the following steps are performed.

(i) Fix the integer variables related to investment costs, i.e., $x_t^{ss,u,i}, x_t^{oltc,i}, n_t^{wd,i}, \bar{P}_t^{pv,i}, n_t^{ees,i}, x_t^{fcb,i}$, $x_t^{scb,i}, x_t^{svc,i}, m_t^{fcb,i}, m_t^{scb,i}, \varkappa_t^{v,i,j}, x_t^{a,i,j}$ and $z_t^{e,i,j}$.

(ii) Set $k := k+1$, $(P^*, Q^*, V^*) = (P,Q,V)^{inc}_{k-1}$ and $I^* = (P^{*2} + Q^{*2})/V^*$. Set $P^{ss,*}, Q^{ss,*}, I^*$ according (4.1)–(4.3). Update M_1, M_2 and M_3. Then, solve the resulting convex QP or MIQP problem.

(iii) Repeat (ii) until $\xi_{feas} \leq \varepsilon_S$.

It is worth indicating that a variation of the proposed technique has been implemented by Marcelo *et al.* (2023), where the solution process is divided only in two stages: relaxed and integral. In the integral stage several MIQP problems are solved reducing the optimization gap along the iterations. However, after several tests it has been note that the integer variables related to investment do not change along the integral stage. Also, it has been noticed that the solution quality depends more on the initial *gap* than on the subsequent *gaps* of the integral stage (despite that they may have a lower value). Thus, the current proposal considers only one iteration for the integral stage (with a reduced optimization gap) and incorporates a feasibility fix stage.

4.2.4 Error coefficient update

It is important to note that the performance of the solution process (including the quality of the solution) depends on the adequate selection of the error coefficients. For example, take large values for M_1, M_2 and M_3 may accelerate the convergence, but it probably will lead to local optimus not close to the global optimal. On the other hand, keep M_1, M_2 and M_3 with small values can make convergence difficult without significant gain in optimality. Thus, an update process that offers equilibrium between convergence and optimality is presented as follows. Note that the subscript $(|k)$ indicates that the parameter or variable value corresponds to the iteration k.

- $k = 2$: For the sake of simplicity, M_1 and M_2 are set as powers of 10. Their significant values are initialized based on the results of the iteration 1, so that each term of f_ξ does not represent more than about 10% of the objective function value (4.12).

$$M_{1|2} = M_{2|2} = M_{3|2} = 10^{\lfloor \log\left(0.1 C_{T|1} / \xi_{max|1}\right) \rceil} \tag{4.12}$$

- $k > 2$: In order to get a soft convergence and not lose optimality looking for feasibility, only the coefficient corresponding to the maximum error can be upgraded, provided it has not improved enough. For that, it is considered that an error improves enough if it is less than or equal to $\varphi\%$ of its previous value (4.13)–(4.15).

$$M_{1|k} = M_{1|k\text{-}1} \cdot 10^{\langle \xi_{\Delta|k\text{-}1} = \xi_{max|k\text{-}1} > \varphi\% \xi_{max|k\text{-}2} \rangle} \tag{4.13}$$

$$M_{2|k} = M_{2|k\text{-}1} \cdot 10^{\langle \xi_{p|k\text{-}1} = \xi_{max|k\text{-}1} > \varphi\% \xi_{max|k\text{-}2} \rangle} \tag{4.14}$$

$$M_{3|k} = M_{3|k\text{-}1} \cdot 10^{\langle \xi_{q|k\text{-}1} = \xi_{max|k\text{-}1} > \varphi\% \xi_{max|k\text{-}2} \rangle} \tag{4.15}$$

Finally, the proposed methodology is summarized in Fig. 10.

Figure 10 – Block diagram of the solution technique methodology

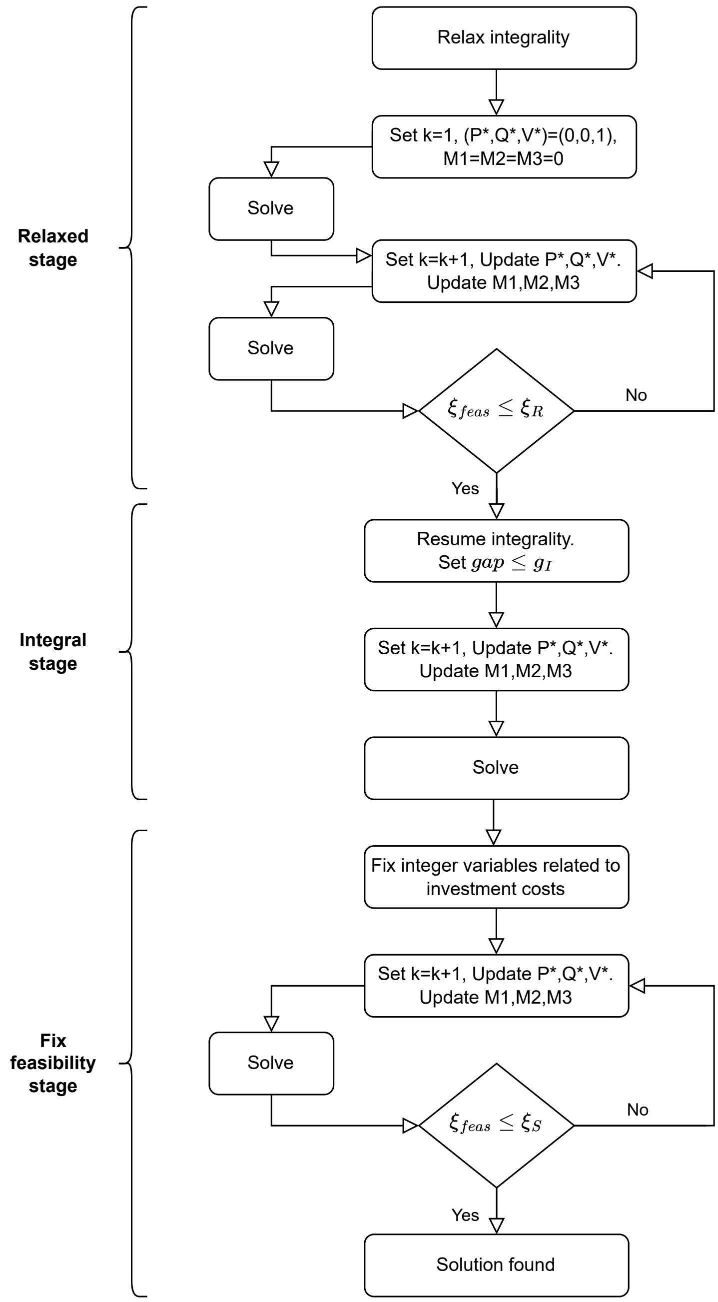

Source: Elaborated by the author.

5 CASE STUDY AND RESULTS

The proposed methodology is implemented in the AMPL language and solved with Gurobi version 10.0.1. The computer used for this purpose has an Intel processor i7-8700@3.20GHz and 16 Gb of RAM. A 69-node distribution system is used to show the performance of the model. On this system, three case studies are carried on in order to show the advantages of considering the uncertainties in the problem modeling and the advantages of properly selecting the ROSs. Thus, Case I consider the problem modeled with forecast values (without uncertainties) and traditional K-means, Case II includes uncertainties and uses traditional K-means, and Case III consider uncertainties and the proposed robust K-means. Additionally, the methodology is computationally implemented on a real 135-node distribution system in order to show the performance of the proposal for simulating real systems.

5.1 TEST SYSTEMS

The 69-node test system is based on that described by Chakravorty and Das (2001). It has a maximum demand of 5,697 kVA (4,625kW and 3,326 kVAr) at the beginning of planning horizon, which is expected to expand to 9,559 kVA (7,841 kW and 5,467 kVAr) at the final of planning horizon. These demands include EV loads and prosumer participation. The number of EVs and the prosumer penetration at the beginning of planning horizon are 28 and 2.5%, respectively. These values are expected to increase to 2959 and 35%, respectively, at the final of planning horizon. The network is mainly composed by a substation (equipped with no-load voltage regulating transformers), conductors and supports. The substation has a nominal power of 7,500 kVA, nominal voltage of 12.66 kV and an elapsed life of 20 years. The capacities of the lines and supports are indicated in the Annex A, which also includes the nominal power of each node of the system at the beginning of the planning horizon.

The real 135-node system corresponds to that presented by Mantovani, Casari and Romero (2000). It has a maximum demand of 20,227 kVA (18,568kW and 8,021 kVAr) at the beginning of planning horizon, which is expected to expand to 34,163 kVA (31,583 kW and 13,023 kVAr) at the final of planning horizon. The number of EVs and the prosumer penetration at the beginning of planning horizon are 104 and 2.5%, respectively. These values are expected to increase to 11,881 and 35%, respectively, at the final of planning horizon. The network is mainly composed by two substations (equipped with no-load voltage regulating transformers), conductors and supports. The substations have nominal powers (and elapsed lifes) of 10 MVA (20 years) and 15 MVA (15 years), at nodes 0 and 1, respectively. The capacities of the lines and supports are indicated in the Annex B, which also includes the nominal power of each node of the system at the beginning of the planning horizon.

The topologies of the 69-node test system and the real 135-node system are shown in Fig. 11 and Fig. 12, respectively.

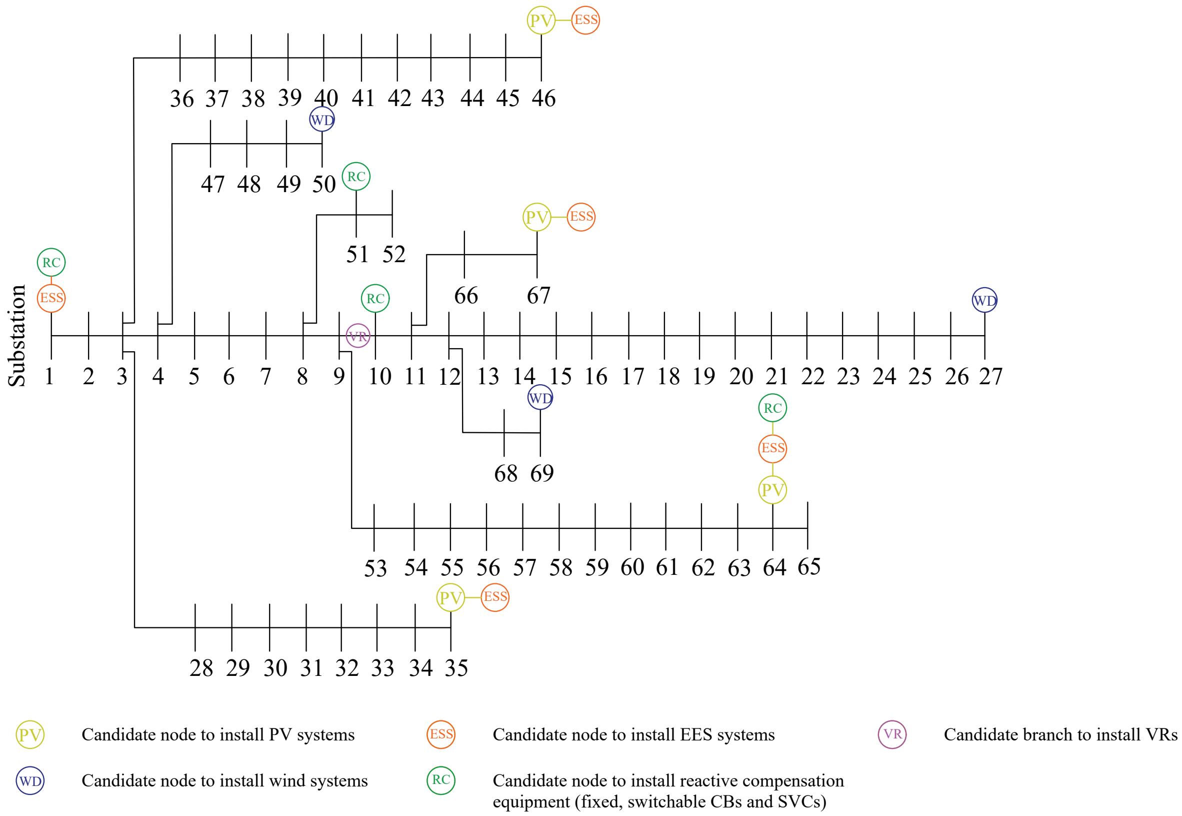

Figure 11 – Topology and candidate location for equipment installation of the 69-node test system

Source: Adapted from Chakravorty and Das (2001).

5.2 PLANNING DATA

Planning data aim at defining the scopes of the system planning and simulating the actual operating, economic and environmental contexts surrounding the distribution system operation. These data are presented below.

- The planning horizon and the duration of each planning period are 20 and 5 years, respectively.
- The discount rate is 10%.

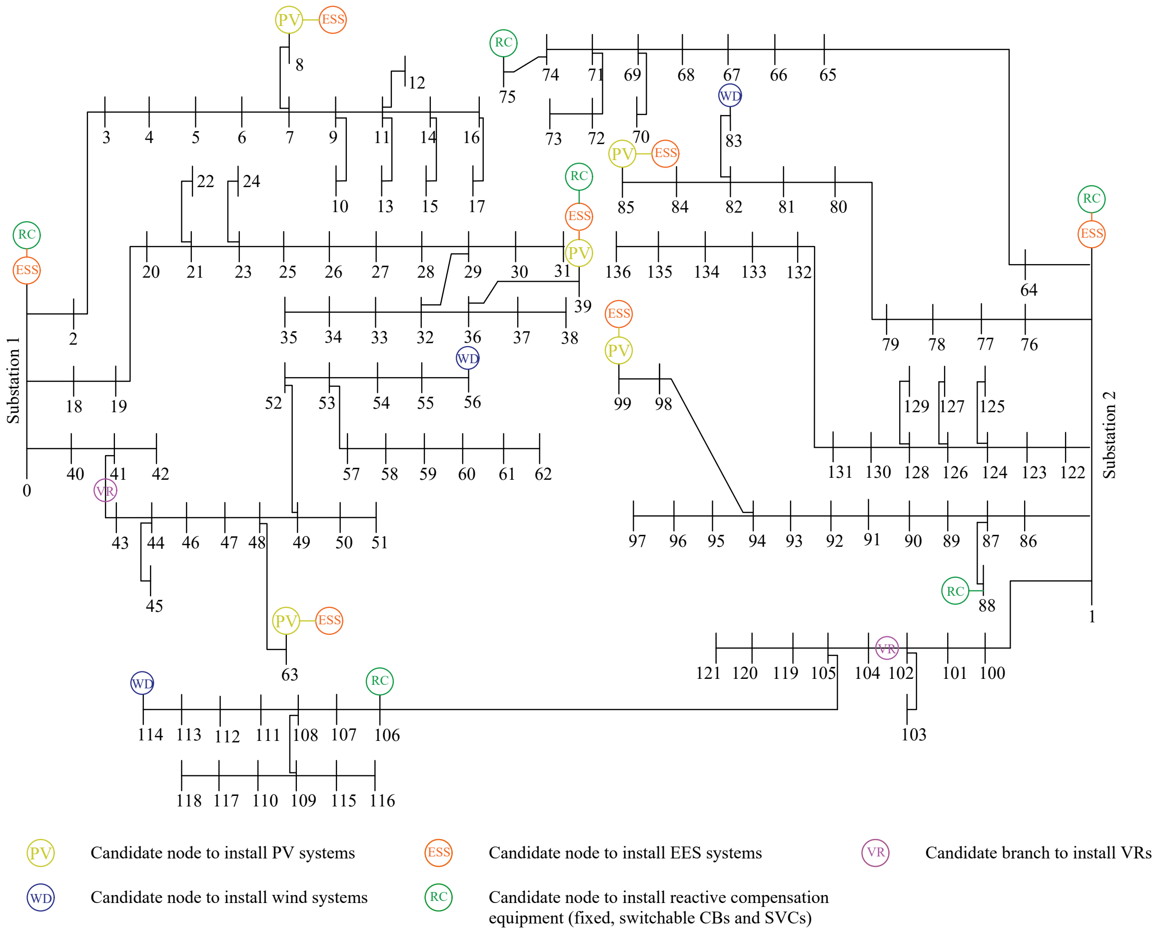

Figure 12 – Topology and candidate location for equipment installation of the real 135-node system

Source: Adapted from Mantovani, Casari and Romero (2000).

- The locations of the distribution systems are in Bahia State, Brazil (latitude: -11.43° and longitude: -42.50°). Thus, the availability and potential of the energy resources considered in this work correspond to this location.

- The price and CO_2 intensity of the energy purchased at substations are given in hourly intervals over a day for each planning period. Their values are presented in the Annex C and are based on the scenario viewer prepared by Gagnon, Cowiestoll and Schwarz (2023).

- The primary voltage of substation transformers are assumed to have a constant value of 1 p.u. The power factor limits established by the TSO at the transmission/distribution interface are 0.90 inductive and 0.95 capacitive. The costs of the substations according their capacities are shown in the Annex D, while the OLTC cost is $12,000.

- DG systems allow to set their power factors between 0.9 inductive and 0.95 capacitive without reducing their nominal powers. Prosumer's DG systems generate energy with a constant inductive power factor of 0.95.

- There are 5 types of conductors and 2 types of structures. The reconductoring costs are shown in the Annex D.

- CBs are made with modules of 300 kVAr (with a maximum of 5). The fixed and variable investment costs for fixed CBs are $3,865 and $860/unit, respectively, while for switchable CBs, they are $6,300 and $950/unit, respectively. The cost of an SVC of 300 kVAr is $10,000.

- There are 4 types of VRs, whose capacities and costs are presented in the Annex D.

- Investment and O&M costs for DG and EES system are obtain from NREL (2023) and are presented in the Annex D.

- The storage duration of EES systems is 4h, i.e., EES systems have the capacity to store energy during 4h at their rated power. Their minimum SOC is 20%.

- The lifetime of the distribution system assets, existing and to be installed, are presented in Table 3.

- The candidate nodes for the installation of DER equipment (DG and EES systems), reactive compensation devices (fixed, switchable CBs and SVCs) and the candidate branches for VR installation, for the 69-node test system and the real 135-node system, are indicated in Fig. 11 and Fig. 12, respectively. It is assumed that some extreme nodes have free surrounded space where DG systems can be allocated. Since PV systems usually present a greater generation in short periods of time (especially around midday) compared to wind systems, they are more predisposed to requiring energy storage. Thus, the allocation of EES systems is considered in the candidate nodes for PV system installation. Reactive compensation devices are allocated in nodes with greater demand of reactive power, central nodes and nodes most distant from the substations. Candidate branches for VR installation correspond to branches that are expected to present large power flow variations.

- The expected quantity of EVs per node for selected years is presented in Appendix A. The power factor of the EV chargers is 0.98. The charging preferences are indicated in the Table 4. It is assumed that EVCSs will be installed at the nodes 17; 41,57; 5, at the beginning of the planning periods 2, 3 e 4, respectively. Here, note that the allocation of EVCSs depends on both the distribution network and the transportation network. Thus, it is beyond the scope of this work. However, to know more about that topic, the works proposed by Mejia *et al.* (2023) and Unterluggauer *et al.* (2022) can be consulted.

- For the first planning period the number of ROSs is 6 and the initial clustering centroids corresponds to the scenarios of minimum demand, maximum demand, minimum PV generation, maximum PV generation, minimum wind generation and maximum wind generation; for the rest of planning periods the number of ROSs is 4 and the initial clustering centroids corresponds to the scenarios of minimum demand, maximum demand, minimum PV generation and minimum wind generation. This difference about the quantity of ROSs is because the main objective of planning problem is to determine the optimal short-term investment actions, therefore the operation of the first planning period is more accurately represented.

- The weights used to determine the robust ROSs are $[w_D, w_R, w_{pv}, w_{wd}] = [1, 0.8, 0.7, 0.35]$ for the operating parameters and $\omega_1^t = \omega_2^t = 2, \forall t \in \Omega_T$ and $\omega_r^t = 1, \forall t \in \Omega_T, r \in \Omega_R^t : r > 2$ for the centroid distances. Thus, since the scenarios of minimum and maximum demand are critical they are set to be more representative.

- The values of the parameters used in the solution technique are $\varepsilon_R = 10, \varepsilon_S = 0.5, g_I = 0.1\%$ and $\varphi\% = 0.7$. Note that the linearization exactness $\varepsilon_I = 0.5$ (kVA) is good enough for planning purposes in a system where the mean power flow is above 1MVA. The desired CO_2 reduction after each planning period is 16.32% in order to achieve the Paris Agreement goals (IRENA, 2019).

5.3 SIMULATION OF THE OPERATING CONDITIONS

In this section the operating conditions of the system are determined over the planning horizon. This is made taken into account the modeling methodologies presented in Chapter 2 and Section 3.1.

In order to show the demand aggregation along the planning horizon, conventional demand, EV load and prosumer generation are simulated for a given day (e.g. day 7 of year 3) of each planning period (Fig. 13). It can be observed how the integrated demand profile resembles duck curves over time due to the increasing penetration of EVs and prosumers (mainly because of these last).

To show the scenario variability achieved by using robust ROSs, the profiles obtained for each planning are shown in Fig. 14. There, the system operating parameters for maximum and minimum demand are represented by the ROSs 1 and 2, respectively. It can be observed that maximum demand usually occurs when prosumer's production (given by PV generation) is

Table 3 – Lifespan of the system assets (years)

Equipament	Lifespan
Substations	35
OLTCs	35
Conductors	35
Supports	35
CBs	20
SVCs	25
VRs	25
PV systems	25
WD systems	25
EES systems	15

Source: Elaborated by the author.

Table 4 – EV charging preferences by charging level (%)

Period	Level 1	Level 2	Level 3
1	80	20	0
2	75	20	5
3	75	20	5
4	70	20	10

Source: Elaborated by the author.

minimum. Also, it is worth indicating that the difference between active and reactive demand profiles becomes accentuated over time (see Fig. 14, planning periods 3 and 4). Additionally, it is important to note that demand variability increases with the penetration of prosumers and EVs, e.g, for the ROSs corresponding to planning period 1, active demand factors vary from 0.4 to 0.94 in Case I, while they vary from 0.15 to 1 for planning period 4. This increased variability also happens because of uncertainties, since forecast uncertainty increases over time.

5.4 RESULTS

In order to effectively discuss the results, they will be structured as follows. It is worth mentioning that the first four points correspond to the implementation of the model on the 69-node distribution test system.

Figure 13 – Demand integration by planning period

Source: Elaborated by the author.

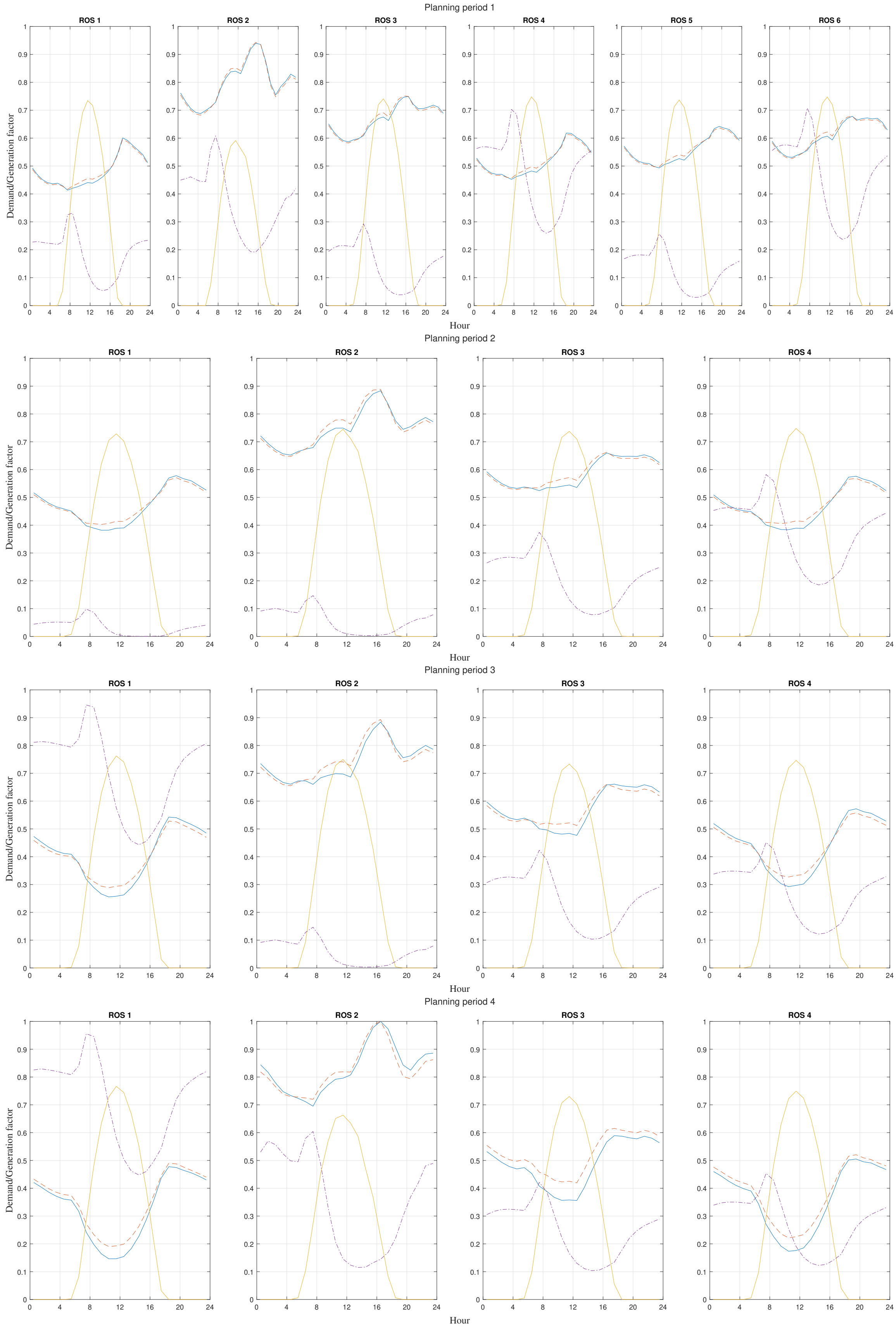

Figure 14 – Robust ROSs for each planning period

Source: Elaborated by the author.

(i) Presentation and analysis of solution overview, in economic terms, for each case study.

(ii) Discussion of the investment plans for Cases I and II.

(iii) Analysis of key aspects of the network operation along the planning horizon.

(iv) Assessment of planning reliability for all cases through simulations on random operating scenarios.

(v) Discussion of the performance of the solution technique

(vi) Presentation and analysis of solution overview, in economic terms, for the Cases I and II, for the real 135-node distribution system.

5.4.1 Solution overview

The solution overview is summarized in Table 5. It shows the costs over the planning horizon corresponding to distribution and energy supply (including the cost of the existing assets). Here, it is worth indicating that this cost structure is preferred over the usual one used in the literature, based on investment and O&M costs, since electricity rates and DISCO accounting are based on this structure. Also, this structure allows to distribute the costs between consumers and prosumers when needed (MARCELO; RUPOLO; MANTOVANI, 2021). This is because consumers are expected to pay both energy and distribution costs, while prosumers only the distribution one.

It can be observed that both distribution and energy costs increase in the order of the Cases I, II and III. Comparing Cases I and II, this happen because Case I only considers expected forecast scenarios, losing the variability carried by possible uncertainty realizations. Thus, the results of the Case I are expected to be less robust and less expensive than Case II. Particularly, in Case I, less is invested in SVCs and EES systems, both devices that add considerable flexibility to the system in terms of reactive and active power, respectively. Regarding Case III in relation to Case II, the costs are increased because Case III considers more robust representative scenarios (it takes more care of the scenarios of maximum and minimum demand). Thus, more investment is put on SVCs instead of fixed CBs, and a greater EES capacity is required. Finally, the energy costs increase because the maximum demand considered in the representative scenarios for each case also increases when considering the uncertainties or the robust approach. In this way, to meet the maximum demand is necessary to anticipate the investments in DG systems, and, although it is more expensive in terms of energy compared that one purchased at substations, it allows to defer the investments in substation upgrades, being the best option in the end. Here, it is worth indicating that the DG systems have increased their costs in the last year and also their long-term forecast values (NREL, 2023). Another important point in the solution overview is

Table 5 – Solution overview: Distribution and energy costs

	Description	Case I	Case II	Case III
Distribution (10^3 USD)	Substations	370.70	370.70	370.70
	OLTCs	0	0	0
	Conductors	164.32	164.82	170.06
	Supports	196.79	194.91	196.58
	Fixed CBs	9.68	4.84	1.84
	Switchable CBs	9.37	9.37	12.60
	SVCs	9.60	19.21	21.88
	VRs	0	0	0
	EES systems	70.82	88.53	123.94
	EES systems (O&M)	13.93	17.42	24.38
	Total distribution cost	**843.22**	**869.79**	**921.98**
Energy (10^3 USD)	Purchased energy	14,444.31	14,386.30	14307.60
	Carbon rate payment	1008.54	1003.63	998.24
	PV systems	269.70	296.04	382.21
	Wind systems	3627.30	3668.23	3668.23
	PV systems (O&M)	23.36	25.17	32.49
	Wind systems (O&M)	595.51	608.05	608.05
	Total energy cost	**19,968.72**	**19,987.42**	**19,996.82**
Aggregate cost (10^3 USD)		**20,811.94**	**20,857.21**	**20,918.80**
Unit aggregate cost (USD/kWh)		**0.0773**	**0.0774**	**0.0777**

Source: Elaborated by the author.

that no voltage regulation devices, as OLTCs and VRs, have been required for the investment plans. This shows that in active distribution systems, voltage regulation can be attained in a more economic way through a proper orchestration of CBs, SVCs, EES systems and reactive support from DG systems. Also, it is worth indicating that reconductoring is an important action that in addition to reducing losses, softens the voltage variations.

5.4.2 Investment plans

The investment plans for Cases I and II are presented in Table 6. The investments required for assets' replacement at the end of their useful life are highlighted in bold while the investments made before that time are done in italics. In the case of substations, it can be observed that the investments correspond to their replacement costs and that capacity upgrade was not needed. About this last point it is important to highlight that a proper planning can defer the traditional investments (since the maximum demand gets to overcome the current capacity of the substations), but since the model does not consider all the realizations of operation uncertainties (which would be computationally intractable), the assessment of planning reliability in terms of substation overload is required. Thus, this point is addressed in Section 5.4.5.

It can be observed, about reconductoring, that several lines and supports need to be upgraded before the end of their useful life (most of them 15 years before). This shows two features about the operation and initial state of the system: the first one is that the currents through the replaced lines are large enough, from the first planning period, to compensate the investment via loss reduction and voltage variation smoothing (to prevent violating the voltage limits); the second one is that the existing network was possibly not properly planned since a good planning generally implies the integral use of the assets. Thus, most of the reconductoring actions proposed at the beginning of the planning horizon probably should have been executed in previous investment plans. Another important fact about using the asset elapsed life information in planning is that at the end of the useful life of a given asset, the decision about selecting a new one is taken considering all the possible options equally, while in the existing planning models, since elapsed life is neglected, the decisions are made considering implicitly that the existing assets can continue working after the end of their lifespan for free within the planning horizon. Thus, the decision-maker is biased to keep the existing asset unless an upgrade compensate the investments. In this way, the upgrade of the lines 21-24, 03-28, 49-50 and 12-50 from type 1 to type 2 probably would not happen with the traditional planning models.

The planning actions about reactive power compensation shows that the joint operation of fixed CBs, switchable CBs and SVCs performs better, and at a lower cost, than using only CBs or SVCs separately as is often done in the literature (XIE *et al.*, 2018; EHSAN; YANG, 2020a; ARIAS *et al.*, 2018; MEJIA *et al.*, 2022). Also, it can be observed that more participation of switchable CBs is required, which makes sense since they offer more flexibility than fixed CBs while they are cheaper than SVCs. Additionally, comparing the Cases I and II is observed that Case II invests more in SVCs than in fixed CBs. This is because the ROSs considered in Case I do not take account for operating uncertainties and therefore their operation variability is lower. Here, note that a constant operation of the system could be handled just with fixed CBs, a medium-variable operation will need additionally switchable CBs or SVCs, and a high-variable one will need SVCs.

The installation of DG systems is mainly to accomplish the CO_2 emission reduction goals. It can be observed that wind system installation predominates over PV systems, although they are more expensive. This is mainly because the price of the energy purchased in the substations is considerably higher at peak hours (GAGNON; COWIESTOLL; SCHWARZ, 2023), when PV systems do not generate energy while wind systems usually do. Another reason is the increasing penetration of prosumers, which accounts for a significant PV system capacity. Thus,

Table 6 – Investment and planning actions

Description	Case I				Case II			
	Period 1	Period 2	Period 3	Period 4	Period 1	Period 2	Period 3	Period 4
Substations (kVA) [node *i* (capacity)]	-	-	-	**1(7500)**	-	-	-	**1(7500)**
Conductors [line *i*-*j* (type)]	*01-09(5),* *09-11(3),* *04-48(5),* *48-49(3),* *09-64(5)*	-	-	**11-14(5), 14-18(2),** **18-21(1), 21-24(2),** **03-28(2), 28-35(1),** **3-36(1), 49-50(2),** **8-52(1), 64-65(1),** **11-67(1), 12-68(2),** **68-69(3),**	*01-09(5),* *09-11(3),* *04-48(5),* *48-49(3),* *09-64(5)*	-	-	**11-15(5), 15-16(3),** **16-22(2), 22-24(3),** **03-28(2), 28-35(1),** **3-36(3), 49-50(5),** **8-52(1), 64-65(1),** **11-67(1), 12-69(5)**
Supports [line *i*-*j* (type)]	*04-48(2),* *09-64(2)*	-	**64-65(1)**	**01-04(2), 09-11(1),** **11-14(2), 14-24(1),** **28-35(1), 3-36(2),** **48-50(1), 8-52(1),** **11-67(1), 12-69(1)**	*04-48(2),* *09-64(2)*	-	**64-65(1)**	**01-04(2), 09-11(1),** **11-15(2), 15-24(1),** **28-35(1), 3-36(2),** **48-50(2), 8-52(1),** **11-67(1), 12-69(2)**
Fixed CBs (kVAr) [node *i* (capacity)]	1(300), 10(300)	-	-	-	1(300)	-	-	-
Switchable CBs (kVAr) [node *i* (capacity)]	64(900)	-	-	-	64(900)	-	-	-
SVCs (kVAr) [node *i* (capacity)]	51(300)	-	-	-	10(300), 51(300)	-	-	-
PV systems (kW) [node *i* (capacity)]	64(138.7)	-	-	64(301)	64(162.6)	-	-	64(164.6)
Wind systems (kW) [node *i* (capacity)]	27(900)	69(1125)	50(900)	27(225), 50(225)	27(900)	69(1125)	50(1125)	27(225)
EES systems (kW) [node *i* (capacity)]	-	-	-	64(400)	-	-	-	64(500)
Required Investment (10^3 USD)	2,481.12	1,992.09	1,383.64	2,134.18	2,522.58	1,992.09	1,694.26	1,718.75

Source: Elaborated by the author.

the allocation of additional PV systems owned by the DISCO is not always beneficial for the network operation. Also, it is important mentioning that the capacity factor for wind systems is slightly greater than for PV systems in the installation area. Additionally, an anticipated investment is made in Case II in relation to Case I in planning period 3 for wind systems. This is because the uncertainties considered in Case II push the maximum demand considered in the model to greater values compared with Case I, and thus more DG systems are required to meet the demand without upgrading the substations.

The installation of EES systems only occurs in the last planning period of the horizon planning. This suggests that currently the use of EES systems still does not compensate their respective investments, but, also, it is worth mentioning that this fact can change in scenarios with more aggressive polices for CO_2 emission reduction, high penetration of prosumers or reduced manufacturing costs. In addition, it can be observed that Case II requires more EES systems than Case I to handle the operating variability from uncertainties, while preventing investments in substation upgrading or DG systems (since an EES system eventually can work as a generator). For example, note that in planning period 4 and Case II it was necessary to add a smaller PV system capacity to the system than in Case I, because Case II required more EES systems.

The required investment costs presented in Table 6 provide valuable information to the planning area of the DISCO. The main value corresponds to the investment cost for the first planning period because its corresponding investment plan needs to be executed in the short-term. For both Case I and II, this is the greatest investment along the planning horizon because it includes most of the planning actions. Some of them because they have immediate impact reducing the operating costs, some are needed to achieve the preset CO_2 emission reduction while the others ensure the proper operation of the system (according the imposed constraints). The expected investment costs for planning periods II and III decrease regarding the planning period I. This is mainly because of the expected cost reduction of DG systems (NREL, 2023). Finally, the investment for planning period IV increases due to the existing substation needs to be replaced at that time (corresponding to the end of its useful life). Thus, it is important considering the elapsed life of the assets in long-term planning because it allows to obtain the real investments that the DISCO has or will have to face.

5.4.3 Network operation analysis

The operation losses are a good indicator to measure the performance of the operation of distribution systems. Thus, their evolution over the planning horizon is addressed in Fig. 15. This analysis is carried out in Case III, but it can be done for any case. First of all it is worth indicating that the losses account just for about 1% of the demand. This is a good indicator of the planning performance. On the other hand, it can be observed that the losses are expected to increase along the planning horizon. A priori, this may seem unfavorable, but it is based on the following facts: the increasing demand causes line losses to increase (basically in a quadratic way); the increasing variability of demand (despite its net value) also increases the line losses; network operation is not always in tune with the stochastic generation from DG systems, thus curtailment is eventually necessary; and the bidirectional operation (charging and discharging) of EES systems is not pretty efficient.

It can be observed that substation transformers account for the second source of losses, thus it is important to include them in the system planning, as done in this work. As observed in Fig. 15, the losses from EES system operation are expected to be significant in the future. Particularly, for the case study, the EES system capacity accounts for less than 10% of the maximum demand; but, in a favorable scenario where the manufacturing costs of the EES system decreases, their use could be extensive taking into account the increasing hourly variation of energy prices (GAGNON; COWIESTOLL; SCHWARZ, 2023). Thus, the cycle efficiency of EES systems will play an important role in the distribution system performance.

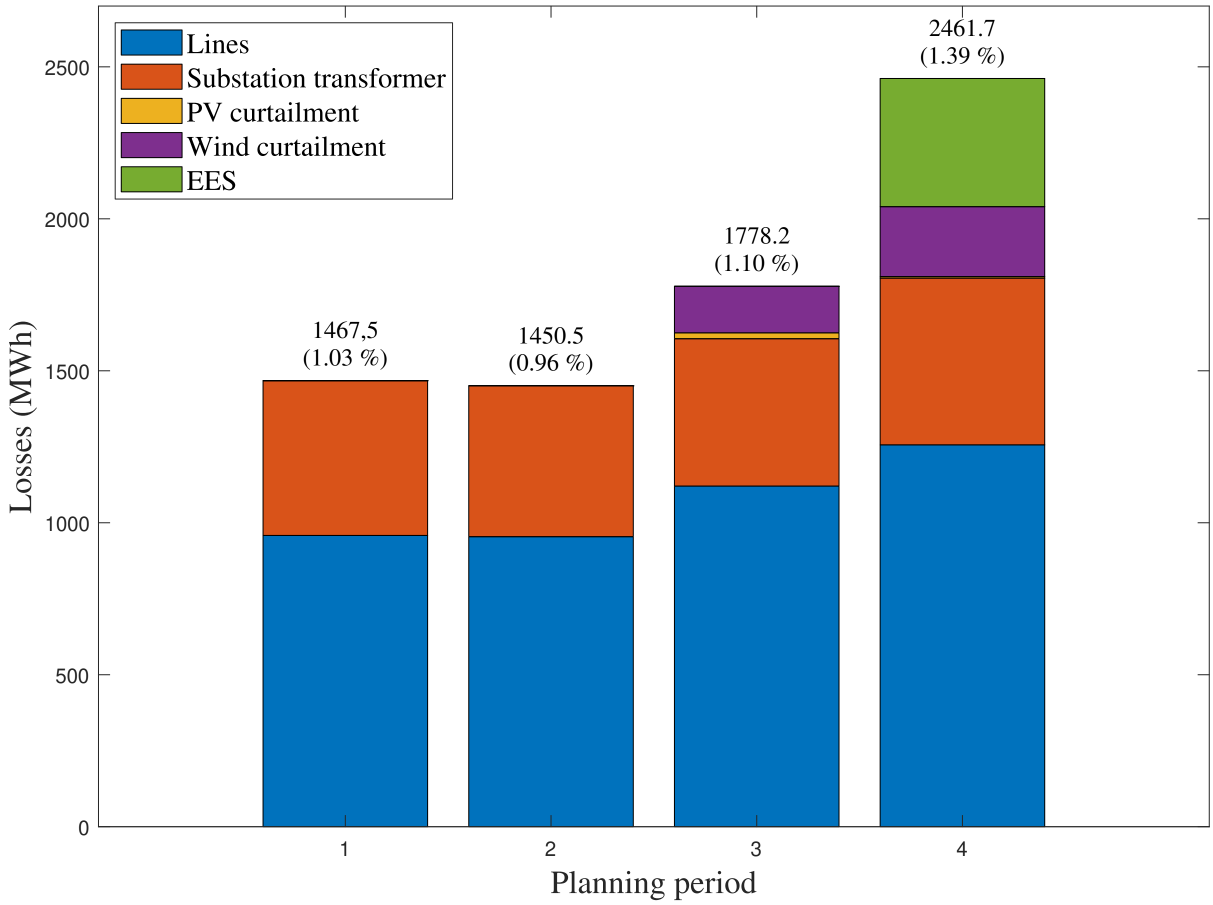

Figure 15 – Losses composition by planning period for Case III

Source: Elaborated by the author.

5.4.4 Performance of the proposed model and solution technique

In order to compare the proposed technique with the traditional approaches, in terms of optimality, feasibility and computational time, the planning problem is also solved using conic relaxation (MISOCP) and the common PWL technique (without binary variables), considering a time limit of 24 h. The test is run on the Case III.

The number of variable blocks considered for the based-PWL model is 40. It is important indicating that the number of variable blocks is inversely proportional to the linearization accuracy when the blocks are taken successively in order. Thus, considering a maximum active power flow of 8,000 kW, the length of each linearization block will be 8000/40=20kW, and the maximum linearization error, 20/2=10kW. For planning purposes and taking into account that a greater number of blocks can lead to models too computationally expensive, is not recommended to use more blocks in the modeling. On the other hand, a lower number of blocks can lead to poor approximations of the original planning problem. It is important to note that the maximum linearization error, previously calculated, can be guaranteed only if the linearization blocks are taken in order. To ensure that, the use of binary variables would be necessary, but it can turn the problem intractable. The performance comparison is shown in Table 7

Table 7 – Performance Overview for the Case III

Description	Proposal	PWL	MISOCP
Objective	20,918.80$^{(a)}$	21,402.01$^{(b)}$	-
Best bound	20,824.84$^{(b)}$	20,840.89$^{(b)}$	20,583.89$^{(a)}$
Max. Feas. Error (ξ_{max}^{lin})	0.06	8,013.48	-
Comp. time (h)	3.83	24	24

corresponding to $^{(a)}$ exact solution,$^{(b)}$ approximate solution

Source: Elaborated by the author.

It can be observed that, in contrast to the PWL model, the proposed technique guarantees solution feasibility within the preset limits. Actually, the PWL technique presents huge feasibility errors for some operating points. For example, the error shown in Table 7 corresponds to the planning period 4, representative day 1, hour 10 and line 63-64. At this point, P=-41.64kW, Q=-316.34kVAr, V=(12.03kV)^2, I=(400A)^2, and clearly $VI \gg P^2+Q^2$. This error is possible in the commom PWL technique, since its formulation does not guarantee that linearization blocks are taken in order from the first one, and because it uses auxiliary variables to handle the reverse power flows, but without using binary variables. Physically, the error can be interpreted as it is more economical to manage the surplus energy through heat dissipation (power losses) than do it through batteries, different planning actions and/or different operating modes. Note that this error occurs at a stage of the planning horizon when the penetration of prosumers is such as the power injection to the transmission system could be unavoidable without storage. Additionally, it is important indicating that depending of the problem, the linearization errors explained above can not occur (even in absence of binary variables). Thus, for example, the commom PWL technique is more suitable for Optimal Power Flow (OPF) problems related to operation than planning. This is because in operation generally minimizing the losses lead to optimal objectives, while in planning, increasing the losses eventually may prevent investment costs, as stated before.

The MISOCP model did not find an integer solution until reaching the time limit of 24 h, verifying that MISOCP is not always suitable for large problems. However, a lower bound for the original non-convex MINLP model is found, which can serve as a reference for evaluating the quality solution of other solution techniques. Also, it is observed that the proposal presents a much better performance than the based-PWL model, since it obtains a better objective in just

16% of the time required by the PWL model to find its best solution, with a maximum feasibility error that is negligible compared with the one of PWL. Also, based on the best bound of the MISOCP solution, it can be guaranteed than the objective obtained with the proposed model is within a gap of 1.6%, which is a good indicator of its quality. Here, note that this MISOCP bound is likely to increase over the solution process.

Additionally, as indicated in Table 7, it is important to note that the proposal can provide a exact solution (not necessarily global optimum) and an approximate best bound, the PWL-based technique can provide an approximate solution and best bound, while the MISOCP approach can provided exact best bounds (relaxed and integral).

The computational times required for solving Cases I, II and III are 2.69 h, 2.73 h and 3.83 h, respectively. Since all the cases have the same size it can be said that the mean time required for the proposed solution technique is about 3 h. It is worth to note that these times are relative short for the planning of a 69-node system, considering the extensive planning actions, the diversity of device types and the number of operating scenarios considered for the long-term multistage planning. Additionally, the recursive nature of the proposed solution technique allows to access incumbent solutions at each iteration, which is an advantage for analysis purposes, mainly for large problems that demand large computationally times.

5.4.5 Planning reliability assessment

In order to evaluate the planning reliability, to know the risks involved in the system operation under uncertainty, and according that to verify (or modify) the investment plans, the planning reliability is addressed and measured in this section in terms of substation overload, conductor overload and voltage limits violation. For that, the investment plans are fixed and the system operation is simulated over different realizations of the random operating parameters (modeled according the Chapter 2). In order to preserve the diversity of the operating scenarios while performing the simulations in a reasonable time, one realization per day, within the planning horizon, is considered. Thus, 1825 simulations are carried out for each planning period. Each simulation consists of an OPF problem that minimizes the energy purchased in substations subject to Kirchhoff's laws, the allowed power exchange flexibility at the transmission/distribution interface (3.18)–(3.19) and the operating conditions of the assets already installed. The results are summarized in Table 8. Note that the values are provided for each planning period in the form P1/P2/P3/P4. Also, the percentage values correspond to the relation between the number of days that present the issue indicated in the column "Description" and the total number of simulated days.

Table 8 – Planning Reliability Assestment

Description	Case I	Case II	Case III
Infeasibility (%)	0/0/0.05/0.55	0/0/0.05/0.49	0/0/0.05/0.22
Substation overload (%)	0/0/0.05/0.27	0/0/0.05/0.27	0/0/0.05/0.27
Substation overload (h)	0/0/2/39	0/0/2/37	0/0/2/29
Conductor overload (%)	0/0/0/0	0/0/0/0	0/0/0/0
Voltage limits violation (%)	0/0/0.05/0	0/0/0/0	0/0/0/0

Source: Elaborated by the author.

The item "infeasibility" indicates how many times the OPF perfomed over the random scenarios results infeasible. Since the Kirchhoff's laws and the operating conditions can be met, an infeasibility implies that the power exchange at substations can not follow the TSO guidelines, i.e., it is possible to have scenarios where the prosumer penetration will be so high that the power injection to the transmission system can be unavoidable (for the given system configuration). Although this is not expected to happen in the next years and its occurrence probability is low, the results suggest research on the link between prosumer participation and the flexibility at the interface transmission/ distribution. Additionally, it can be observed how the infeasibility issue decreases with robust ROSs are used, and how it increases when uncertainties are not considered.

Probably the most determining factor in the planning reliability assessment is the substation overload, since it represents the main source of energy supply. The low percentages of substation overload suggest that its capacity upgrade could be deferred, but it is worth indicating that this perspective is from now and it can change in the future when new operating scenarios are considered. Also, it can be observed that, despite the number of days with substation overload is the same for all cases, the number of hours within that days decreases as the uncertainties are considered or robust ROSs are used. About conductor operation, it is observed that no conductor is expected to present overload issues for any case along the planning horizon. This is because, despite not considering the stochastic nature of the system operation, the operating cost is reduced using generally oversized conductors. Note that this fact is not seen a priori but through the optimization process. Finally, there is only one day with violation of the voltage limits in the Case I while there is not such a issues in Cases II and III. Here, it is worth mentioning that the voltage profile smooths out in the planning period 4 after the installation of EES systems.

Finally, it is worth indicating that the main goal of multistage planning is to determine the optimal investment plan to be executed in the short-term, taking advantage of the knowledge and forecast of future events. Also, the investment plans corresponding to the subsequent planning periods are good references about what is expected to happen, but, for its application, they should be revalidated as the forecast uncertainties are being realized. Consequently, for practical purposes it is recommended to perform a multistage (and long-term) planning at the beginning of every planning period whose investment plan needs to be determined.

5.4.6 Solution overview for the real 135-node distribution system

The solution overview for the real 135-node distribution system is summarized in Table 9 considering the Cases I and III. It can be observed that greater investment in substations is required for Case III. This is because the robust ROSs considered in this case emphasize in scenarios of maximum demand. Thus, the maximum demand considered in Case III is greater that the one considered in Case I. Specifically, in Case III it is necessary to anticipate for one planning period the capacity upgrade of both substations. Since this can be considerably expensive, a temporal repowering of the substation could be an option; but, since this event is expected to happen just in the second half of the planning horizon, it is better to be addressed with more certainty in a subsequent planning. A different fact with respect to the 69-node distribution system, it is that for the real 135-node system, the installation of OLTCs is required for both cases. This is probably because the 69-node system is composed only of one main feeder, while in the real 135-node come out several feeders from each substation. Note that if a given power flow is distributed along a unique feeder, the voltage variation along that feeder is expected to be greater than the voltage variation obtained if the power flow is distributed by several feeders. In this way, the permissible OLTC operating range for one-feeder systems is less than the one for several-feeder systems, making OLTC installation more attractive for this last case. In contrast, VR installation could be a good option for systems composed only of one main long feeder.

It can be verified that greater investment is required for switchable CBs than for fixed CBs in the Case III. This is because this case consider more variable operating scenarios due to uncertainties and its robust nature. An interesting point about the reactive compensation for the real 135-node system is that its corresponding investment is less than the double of the one for the 69-node system, despite the reactive power demand for the 135-node system is more than twice the one for the 69-node system. Also, the required investment are relatively low in both systems. This is because the reactive compensation is mainly done by substations and DG systems, e.g., PV systems deliver up to 1200kVAr while wind systems 1500kVAr. Additionally, it is worth mentioning that this model was solved considering a time limit of 24h for the integral stage, obtaining a gap of 2.7% at the final of this time.

Table 9 – Solution overview for the real 135-node system: Distribution and energy costs

	Description	Case I	Case III
Distribution (10^3 USD)	Substations	1,188.03	1,431.69
	OLTCs	45.21	45.21
	Conductors	324.34	324.14
	Supports	377.12	376.79
	Fixed CBs	22.00	15.84
	Switchable CBs	10.28	21.78
	SVCs	28.81	28.81
	VRs	0	0
	EES systems	2,366.84	2,328.42
	EES systems (O&M)	462.20	455.51
	Total distribution cost	**4,824.84**	**5,028.20**
Energy (10^3 USD)	Purchased energy	55,855.38	55,999.24
	Carbon rate payment	3,966.95	3,966.85
	PV systems	7,202.06	8,668.04
	Wind systems	11,564.14	9,678.89
	PV systems (O&M)	634.76	752.65
	Wind systems (O&M)	1,800.36	1,605.62
	Total energy cost	**81,023.65**	**80,671.29**
Aggregate cost (10^3 USD)		**85,848.49**	**85,699.49**

Source: Elaborated by the author.

6 CONCLUSIONS AND FUTURE WORKS

In this work, a multistage planning model for active distribution systems under uncertainty has been proposed. In order to handle the uncertainties a scenario-based two-stage stochastic approach has been used. Unlike the traditional models based on two-stage stochastic programming, the proposed model has modeled and used the uncertainties associated with the operating parameters in order to get more realistic and reliable representative operating scenarios (ROSs). Thus, the uncertainties from conventional demand, EVs, prosumers, and renewable energy resources have been addressed.

6.1 CONCLUSIONS

The results show that considering the operating uncertainties leads to more robust investment plans than the traditional approach where just the expected forecast values are considered. Additionally, this work has implemented a novel robust k-means method to obtain robust ROSs that leads to more robust investment plans compared with those obtained using the traditional K-means. In general, it has been shown that the planning robustness, under a scenario-based two-stage stochastic approach, can be increased through the proper selection of ROSs.

Also, for the sake of applicability in the industry, important realistic aspects about planning and operation of distribution systems have been considered in this work, as the elapsed life of the existing assets and substation transformer losses. It has been shown that considering the elapsed life of the existing assets modifies the replacement times and the selection of the conductors. Also, its use leads to realistic information about the investments values, which is important for DISCO's accounting.

Additionally, the work has presented the most complete portfolio of planning actions so far in order to obtain the best planning configuration and to draw conclusions about the interaction of the different devices involved in the system operation. Thus, it has been concluded that the joint operation of fixed CBs, switchable CBs and SVCs performs better than the individual operation of that devices.

The results show a high performance of the proposed model and solution technique, obtaining high-quality and feasible solutions for the planning problem in relative short times. Feasibility has been guaranteed regarding the original non-convex MINLP problem. CO_2 emission reduction goals have been met, mainly, through the installation of PV, wind and EES systems.

Finally, a post-planning stage to address and measure the planning reliability in terms of substation and conductor overload as well as voltage limits violation has been implemented. It has been shown that this stage is important and necessary when using a scenario-based two-stage stochastic approach, since a priory it can not be known how the system will react to unexpected scenarios from uncertainty realizations.

6.2 FUTURE WORKS

Future works can consider the following topics:

1. The analysis and exploitation of the flexibility at the transmission/distribution interface considering the increasing penetration of prosumers and distributed independent producers.
2. The implementation of robust and chance-constraint models for the planning of active distribution systems and the analysis of pros and cos of each uncertainty approach (stochastic, robust and chance constraint).
3. The adequacy and specialization of the proposed solution technique for general OPF problems considering different problem sizes (with focus on large-scale problems).
4. The developing of a planning model that minimizes the distribution system costs while maximizing the profit of distributed independent producers.

BIBLIOGRAPHY

ADAMO, C. D.; BUCHHOLZ, B.; ABBEY, C.; KHATTABI, M.; JUPE, S.; PILO, F. Development and operation of active distribution networks : Results of CIGRE C6.11 working group. *In*: INTERNATIONAL CONFERENCE AND EXHIBITION ON ELECTRICITY DISTRIBUTION, 21., 2011, Frankfurt. **Proceedings** [...]. Paris: CIGRE, 2011. Cited on page 20.

AL-HANAHI, B.; AHMAD, I.; HABIBI, D.; MASOUM, M. A. Charging infrastructure for commercial electric vehicles: Challenges and future works. **IEEE Access**, IEEE Inc., Piscataway, v. 9, p. 121476–121492, Aug. 2021. Cited on page 32.

ARASTEH, H.; SEPASIAN, M. S.; VAHIDINASAB, V.; SIANO, P. Sos-based multiobjective distribution system expansion planning. **Electric Power Systems Research**, Elsevier Ltd, Amsterdam, v. 141, p. 392–406, Dec. 2016. Cited on page 21.

ARIAS, N. B.; TABARES, A.; FRANCO, J. F.; LAVORATO, M.; ROMERO, R. Robust joint expansion planning of electrical distribution systems and EV charging stations. **IEEE Transactions on Sustainable Energy**, Piscataway, v. 9, n. 2, p. 884–894, Apr. 2018. Cited 2 times on pages 24 and 70.

BELOTTI, P.; KIRCHES, C.; LEYFFER, S.; LINDEROTH, J.; LUEDTKE, J.; MAHAJAN, A. Mixed-integer nonlinear optimization. **Acta Numerica**, Cambridge University Press, Cambridge, v. 22, p. 1–131, 5 2013. Cited on page 21.

BHASKAR, P.; STEHLY, T. **Technology Innovation Pathways for Distributed Wind Balance-of-System Cost Reduction**. 2021. Available from Internet: www.nrel.gov/publications. Cited on page 47.

BLIEK, C.; BONAMI, P.; LODI, A. Solving mixed-integer quadratic programming problems with IBM-CPLEX: a progress report. *In*: RAMP SYMPOSIUM, 26., 2014, Tokio. **Proceedings** [...]. Tokio: ORSJ, 2014. Cited on page 56.

BOSCHETTI, M. A.; MANIEZZO, V. Matheuristics: using mathematics for heuristic design. **4OR - A Quarterly Journal of Operations Research**, Springer, Berlin, v. 20, n. 2, p. 173–208, Jun. 2022. Cited 3 times on pages 21, 22, and 54.

CAPITANESCU, F.; OCHOA, L. F.; MARGOSSIAN, H.; HATZIARGYRIOU, N. D. Assessing the potential of network recon fi guration to improve distributed generation hosting capacity in active distribution systems. **IEEE Transactions on Power Systems**, IEEE, Piscataway, v. 30, n. 1, p. 346–356, Jan. 2015. Cited on page 21.

CHAKRAVORTY, M.; DAS, D. Voltage stability analysis of radial distribution networks. **International Journal of Electrical Power & Energy Systems**, Elsevier Ltd, Amsterdam, v. 23, n. 2, p. 129–135, Feb. 2001. Cited 3 times on pages 60, 61, and 90.

DING, F.; MEMBER, S.; BAGGU, M. M. Coordinated use of smart inverters with legacy voltage regulating devices in distribution systems with high distributed PV penetration-increase CVR energy savings. **IEEE Transactions on Smart Grid**, Piscataway, v. 14, Jul. 2018. Cited on page 47.

EHSAN, A.; YANG, Q. Active distribution system reinforcement planning with EV charging stations - part I: Uncertainty modeling and problem formulation. **IEEE Transactions on Sustainable Energy**, Institute of Electrical and Electronics Engineers Inc., Piscataway, v. 11, p. 970–978, Apr 2020. Cited 3 times on pages 22, 25, and 70.

EHSAN, A.; YANG, Q. Active distribution system reinforcement planning with EV charging stations-part II: Numerical results. **IEEE Transactions on Sustainable Energy**, Institute of Electrical and Electronics Engineers Inc., Piscataway, v. 11, p. 979–987, Apr 2020. Cited on page 25.

ELLIS, A.; NELSON, R.; ENGELN, E. V.; WALLING, R.; J.MACDOWELL; CASEY, L.; SEYMOUR, E.; PETER, W.; BARKER, C.; KIRBY, B.; WILLIAMS, J. R. Reactive power performance requirements for wind and solar plants. *In*: IEEE POWER AND ENERGY SOCIETY GENERAL MEETING, 2012, San Diego. **Proceedings** [...]. Piscataway: IEEE, 2012. Cited on page 47.

EMPRESA DE PESQUISA ENERGÉTICA – EPE. **Painel de Dados de Micro e Minigeração Distribuída**. 2023. Available from Internet: http://dashboard.epe.gov.br/apps/pdgd/. Cited on page 37.

FLUCHS, S. The diffusion of electric mobility in the european union and beyond. **Transportation Research Part D: Transport and Environment**, Elsevier Ltd, Amsterdam, v. 86, Set. 2020. Cited on page 32.

FRANCO, J. F.; RIDER, M. J.; LAVORATO, M.; ROMERO, R. Optimal conductor size selection and reconductoring in radial distribution systems using a mixed-integer LP approach. **IEEE Transactions on Power Systems**, Piscataway, v. 28, n. 1, p. 10–20, Feb. 2013. Cited on page 20.

GAGNON, P.; COWIESTOLL, B.; SCHWARZ, M. **Scenario Viewer | Standard Scenarios 2022**. 2023. Available from Internet: https://scenarioviewer.nrel.gov. Cited 5 times on pages 62, 70, 73, 96, and 97.

GARCÍA-CEREZO, A.; BARINGO, L.; GARCÍA-BERTRAND, R. Representative days for expansion decisions in power systems. **Energies**, MDPI, Basel, v. 13, n. 2, Jan. 2020. Art. no. 335. Cited on page 40.

GEORGILAKIS, P. S.; HATZIARGYRIOU, N. D. Optimal distributed generation placement in power distribution networks: Models, methods, and future research. **IEEE Transactions on Power Systems**, IEEE, Piscataway, v. 28, n. 3, p. 3420–3428, Aug. 2013. Cited on page 20.

HAGHIGHAT, H.; ZENG, B. Stochastic and chance-constrained conic distribution system expansion planning using bilinear benders decomposition. **IEEE Transactions on Power Systems**, Institute of Electrical and Electronics Engineers Inc., Piscataway, v. 33, n. 3, p. 2696–2705, May 2018. Cited on page 21.

HOME-ORTIZ, J. M.; POURAKBARI-KASMAEI, M.; LEHTONEN, M.; MANTOVANI, J. R. S. A mixed integer conic model for distribution expansion planning: Matheuristic approach. **IEEE Transactions on Smart Grid**, Piscataway, v. 11, n. 5, p. 3932–3943, Sep. 2020. Cited 2 times on pages 22 and 25.

HU, J.; WU, J.; AI, X.; LIU, N. Coordinated energy management of prosumers in a distribution system considering network congestion. **IEEE Transactions on Smart Grid**, Piscataway, v. 12, n. 1, p. 468–478, Jan. 2021. Cited on page 20.

IEA. **IEA Energy Atlas**. 2020. Available from Internet: http://energyatlas.iea.org/#!/tellmap/-1118783123/2. Cited on page 52.

IRENA. **Global Energy Transformation: A Roadmap to 2050 (2019 Edition)**. 2019. Available from Internet: https://www.irena.org/publications/2019/Apr/Global-energy-transformation-A-roadmap-to-2050-2019Edition. Cited on page 64.

JAYASEKARA, N.; MEMBER, S.; MASOUM, M. A. S.; MEMBER, S.; WOLFS, P. J.; MEMBER, S. Optimal operation of distributed energy storage systems to improve distribution network load and generation hosting capability. **IEEE Transactions on Sustainable Energy**, IEEE, Piscataway, v. 7, n. 1, p. 250–261, Jan. 2016. Cited on page 21.

LIMA, T. D. D.; FRANCO, J. F.; LEZAMA, F.; SOARES, J. A specialized long-term distribution system expansion planning method with the integration of distributed energy resources. **IEEE Access**, Piscataway, v. 10, p. 19133–19148, Jan. 2022. Cited 2 times on pages 22 and 25.

MAHDI, M. A.; HOSNY, K. M.; ELHENAWY, I. Scalable clustering algorithms for big data: A review. **IEEE Access**, IEEE Inc., Piscataway, v. 9, p. 80015–80027, May. 2021. Cited on page 40.

MANTOVANI, J. R. S.; CASARI, F.; ROMERO, R. A. Reconfiguração de sistemas de distribuição radiais utilizando o critério de queda de tensão. **SBA Controle & Automação**, SBA, Campinas, v. 11, p. 150–159, Sep. 2000. Cited 3 times on pages 60, 62, and 95.

MARCELO, J. A.; MUÑOZ-DELGADO, G.; CONTRERAS, J.; MANTOVANI, J. R. S. A novel solution technique for the expansion planning of modern distribution systems. *In*: IEEE INTERNATIONAL CONFERENCE ON ENVIRONMENT AND ELECTRICAL ENGINEERING AND IEEE INDUSTRIAL AND COMMERCIAL POWER SYSTEMS EUROPE (EEEIC / I&CPS EUROPE), 2023, Madrid. **Proceedings** [...]. Madrid: IEEE, 2023. Cited 2 times on pages 26 and 58.

MARCELO, J. A.; RUPOLO, D.; MANTOVANI, J. R. A new approach to determine a distribution network usage fee for distributed generators. *In*: IEEE PES INNOVATIVE SMART GRID TECHNOLOGIES EUROPE (ISGT EUROPE), 2021, Espoo. **Proceedings** [...]. Piscataway: IEEE, 2021. Cited on page 68.

MEJIA, M. A.; FRANCO, J. F.; MACEDO, L. H.; MUÑOZ-DELGADO, G.; CONTRERAS, J. Integrated planning of active distribution systems and charging stations for plug-in electric vehicles considering the vehicular traffic network. *In*: IEEE INTERNATIONAL CONFERENCE ON ENVIRONMENT AND ELECTRICAL ENGINEERING AND IEEE INDUSTRIAL AND COMMERCIAL POWER SYSTEMS EUROPE (EEEIC / I&CPS EUROPE), 2023, Madrid. **Proceedings** [...]. Piscataway: IEEE, 2023. Cited on page 64.

MEJIA, M. A.; MACEDO, L. H.; MUNOZ-DELGADO, G.; CONTRERAS, J.; PADILHA-FELTRIN, A. Multistage planning model for active distribution systems and electric vehicle charging stations considering voltage-dependent load behavior. **IEEE Transactions on Smart Grid**, IEEE, Piscataway, v. 13, n. 2, p. 1383–1397, Mar. 2022. Cited 4 times on pages 21, 22, 26, and 70.

MELGAR-DOMINGUEZ, O. D.; POURAKBARI-KASMAEI, M.; MANTOVANI, J. R. S. Robust short-term electrical distribution network planning considering simultaneous allocation of renewable energy sources and energy storage systems. *In*: **Robust Optimal Planning and Operation of Electrical Energy Systems**. Springer International Publishing, 2019. p. 145–175. Available from Internet: https://link.springer.com/chapter/10.1007/978-3-030-04296-7_9. Cited on page 24.

MELGAR-DOMINGUEZ, O. D.; POURAKBARI-KASMAEI, M.; MANTOVANI, S. Adaptive robust short-term planning of electrical distribution systems considering siting and sizing of renewable energy based dg units. **IEEE Transactions on Sustainable Energy**, Piscataway, v. 10, n. 1, p. 158–169, Jan. 2019. Cited on page 21.

MONTOYA-BUENO, S.; MUÑOZ, J. I.; CONTRERAS, J. A stochastic investment model for renewable generation in distribution systems. **IEEE Transactions on Sustainable Energy**, Piscataway, v. 6, n. 4, p. 1466–1474, Oct. 2015. Cited on page 37.

NREL. **Annual Technology Baseline**. 2023. Available from Internet: https://atb.nrel.gov/electricity/2023/data. Cited 5 times on pages 63, 68, 72, 99, and 100.

OPERADOR NACIONAL DO SISTEMA ELÉTRICO – ONS. **Histórico da Operação**. 2023. Available from Internet: http://www.ons.org.br/paginas/resultados-da-operacao/historico-da-operacao. Cited on page 30.

PEREIRA, B. R.; COSSI, A. M.; MANTOVANI, J. R. Multiobjective short-term planning of electric power distribution systems using NSGA-II. **Journal of Control, Automation and Electrical Systems**, Berlin, v. 24, p. 286–299, 2013. Cited on page 23.

POURAKBARI-KASMAEI, M.; LEHTONEN, M.; CONTRERAS, J.; MANTOVANI, R. S. Carbon footprint management : A pathway toward smart emission abatement. **IEEE Transactions on Industrial Informatics**, Piscataway, v. 16, n. 2, p. 935–948, Feb. 2020. Cited on page 21.

PRILLIMAN, M. J.; HANSEN, C. W.; KEITH, J. M. F.; JANZOU, S.; THERISTIS, M.; SCHEINER, A.; OZAKYOL, E. **Quantifying Uncertainty in PV Energy Estimates Final Report**. 2023. Available from Internet: www.nrel.gov/publications. Cited on page 35.

QUIRÓS-TORTÓS, J.; OCHOA, L. F.; LEES, B. A statistical analysis of EV charging behavior in the UK. *In*: PES INNOVATIVE SMART GRID TECHNOLOGIES LATAM, 2015, Montevideo. **Proceedings** [...]. Piscataway: IEEE, 2015. p. 445–449. Cited on page 35.

ROALD, L. A.; POZO, D.; PAPAVASILIOU, A.; MOLZAHN, D. K.; KAZEMPOUR, J.; CONEJO, A. Power systems optimization under uncertainty: A review of methods and applications. **Electric Power Systems Research**, Elsevier Ltd, Amsterdam, v. 214, 1 2023. Cited on page 22.

SAFIGIANNI, A. S.; SALIS, G. J. Optimum voltage regulator placement in a radial power distribution network. **IEEE Transactions on Power Systems**, Piscataway, v. 15, n. 2, p. 879–886, May 2000. Cited on page 20.

SHA, S.; FOTUHI-FIRUZABAD, M. Investigating the impacts of plug-in hybrid electric vehicles on power distribution systems. **IEEE Transactions on Smart Grid**, Piscataway, v. 4, n. 3, p. 1351–1360, Sep. 2013. Cited on page 21.

SHAHEEN, A. M.; EL-SEHIEMY, R. A. Optimal coordinated allocation of distributed generation units / capacitor banks / voltage regulators by EGWA. **IEEE Systems Journal**, Piscataway, v. 15, n. 1, p. 257–264, Mar. 2021. Cited on page 20.

SOLARGIS; ESMAP; GROUP, W. B. **Global Solar Atlas 2.0**. 2023. Available from Internet: https://globalsolaratlas.info/map. Cited on page 37.

STANKOVIĆ, S.; SÖDER, L.; HAGEMANN, Z.; REHTANZ, C. Reactive power support adequacy at the DSO/TSO interface. **Electric Power Systems Research**, Elsevier Ltd, Amsterdam, v. 190, Aug. 2021. Cited on page 46.

SUNDHARARAJAN, S.; PAHWA, A. Optimal selection of capacitors for radial distribution systems using a genetic algorithm. **IEEE Transactions on Power Systems**, Piscataway, v. 9, n. 3, p. 1499–1507, Aug. 1994. Cited on page 20.

TABARES, A.; FRANCO, J. F.; LAVORATO, M.; RIDER, M. J. Multistage long-term expansion planning of electrical distribution systems considering multiple alternatives. **IEEE Transactions on Power Systems**, IEEE Inc., Piscataway, v. 31, n. 3, p. 1900–1914, May 2016. Cited 3 times on pages 21, 24, and 51.

Technical University of Denmark (DTU); VORTEX; ESMAP; GROUP, W. B. **Global Wind Atlas 3.0**. 2023. Available from Internet: https://globalwindatlas.info/. Cited on page 37.

UNTERLUGGAUER, T.; RICH, J.; ANDERSEN, P. B.; HASHEMI, S. Electric vehicle charging infrastructure planning for integrated transportation and power distribution networks: A review. **eTransportation**, Elsevier B.V., Amsterdam, v. 12, 5 2022. Cited on page 64.

VAHIDINASAB, V.; MEMBER, S.; TABARZADI, M. Overview of electric energy distribution networks expansion planning. **IEEE Access**, IEEE, Piscataway, v. 8, p. 34750–34769, Feb. 2020. Cited on page 20.

VELLOSO, A.; POZO, D.; STREET, A. Distributionally robust transmission expansion planning: A multi-scale uncertainty approach. **IEEE Transactions on Power Systems**, IEEE Inc., Piscataway, v. 35, p. 3353–3365, Set. 2020. Cited on page 30.

XIE, S.; HU, Z.; ZHOU, D.; LI, Y.; KONG, S.; LIN, W.; ZHENG, Y. Multi-objective active distribution networks expansion planning by scenario-based stochastic programming considering uncertain and random weight of network. **Applied Energy**, Elsevier Ltd, Amsterdam, v. 219, p. 207–225, 6 2018. Cited 4 times on pages 21, 22, 24, and 70.

ZENG, B.; MEMBER, S.; ZHANG, J.; YANG, X.; MEMBER, S. Integrated planning for transition to low-carbon distribution system with renewable energy. **IEEE Transactions on Power Systems**, IEEE, Piscataway, v. 29, n. 3, p. 1153–1165, May 2014. Cited on page 21.

APPENDIX A - EXPECTED QUANTITY OF EVS

Table 10 – Expected number of EVs by node for selected years

Node	year				Node	year			
	5	10	15	20		5	10	15	20
1	0	0	0	0	36	1	3	8	16
2	1	3	8	16	37	1	3	8	16
3	1	3	8	16	38	1	3	8	16
4	1	3	8	16	39	1	3	7	15
5	1	3	8	16	40	1	3	7	15
6	1	3	8	16	41	1	3	8	16
7	1	5	12	26	42	1	3	8	16
8	3	9	23	48	43	1	2	6	12
9	1	4	9	19	44	1	3	8	16
10	1	3	9	18	45	1	5	12	25
11	5	18	44	93	46	1	5	12	25
12	5	18	44	93	47	1	3	8	16
13	1	5	12	25	48	3	10	24	51
14	1	5	12	25	49	14	47	118	246
15	1	3	8	16	50	14	47	118	246
16	2	6	14	29	51	1	5	12	26
17	2	7	18	39	52	1	4	11	23
18	2	7	18	39	53	2	5	13	28
19	1	3	8	16	54	1	3	8	17
20	1	4	9	19	55	1	3	7	15
21	4	14	35	73	56	1	3	7	15
22	2	6	15	32	57	1	3	8	16
23	1	3	8	16	58	1	3	8	16
24	1	3	9	18	59	4	12	31	64
25	1	3	8	16	60	1	3	8	16
26	1	3	9	18	61	46	153	381	796
27	1	3	9	18	62	1	4	10	21
28	1	3	8	16	63	1	3	8	16
29	1	3	8	16	64	8	28	69	145
30	1	3	8	16	65	2	7	18	38
31	1	3	8	16	66	1	2	6	12
32	1	3	9	18	67	1	2	6	12
33	1	3	9	18	68	1	3	9	18
34	1	2	6	12	69	1	3	9	18
35	1	2	6	12					

Source: Elaborated by the author.

APPENDIX B - SCIENTIFIC PRODUCTION

The articles produced during the Ph.D. program, related directly or indirectly to this thesis, are presented below. The articles include those already published as those under review. The articles have been submitted to international journals classified with CAPES A1 qualifications or presented in renowned international conferences.

1. Marcelo, J. A., Muñoz-Delgado, G., Contreras, J. and Mantovani, J. R. S. (2023). Multistage Planning for Active Power Distribution Systems Under Uncertainty. Applied Energy. (Under review)
2. Marcelo, J. A., Muñoz-Delgado, G., Rupolo, D., Contreras, J. and Mantovani, J. R. S. (2023). Multistage Planning for Active Power Distribution Systems With Increasing Penetration of Prosumers and Electric Vehicles. Sustainable Energy, Grids and Networks. (Under review)
3. Marcelo, J. A., Muñoz-Delgado, G., Contreras, J. and Mantovani, J. R. S. (2023). A Novel Solution Technique for the Expansion Planning of Modern Distribution Systems. 2023 IEEE International Conference on Environment and Electrical Engineering and 2023 IEEE Industrial and Commercial Power Systems Europe (EEEIC / I&CPS Europe), 15, 1–6. https://doi.org/10.1109/EEEIC/ICPSEurope57605.2023.10194884 (Eligible for Publication by IEEE Industry Applications Society)
4. Marcelo, J. A., Rupolo, D. and Mantovani, J. R. S. (2021). A New Approach to Determine a Distribution Network Usage Fee for Distributed Generators. 2021 IEEE PES Innovative Smart Grid Technologies Europe (ISGT Europe), 01–05. https://doi.org/10.1109/ISGTEurope52324.2021.9640015

ANNEX A - TEST SYSTEM OF 69 NODES

Table 11 – Data of the 69-node test system

Line		Load (N2)		Length (m)	Conductor		Support	
N1	N2	P(kW)	Q(kVar)		Type	Elap. Life (years)	Type	Elap. Life (years)
1	2	25	20	20	4	20	2	20
2	3	25	20	50	4	20	2	20
3	4	25	20	50	4	20	2	20
4	5	25	20	20	3	20	1	20
5	6	25	20	350	3	20	1	20
6	7	40.4	30	360	3	20	1	20
7	8	75	54	90	3	20	1	20
8	9	30	22	50	2	20	1	20
9	10	28	19	550	1	20	1	20
10	11	145	104	120	1	20	1	20
11	12	145	104	470	1	20	1	20
12	13	40	25	690	1	20	1	20
13	14	40	27.5	700	1	20	1	20
14	15	25	20	710	1	20	1	20
15	16	45.5	30	130	1	20	1	20
16	17	60	35	250	1	20	1	20
17	18	60	35	50	1	20	1	20
18	19	25	10	220	1	20	1	20
19	20	30	18	140	1	20	1	20
20	21	114	81	230	1	20	1	20

Line		Load (N2)		Length (m)	Conductor		Support	
N1	N2	P(kW)	Q(kVar)		Type	Elap. Life (years)	Type	Elap. Life (years)
21	22	50	35	10	1	20	1	20
22	23	25	20	110	1	20	1	20
23	24	28	20	230	1	20	1	20
24	25	25	20	500	1	10	1	10
25	26	28	20	210	1	10	1	10
26	27	28	20	120	1	10	1	10
3	28	26	18.6	50	1	20	1	20
28	29	26	18.6	40	1	20	1	20
29	30	25	20	270	1	20	1	20
30	31	25	20	50	1	20	1	20
31	32	28	20	230	1	20	1	20
32	33	28	20	560	1	20	1	20
33	34	19	28	1140	1	20	1	20
34	35	18	12	980	1	20	1	20
3	36	26	18.55	50	1	20	1	20
36	37	26	18.55	40	1	10	1	10
37	38	25	20	70	1	10	1	10
38	39	24	17	20	1	10	1	10
39	40	24	17	50	1	10	1	10
40	41	25	20	490	1	10	1	10
41	42	25	20	210	1	10	1	10
42	43	18	13	30	1	10	1	10
43	44	25	20	10	1	10	1	10
44	45	39.22	26.3	70	1	10	1	10
45	46	39.22	26.3	50	1	10	1	10
4	47	25	20	40	1	20	1	20
47	48	79	56.4	60	1	20	1	20
48	49	384.7	274.5	190	1	20	1	20
49	50	384.7	274.5	50	1	20	1	20
8	51	40.5	28.3	60	1	20	1	20

Line		Load (N2)		Length (m)	Conductor		Support	
N1	**N2**	**P(kW)**	**Q(kVar)**		**Type**	**Elap. Life (years)**	**Type**	**Elap. Life (years)**
51	52	36	27	220	1	20	1	20
9	53	43.5	35	120	1	20	1	20
53	54	26.4	19	140	1	20	1	25
54	55	24	17.2	190	1	20	1	25
55	56	24	17.2	190	1	20	1	25
56	57	25	20	1060	1	20	1	25
57	58	25	20	520	1	20	1	25
58	59	100	72	200	1	20	1	25
59	60	25	20	260	1	20	1	25
60	61	1244	888	340	1	20	1	25
61	62	32	23	60	1	20	1	25
62	63	25	20	100	1	20	1	25
63	64	227	162	470	1	20	1	25
64	65	59	42	690	1	20	1	25
11	66	18	13	130	1	20	1	20
66	67	18	13	50	1	20	1	20
12	68	28	20	490	1	20	1	20
68	69	28	20	50	1	20	1	20

Source: Adapted from Chakravorty and Das (2001).

ANNEX B - REAL SYSTEM OF 135 NODES

Table 12 – Data of the real 135-node system

Line		Load (N2)		Length (m)	Conductor		Support	
N1	N2	P(kW)	Q(kVar)		Type	Elap. Life (years)	Type	Elap. Life (years)
0	2	0.0	0.0	460	3	25	1	20
2	3	47.8	19.0	50	3	25	1	20
3	4	42.6	16.9	210	2	25	1	20
4	5	87.0	34.6	90	2	25	1	20
5	6	311.3	123.9	150	2	25	1	20
6	7	148.9	59.2	110	1	25	1	20
7	8	238.7	95.0	80	1	20	1	20
7	9	62.3	24.8	40	1	20	1	20
9	10	124.6	49.6	350	1	20	1	20
9	11	140.2	55.8	70	1	20	1	20
11	12	116.8	46.5	270	1	15	1	15
11	13	249.2	99.1	610	1	15	1	15
11	14	291.4	116.0	80	1	15	1	15
14	15	303.7	120.8	340	1	15	1	15
14	16	215.4	85.7	40	1	15	1	15
16	17	198.6	79.0	200	1	15	1	15
0	18	0.0	0.0	320	2	20	1	20
18	19	0.0	0.0	50	2	20	1	20
19	20	0.0	0.0	210	2	20	1	20

Line		Load (N2)		Length (m)	Conductor		Support	
N1	N2	P(kW)	Q(kVar)		Type	Elap. Life (years)	Type	Elap. Life (years)
20	21	30.1	14.7	100	2	20	1	20
21	22	231.0	112.9	470	1	20	1	20
21	23	60.3	29.5	120	1	20	1	20
23	24	231.0	112.9	200	1	20	1	20
23	25	120.5	58.9	20	1	20	1	20
25	26	0.0	0.0	30	1	20	1	20
26	27	57.0	27.9	50	1	20	1	20
27	28	364.7	178.3	80	1	20	1	20
28	29	0.0	0.0	20	1	20	1	20
29	30	124.6	60.9	130	1	20	1	20
30	31	57.0	27.9	270	1	20	1	20
29	32	0.0	0.0	40	1	20	1	20
32	33	85.5	41.8	60	1	20	1	20
33	34	0.0	0.0	280	1	20	1	20
34	35	396.7	194.0	80	1	20	1	20
32	36	0.0	0.0	50	1	20	1	20
36	37	181.2	88.6	250	1	20	1	20
37	38	242.2	118.4	180	1	20	1	20
36	39	75.3	36.8	40	1	20	1	20
0	40	0.0	0.0	460	3	20	1	20
40	41	12.5	5.3	160	3	20	1	20
41	42	62.7	26.6	1980	1	20	1	20
41	43	0.0	0.0	50	3	20	1	20
43	44	117.9	50.0	100	3	20	1	20
44	45	62.7	26.6	540	1	20	1	20
44	46	172.3	73.0	60	2	20	1	20
46	47	458.6	194.4	130	2	20	1	20
47	48	263.0	111.5	40	1	20	1	20
48	49	235.8	99.9	80	1	20	1	20
49	50	0.0	0.0	190	1	20	1	20

Line		Load (N2)		Length (m)	Conductor		Support	
N1	N2	P(kW)	Q(kVar)		Type	Elap. Life (years)	Type	Elap. Life (years)
50	51	109.2	46.3	190	1	20	1	20
49	52	0.0	0.0	30	1	20	1	20
52	53	72.8	30.9	20	1	20	1	20
53	54	258.5	109.6	40	1	20	1	20
54	55	69.2	29.3	20	1	20	1	20
55	56	21.8	9.3	10	1	20	1	20
53	57	0.0	0.0	70	1	20	1	20
57	58	20.5	8.7	170	1	20	1	20
58	59	150.5	63.8	280	1	20	1	20
59	60	220.7	93.6	340	1	20	1	20
60	61	92.4	39.2	220	1	20	1	20
61	62	45.0	20.0	140	1	20	1	20
48	63	226.7	96.1	90	1	15	1	20
1	64	0.0	0.0	10	2	20	1	20
64	65	294.0	117.0	180	1	20	1	20
65	66	83.0	33.0	260	1	20	1	20
66	67	83.0	33.0	220	1	20	1	20
67	68	103.8	41.3	220	1	20	1	20
68	69	176.4	70.2	110	1	20	1	20
69	70	83.0	33.0	370	1	15	1	15
69	71	217.9	86.7	40	1	15	1	15
71	72	23.3	9.3	470	1	15	1	15
72	73	5.1	2.0	680	1	15	1	15
71	74	72.6	28.9	50	1	15	1	15
74	75	406.0	161.5	880	1	15	1	15
1	76	0.0	0.0	10	2	20	1	20
76	77	100.2	42.5	490	1	20	1	20
77	78	142.5	60.4	150	1	20	1	20
78	79	96.0	40.7	140	1	20	1	20
79	80	300.5	127.4	30	1	20	1	20

Line		Load (N2)		Length (m)	Conductor		Support	
N1	N2	P(kW)	Q(kVar)		Type	Elap. Life (years)	Type	Elap. Life (years)
80	81	141.2	59.9	410	1	20	1	20
81	82	279.8	118.6	230	1	20	1	20
82	83	87.3	37.0	380	1	20	1	20
82	84	243.8	103.4	70	1	20	1	20
84	85	247.8	105.0	380	1	20	1	20
1	86	0.0	0.0	20	3	25	1	25
86	87	89.9	38.1	570	3	25	1	25
87	88	1137.3	482.1	70	1	20	1	20
87	89	458.3	194.3	290	1	25	1	20
89	90	385.2	163.3	50	1	25	1	20
90	91	0.0	0.0	50	1	25	1	20
91	92	79.6	33.7	220	1	25	1	20
92	93	87.3	37.0	60	1	25	1	20
93	94	0.0	0.0	90	1	25	1	20
94	95	74.0	31.4	200	1	25	1	20
95	96	232.1	98.4	150	1	25	1	20
96	97	141.8	60.1	180	1	25	1	20
94	98	0.0	0.0	70	1	20	1	20
98	99	76.4	32.4	90	1	10	1	20
1	100	0.0	0.0	10	3	20	1	20
100	101	51.3	21.8	230	3	20	1	20
101	102	59.9	25.4	160	3	20	1	20
102	103	90.7	38.5	1530	1	20	1	20
102	104	2.1	0.9	630	3	20	1	20
104	105	16.7	7.1	960	3	20	1	20
105	106	1506.5	638.6	440	2	20	1	20
106	107	313.0	132.7	140	1	20	1	20

Line		Load (N2)		Length (m)	Conductor		Support	
N1	N2	P(kW)	Q(kVar)		Type	Elap. Life (years)	Type	Elap. Life (years)
107	108	79.8	33.8	140	1	20	1	20
108	109	51.3	21.8	370	1	20	1	20
109	110	0.0	0.0	360	1	20	1	20
108	111	202.4	85.8	30	1	20	1	20
111	112	60.8	25.8	320	1	20	1	20
112	113	45.6	19.3	580	1	20	1	20
113	114	0.0	0.0	380	1	20	1	20
109	115	157.1	66.6	520	1	20	1	20
115	116	0.0	0.0	720	1	20	1	20
110	117	250.1	106.0	730	1	20	1	20
117	118	0.0	0.0	320	1	20	1	20
105	119	69.8	29.6	220	1	20	1	20
119	120	32.1	13.6	100	1	20	1	20
120	121	61.1	25.9	80	1	20	1	20
1	122	0.0	0.0	10	2	20	1	10
122	123	94.6	46.3	430	1	20	1	10
123	124	49.9	24.4	30	1	20	1	10
124	125	123.2	60.2	350	1	20	1	20
124	126	78.4	38.3	20	2	20	1	20
126	127	145.5	71.1	350	1	20	1	20
126	128	21.4	10.4	70	1	20	1	20
128	129	74.8	36.6	80	1	20	1	20
128	130	227.9	111.4	90	1	20	1	20
130	131	35.6	17.4	30	1	20	1	20
131	132	249.3	121.9	60	1	20	1	20
132	133	316.7	154.8	110	1	20	1	20
133	134	333.8	163.2	250	1	20	1	20
134	135	249.3	121.9	270	1	20	1	20
135	136	60.0	5.0	200	1	20	1	20

Source: Adapted from Mantovani, Casari and Romero (2000).

ANNEX C - ENERGY PRICES AND CO_2 INTENSITY

Table 13 – Hourly average energy prices for each planning period ($/MWh)

Hour	Period 1	Period 2	Period 3	Period 4
1	46.8	45.3	43.7	40.3
2	44.0	42.4	40.1	38.9
3	42.9	41.4	39.4	38.2
4	42.5	41.2	39.4	38.2
5	43.0	42.1	39.7	38.5
6	44.7	46.5	42.4	40.1
7	47.1	51.0	42.6	38.0
8	46.9	41.4	33.3	29.8
9	45.0	35.1	26.9	24.0
10	45.1	33.5	23.9	21.0
11	47.8	35.4	24.7	21.6
12	48.6	36.0	25.0	22.4
13	50.6	38.0	26.2	23.3
14	53.0	40.0	26.6	23.8
15	55.3	42.3	27.3	24.5
16	57.6	47.2	31.4	28.2
17	61.0	59.6	45.7	45.0
hg	71.3	97.0	119.3	138.8
19	95.3	141.1	196.0	190.7
20	90.3	128.1	180.7	175.4
21	92.7	109.5	145.5	141.8
22	84.0	103.5	125.8	116.1
23	65.0	68.0	64.6	59.0
24	55.6	55.0	48.6	46.0

Source: Adapted from Gagnon, Cowiestoll and Schwarz (2023).

Table 14 – Hourly average CO_2 intensity for each planning period ($kgCO_2/MWh$)

Hour	Period 1	Period 2	Period 3	Period 4
1	415	404	402	362
2	411	396	400	365
3	413	398	402	370
4	416	403	409	377
5	422	412	417	383
6	433	422	415	374
7	431	395	360	314
8	413	348	299	255
9	388	300	243	199
10	372	275	216	175
11	373	270	207	167
12	380	276	206	167
13	387	283	209	168
14	390	287	209	167
15	394	294	213	170
16	404	311	232	187
17	430	366	300	252
18	464	435	372	322
19	490	495	448	398
20	501	504	457	401
21	497	486	432	373
22	486	471	426	368
23	459	451	424	371
24	431	423	416	369

Source: Adapted from Gagnon, Cowiestoll and Schwarz (2023).

ANNEX D
INVESTMENT AND O&M COSTS RELATED TO PLANNING ACTIONS

Table 15 – Substation costs

Capacity (MVA)	Cost ($)
7.5	410,620
10	533,800
15	780,150
20	1,026,500

Source: Elaborated by the author.

Table 16 – Conductor replacement costs

X	Y				
	AA1	AA2	AA3	AA4	AA5
AA1	6,500	7,830	10,170	11,500	12,830
AA2	-	8,500	10,830	12,170	13,500
AA3	-	-	12,000	13,300	14,670
AA4	-	-	-	14,000	15,330
AA5	-	-	-	-	16,000

X: initial type, Y: final type

Source: Elaborated by the author.

Table 17 – Support replacement costs

X	Y	
	E1	E2
E1	10500	11500
E1	-	12000

X,Y: initial/final type

Source: Elaborated by the author.

Table 18 – VR costs

Type	Capacity (A)	Cost($)
1	50	4510
2	100	8960
3	200	17870
4	300	26780

Source: Elaborated by the author.

Table 19 – Investment costs of DER systems

System	**Cost ($/kW)**			
	Period 1	**Period 2**	**Period 3**	**Period 4**
PV	1782	1501	1219	1051
Wind*	3191	2361	2008	1827
EES	2197	1729	1550	1449

*Applicable for a wind system unit of 225kW

Source: Adapted from NREL (2023).

Table 20 – O&M costs of DER systems ($/kW)

Year	System		
	PV	**Wind**	**EES**
1	18	36	51
2	18	36	49
3	17	36	47
4	17	36	45
5	16	35	43
6	16	35	42
7	15	35	40
8	15	35	40
9	14	35	39
10	14	35	39
11	13	35	38
12	13	35	38
13	13	35	38
14	12	34	37
15	12	34	36
16	12	34	36
17	12	34	35
18	12	34	35
19	12	34	34
20	11	34	34

Source: Adapted from NREL (2023).